Development of competitive algal growth model applicable to eutrophic lakes for the suppression of cyanobacterial blooms

February 2023

Jingnan Li

Graduate School of Science and Engineering

CHIBA UNIVERSITY

（千葉大学審査学位論文）

富栄養湖沼に適用可能なアオコ抑制のための新規藻類競合モデルの開発

2023 年 2 月

融合理工学府
先進理化学専攻 共生応用化学コース
李　婧男

Ph. D. thesis submitted in particle fulfillment of the requirements for the degree of Ph.D. in Graduate School of Science and Engineering, Chiba University, Japan.

Affiliation:

Department of Applied Chemistry and Biotechnology, Division of Advanced Science and Technology, Graduate School of Science and Engineering, Chiba University.
1-33, Yayoi-cho, Inage-ku, Chiba-shi, Chiba, 263-8522, Japan

Supervisor:

Assoc. Prof. Yoshimasa Amano
Department of Applied Chemistry and Biotechnology, Graduate School of Engineering, Chiba University

Examiners:

Prof. Naofumi Uekawa
Department of Applied Chemistry and Biotechnology, Graduate School of Engineering, Chiba University

Prof. Takashi Karatsu
Department of Applied Chemistry and Biotechnology, Graduate School of Engineering, Chiba University

Assoc. Prof. Masumi Yamada
Department of Applied Chemistry and Biotechnology, Graduate School of Engineering, Chiba University

Prof. Motoi Machida
Department of Applied Chemistry and Biotechnology, Graduate School of Engineering, Chiba University

Assoc. Prof. Yoshimasa Amano
Department of Applied Chemistry and Biotechnology, Graduate School of Engineering, Chiba University

Declaration

I hereby declare that this submission is my own work and that, to the best of my knowledge and belief, it contains no material which to a substantial extent has been accepted for the award of any other degree or diploma of the university or other institute of higher learning, expect where due acknowledgement has been made in the text.

Jingnan Li

Chiba

February 2023

Acknowledgements

The present study was carried out under the supervision of Assoc. Prof. Yoshimasa Amano of Graduate School of Engineering, Chiba University.

I would like to express my sincere gratitude to Assoc. Prof. Yoshimasa Amano. In the past three years, Assoc. Prof. Amano has strictly requested my study and research, and gave me guidance and opinion patiently. He has made guiding opinions and recommendations on the research direction of the thesis and gave careful advice to grow me as a research scientist.

I would like to express my gratitude to Prof. Motoi Machida for his guide and support in my research and daily life. He gave me a lot of guidance and help in experimental operation and the English writing of the thesis.

I also would like to thank Prof. Naofumi Uekawa, Prof. Takashi Karatsu and Assoc. Prof. Masumi Yamada for reviewing and providing comments and advice of the present thesis.

I want to thank my most close friend Mengze Wang for listening, offering me advice and taking care of my daily life during the three years. Special thanks to my other friends: Kai Wei, Jinghan Yuan, and Zimu Li.

Last but not least, I am especially grateful to my parents, who supported me emotionally and financially. I always knew that they believed in me and wanted the best for me. Thank they for teaching me that my job in life was to learn and to be myself; only then could I insist on science research.

Abstract

Human activities became more and more frequent nowadays, with that increasing amounts of agricultural and industrial wastes are being discharged into water bodies. As a result, the phenomenon of eutrophication is becoming more and more common worldwide. Combined with the recent effect of global warming problem, cyanobacterial blooms break out more frequently in eutrophic lakes. Cyanobacterial blooms deteriorate water quality causing severe water problems as well as disrupting the balance of the aquatic ecosystem. In order to prevent cyanobacterial blooms in advance by predicting the proliferation of cyanobacteria, several models have been proposed. However, there was still a lack of models that were able to accurately predict the cyanobacterial bloom occurrence. The understanding of the comprehensive impact of temperature, nutrient concentrations, and competitors on the proliferation of cyanobacteria was also limited. Therefore, it is vital to simulate the impacts of these factors for the improvement of the accuracy of the models.

This study aimed to explore the growth mechanism of *Microcystis* sp. cyanobacterium and its competitor *Cyclotella meneghiniana* diatom under various environmental conditions and develop an accurate growth prediction model. The temperature sensitivities of both species were discussed, and the effect of nutrient concentration and dilution rate on the competition characteristics for the two species were examined. Based on the different research contents, this study was divided into the following aspects:

(1) The temperature-related growth characteristics of *Microcystis* sp. and its competitor *C. meneghiniana* were examined in a series of monoculture experiments at different temperatures. Then, the temperature-related term for each species was established for a previously developed growth competition model, which was difficult

to be applied to actual lakes due to the lack of temperature-related term. Based on experimental results, the highest temperature-dependent growth rate for *C. meneghiniana* was calculated to be 0.64 day^{-1} at 29°C and that for *Microcystis* sp. was 0.65 day^{-1} at 37°C. The coefficient ε, which reflects the extent of the biovolume change affected by temperature, was 19.4 for *C. meneghiniana* and 8.7 for *Microcystis* sp., indicating that *C. meneghiniana* is more sensitive to the temperature than *Microcystis* sp. Moreover, cocultivation experiments at low temperature (20°C) and high temperature (30°C) were conducted to verify the influence of these temperature-dependent growth characteristics on the interspecific interaction. The biovolume in saturation and dominant species were portrayed in the two temperature groups to assess the effect of temperature on their interaction. The effect of temperature on the cyanobacterial bloom formation was also discussed by comparing experimental results with the observed situation in the field of Lake Tega, Japan.

(2) Since the overestimation of the amount of nutrient uptake was always observed in the previous model, especially under low temperatures, due to the use of the Michaelis-Menten model for nutrient uptake term. In this study, monoculture experiments of *Microcystis* sp. and *C. meneghiniana* were conducted to examine their growth and estimate their nutrient uptake parameters under low temperature (20°C). Cocultivation experiments were also performed under various nitrogen concentrations and dilution rates at 20°C to explore the different nutrient uptake characteristics of the two species. Based on the experimental results, the nutrient uptake term was further derived by relating the nutrient uptake rate to biovolume density. The result showed that the overestimation was reduced, and the accuracy of the model prediction was improved. The coefficient of determination (R^2) increased mostly from 0.26 to 0.84. Under sufficient phosphorus concentrations, the critical value of nitrogen concentration that effectively suppressed *Microcystis* sp. proliferation was portrayed to be 0.31 mg-N L^{-1} under low temperature by the improved model.

(3) In order to clarify the effective dilution rate to suppress *Microcystis* growth and their blooms formation, the growth competition model developed for eutrophic

conditions was utilized. Cocultivation experiments of *Microcystis* sp. and *C. meneghiniana* under limited phosphorus and sufficient nitrogen concentration with various dilution rates were conducted to investigate the mechanisms of dilution effect and verify the broad applicability of the developed model. Experimental results revealed that there was rarely a remarkable discrepancy in *Microcystis* sp. cell density among different dilution groups ($p > 0.05$), while *C. meneghiniana* cell density was significantly different between groups ($p < 0.05$). The accuracy of the simulation model under limited phosphorus as well as sufficient nitrogen concentration was verified by comparing the simulated value with experimental results. Based on the simulated results, it was suggested that a dilution rate over 13.3% can suppress *Microcystis* growth effectively in Lake Tega, as a case study. The predicted data were also compared with the actual data collected over years in Lake Tega, and the effectiveness of the model simulation has been confirmed.

Abstract

List of contents

Chapter 1 General introduction

1.1 Microalgae and cyanobacteria

Microalgae and cyanobacteria are the primary producers in aquatic ecosystems, for their carbon fixation ability by photosynthesis. They can be found in oceans, lakes, rivers, and some ponds, and are even able to live and proliferate in severe water environments like highly contaminated water [1]. Microalgae are a diverse group of unicellular organisms [2], and some of them can form colonies on surface layer which can be visually observed [3]. Cyanobacteria, also known as blue-green algae, are a kind of gram-negative photosynthetic autotrophic prokaryote, emerged on the earth billions of years ago. They fulfill key roles in the cycling of biological substances, and cosmopolitan inhabit in fresh-, marine- and various aquatic environments [4]. Furthermore, cyanobacteria are also one of the earliest organisms to carry out photosynthesis. The photosynthesis of cyanobacteria has changed the atmospheric composition and provided the material basis (carbon dioxide) and development conditions (oxygen) for the survival of animals and plants. They also play a key role in the formation of atmosphere oxygen [5]. Approximately 30% of total oxygen in atmosphere is produced by cyanobacterial photosynthesis [6]. Some cyanobacterial species can fix the atmospheric N_2 to enhance the soil fertility. Thus, similar to other prokaryotic bacteria, the recently increasing utilization of cyanobacteria as bioinoculants for soil fertility has improved the soil physicochemical characteristics such as water-holding capacity and mineral nutrient status of the degraded lands [7].

Meanwhile, the biofuel utilization of cyanobacteria has been also focused to supplement the fossil fuels' drain [8]. Both microalgae and cyanobacteria are considered to be the important promising sources for biodiesel production, because their cultivated time is short and oil content is high [9]. Compared with the contaminating components produced by fossil fuels combustion such as SO_2, NO,

CO_2, and NO_2 [10], the cyanobacteria can conversely fix CO_2 by photosynthesis. A part of the main chemical compounds produced by engineered cyanobacteria are alcohols, diols and some other hydrocarbons [11], whose combustion products contain H_2O and other environment friendly compounds.

However, the invasion of cyanobacteria to aquatic ecosystems has also been discussed in recent decades. There are many categories of cyanobacteria. It is recognized that about 150 genera and 2000 species are belonged to cyanobacteria [12, 13]. The existing morphometrics of cyanobacteria are generally observed in single cells, colonies, and filaments [14, 15]. There are some species that can produce toxins to impact terrestrial and aquatic organisms. Though they appear unable to colonize, invade and grow in human or other aquatic organisms, the toxic substances can destroy the organs of organisms or even kill other non-toxic algae directly [4] making the toxic cyanobacterial dominance, and thereby, leading to cyanobacterial blooms outbreak.

Among these algal species, of particular concern is *Microcystis* that is frequently observed in cyanobacterial blooms, *Microcystis* blooms are the most widespread and harmful in cyanobacterial blooms [16]. *Microcystis aeruginosa* is a typical cyanobacterial bloom-forming species, generally growing and metabolizing in freshwater lakes [17]. The hepatotoxic secondary metabolites produced by not only *M. aeruginosa* but also some other *Microcystis* species are called microcystins [18]. At least 65 isoforms of microcystins produced by *Microcystis* have been identified [19], which will poison other coexisting algae leading to the proliferation of *Microcystis*. Moreover, *Microcystis* is a kind of gas-vacuolate cyanobacteria, and their dominance is often attributed to their buoyancy [20]. It often assembles a thick layer on the water surface forming blooms, and sometimes the thick layer accumulates in piles and floats on the shore. After *Microcystis* death, they will be decomposed by bacteria. The dissolved oxygen in water will decrease due to this process, causing deaths of fish and other organisms [21] and, consequently resulting in the collapse of water ecosystems.

1.2 Cyanobacterial blooms and its harmfulness

Cyanobacteria proliferate rapidly with overwhelming dominance when environmental conditions are supporting their growth. Abundant nutrients, prolonged warm temperatures (22^{o}C - 30^{o}C) and relatively calm weather conditions can support the cyanobacterial growth in the water column, and when hydraulic conditions permit, the hyper-proliferated cyanobacteria can float on the water surface forming blooms [17, 22]. Cyanobacterial blooms are first defined as the aggregation of dispersing buoyant planktonic cyanobacteria on the water surface by Reynolds [23]. The harmful effect caused by cyanobacterial blooms mainly act on environments, ecosystems, and biological health [24-28].

As for the effect on the perception of environment, a large amount of cyanobacteria gather on the water surface, causing the water color turns green. Some aquatic animals die due to the water quality caused by the blooms [13]. Furthermore, not only the animal carcasses will be deteriorated to release an odor smell, but also the cyanobacteria itself will make the water turn to smell unpleasant [29].

Fig. 1-1 Cyanobacterial blooms in Lake Senba, Japan (2019)

When it comes to the effect on aquatic ecosystems, microcystins secreted by cyanobacteria caused the death of fish, shellfish, and other aquatic organisms. Besides, cyanobacterial blooms in the water can block the holes on the gills of fish and shellfish leading to death by choking their breath [30-32]. The outbreak of

cyanobacterial blooms seriously affects the survival of aquatic organisms and destroys the ecological balance.

Microcystins can be also accumulated step by step along the food chain, entering the human and other organisms' body, which will threaten the health of them [33]. The treatment of cyanobacterial blooms for water purification is difficult, which may clog the filtration treatment equipment. Methods for the removal of some certain unknown toxins produced by cyanobacteria are still unclear, making a water supply safety hazard [34].

1.3 Eutrophication and cyanobacteria bloom

Cyanobacterial blooms are a common phenomenon in eutrophic lakes [35, 36], and are a representative feature of eutrophication [37, 38].

Eutrophication can be recognized as the sum of the effects of the excessive growth of phytoplankton, that breaks the balance of primary and secondary productivity [39]. Eutrophication can be greatly accelerated by human activities that increase the rate of nutrient input in a water body, due to rapid urbanization, industrialization and intensifying agricultural production [40].

The eutrophication in nature is originally a slow process of lake aging and productivity enhancement, usually taking thousands of years [41]. However, with the development of human activities, the eutrophication rapidly proceeds has been a global environmental problem. As a result, cyanobacterial blooms are observed more and more frequently in recent years.

According to the survey report, it is portrayed that among the 480 lakes with area of more than one hectare in Japan, 181 lakes were in eutrophic status, accounting for 33% in the total number [42]. In contrast, the number of oligotrophic lakes was 124, accounting for 26%, which was less than that of eutrophic lakes. The features of eutrophic status in lake are increasingly high nutrient concentrations, more and more simple phytoplankton community structure and lower biodiversity. The survey also displayed that the dominant bloom-forming species in inland lakes in Japan are

Microcystis, *Anabaena*, and *Aphanizomenon* adapting to the eutrophic environment [43]. The rapid growth of these cyanobacterial populations often results in the appearance of blooms.

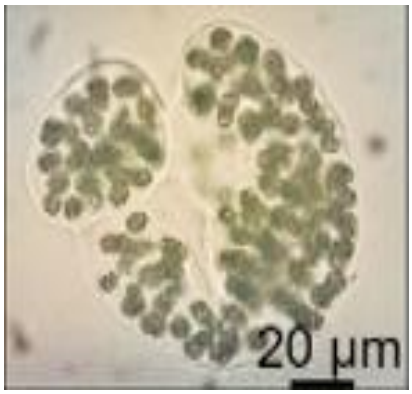

Fig. 1-2 The genus *Microcystis*

However, the problem of eutrophication can not be managed significantly within a short period of time. According to the experience of lake management worldwide, with 20-30 years of high-intensity pollution control, most lakes have been gradually recovered from the status of eutrophication to mesotrophic and oligotrophic [44]. It can be anticipated that the water environment in Japan will still suffer the risk of cyanobacterial blooms in the next few decades. Therefore, it is necessary to predict the timing of appearance and intensity of cyanobacterial blooms in lakes. The early warning and forecasting of the development trend of cyanobacterial blooms needs to be developed so that the measures can be taken to control and reduce the pollution caused by cyanobacterial blooms.

1.4 Mechanism of cyanobacterial bloom formation and its influential factors

It is important for the early warning and management of cyanobacteria to explore the mechanism of cyanobacterial bloom occurrence [45, 46]. However, the mechanism is complex, and there may be multiple factors in the mechanisms [47-49].

Most of the current studies agree that the formation of cyanobacterial blooms was generally caused by the physiological characteristics of cyanobacteria themselves, and the interaction with physical, chemical, and biological factors [38, 45].

There has still not been absolute definition of cyanobacterial bloom so far. Though Reynolds [23] defined cyanobacterial blooms as the aggregation of dispersing buoyant planktonic cyanobacteria on the water surface, Pearl et al. [38] believed that cyanobacterial blooms can also occur at a specific locations below the water surface, which is related to light intensity, nutrient concentrations, and the location of the thermocline. Meanwhile, there are some limnological scientists, who consider that cyanobacterial blooms were formed when the chlorophyll-a concentration in lake show over 10 μg L^{-1} or the cyanobacterial cell density reached 2.0×10^4 cells mL^{-1} [50, 51].

1.4.1 Research progress of cyanobacteria bloom formation mechanism

The mechanism of cyanobacterial bloom formation is complex, including vertical stratification of the water column, changes in nutrient concentration, and longer hydraulic residence times, among others [47, 50]. The outbreak of cyanobacterial bloom is the result of complex interaction among biological, physical, and chemical factors which compose the optimal conditions for the bloom formation.

Reynolds [23] and Walsby [52] argued that, before cyanobacterial blooms occur, three conditions must be qualified: (i) sufficient cyanobacterial cell density in the lake, (ii) cyanobacterial cells have excessive buoyancy, and (iii) the hydrodynamic force is not strong enough to offset the buoyancy of the cyanobacterial cell.

From these arguments, the importance of the cyanobacterial buoyancy and cell density in the formation of cyanobacterial blooms can be recognized. In addition, Dokulil and Dokulil [53] suggested that eutrophication would lead to a decrease in phytoplankton community biodiversity, which eventually causes the cyanobacterial

dominance, and the dominance as a result of interspecific competition may also result in cyanobacterial blooms. Thus, the study of cyanobacterial dominance has also been a hot issue.

The outbreak of cyanobacterial blooms at water surface is always observed in the environment of high temperature in summer, high light intensity and steady hydraulic conditions. In some cases, the outbreak of the cyanobacterial blooms was very quick, which has led to the misunderstanding that cyanobacteria can grow very fast in a short period and occur suddenly [54, 55]. This misunderstanding has led to the perception in media reports and even professional literature that the occurrence of cyanobacteria bloom is unpredictable and break suddenly.

However, Yang et al. [56] found that the conclusion of their research could not support the bias for the mechanism of cyanobacterial bloom occurrence. They found that cyanobacterial blooms were not caused by the suddenly increased cell density but caused by a gradual bloom-development and bloom-forming process. The process includes the transformation of cyanobacterial cells from a dormant state to revived state, gradual increase in cell density, and the aggregation and floatation of cyanobacterial cells. The microscopic observation reveal that a large population of *Microcystis* has been already suspended in the water body prior to the bloom formation. Once meteorological and hydrological conditions changed to suitable for cyanobacterial proliferation, *Microcystis* will aggregate and float on the water surface, while the species other than *Microcystis* below the water surface decreases significantly. The description “outbreak” only displays the spatial locational change of large cyanobacterial community in a short time, which was mainly due to the wind action, but not a description of sudden increase in cell density. In conclusion, the occurrence of cyanobacterial blooms is indeed an instantaneous outbreak in terms of phenological phenomena, but it is essentially a gradual and predicational process.

(a) Bloom forming mechanism of cell density accumulation

Both Reynolds [23] and Zhang et al. [57] indicated that, before the occurrence of

cyanobacterial blooms, there is a process of biomass and cell density accumulation. The premise of the cyanobacterial bloom occurrence was that there has been a large amount of cell density. Cyanobacterial blooms are the phenomenon of these accumulated cells gathering and floating on the water surface.

(b) Bloom forming mechanism of cyanobacteria buoyancy

The regulation of buoyancy by cyanobacteria is an important mechanism for the formation of cyanobacterial blooms [58-60]. Many cyanobacterial species have gas vesicles in cells which enable them to float on the water surface [23]. Gas vesicle is a subcellular structure filling air and generally cylindrical or spindle shape [22]. The protein in cyanobacterial cells can control the gas vesicles size and shape to regulate the cell buoyancy to change vertical distribution, diurnal migration, and bloom-forming ability. This ability to control buoyancy allows cyanobacteria to better adapt to environmental changes, e.g. floating to the water surface to access to sunlight. On the other hand, cyanobacteria such as *Microcystis* can form colony by growth and the production of extracellular polysaccharides (EPS). The cyanobacterial colony can enhance the rate of sinking and upwelling, and can also reduce the loss of biomass due to cell deposition [51].

Factors affecting the cyanobacterial buoyancy are cell size and shape, aounts of protein, nucleic acid, carbohydrate and cellular phosphate concentration, and the structure and function of gas vesicle [23]. Cellular carbohydrate contents will change with different light intensity, which alter the cellular buoyancy [61]. There have been many studies, pointing out that the alteration of carbohydrate contents in *Microcystis* cell is one of the main influential factors for the buoyancy regulation [62-64].

(c) Bloom forming mechanism of cyanobacterial community succession

Some studies have examined the mechanism of cyanobacterial bloom formation in ecosystem scale, using phytoplankton succession dynamics combined with community diversity to study the dynamics of *M. aeruginosa* in eutrophic lakes [47,

65, 66]. They explored that in the absence of blooms, if both successional dynamics were few and community diversity was low, then *Microcystis* blooms would occur quickly. Conversely, if both successional dynamics and community diversity were high for a considerable period of time, they would not lead to cyanobacterial blooms.

(d) Summary

The growth and biomass of cyanobacteria, buoyancy control mechanisms, and the succession of dominant species in phytoplankton community are the most direct mechanisms responsible for the formation of cyanobacterial blooms. Therefore, the growth characteristics of cyanobacteria and changes of morphology and intracellular components during the growth process are of great importance to study the biomass accumulation and cell buoyancy changes. Meanwhile, the succession of dominant cyanobacterial species will be affected by many factors and is important for the prediction of cyanobacterial blooms.

1.4.2 Affecting factors for cyanobacterial bloom formation

In aquatic environments, cyanobacterial species usually keep in low density. However, cyanobacterial cells can rapidly proliferate when the environmental conditions changed to be supporting the growth of cyanobacteria. These conditions include physical, chemical, and biological factors. The hydrological conditions, water temperature [67-69], and light intensity belong to physical condition, which affect cellular properties, spatial distribution, and community composition, relating to cyanobacteria bloom formation. The chemical factors include nutrient salts (nitrogen and phosphorus) nutritional salty, micro-nutrient element, CO_2 and so on. The biological factors mainly influence the proliferation of cyanobacteria by the predation from high trophic levels and viral bacterial attack [70].

(a) Temperature

Single-cell algae are ectothermic organisms. So, they need to obtain their heat from environment. It is unable to maintain its intracellular heat to keep temperature in cell constant at various surrounding water temperatures. Changes in water temperature will rapidly lead to changes in the metabolic rate and chemical reactions in algal cell. This kind of change can affect the proliferation of cyanobacteria, visually manifested in the difference in the cell growth rate and chlorophyll-a concentrations.

Ganf [71] has found that the preferable temperature range of *Microcystis* spp. growth was from 24^{o}C to 34^{o}C. Paerl and Huisman [72] also suggested that *Microcystis* spp. presented the maximal growth rate at 25^{o}C or higher, and the increase in cells was always observed between 20^{o}C and 30^{o}C [73]. Moreover, there has also been studies, portraying that cyanobacteria can grow better at higher temperature (> 25^{o}C) compared with other phytoplankton such as microalgae and diatoms [58, 60, 74], which make cyanobacteria dominate at high temperature.

(b) Illumination

Cyanobacteria are photosynthetic autotrophs, and they must rely on photosynthesis to synthesize carbohydrates. The substances produced by photosynthesis are the material basis for nutrition, development, growth, and other life activities.

The reaction center of the photosynthetic system in cyanobacteria is similar to that of other eukaryotic algae, in which they contain chlorophyll-a. However, the antennae of the photosynthetic system of cyanobacteria does not contain chlorophyll-a. The photosynthetic pigments contained in cyanobacteria are mainly phycobiliproteins, including phycocyanin, allophycocyanin, and phycoerythrin. These proteins allow cyanobacteria to use the green, yellow, and orange parts of light that are not available to other algae, thus having a wider light absorption band than other algae. This kind of characteristics allow cyanobacteria to use the effective light in underwater more

efficiently and grow in low-light environment [74]. Huisman et al. [75] conducted experiments setting lights as a influential factor in competition and suggested that each alga has the critical light intensity. When the effective light intensity decreases to below this threshold, alga can not grow properly and be eliminated. Algae with lower critical light intensities were more capable of becoming dominant when light was limited [76]. Among the cyanobacterial species of *M. aeruginosa*, two other green algae, *Chlorella*, and *Phyllostachys*, which Huisman et al. [75] used for their study, both *M. aeruginosa* and *Chlorella* had lower critical light intensities than *Phyllostachys*, and both of them were dominant in mixed cultures with *Phyllostachys*. Furthermore, Davis and Koop [77] discovered that light attenuation and thermogenic stratification were causative factors for the occurrence of cyanobacterial blooms in some rivers in western Australia.

(c) Nutrient salts

Nitrogen (below N) and phosphorus (below P) are necessary nutrients for phytoplankton. Due to the development of agriculture and industry as well as population increase, the nutrients are increasingly being discharged into water bodies [78, 79]. Excessive input of them has been considered as the main cause of cyanobacterial blooms. Studies of nutrient dynamics have displayed that an increase in nutrient concentration could accelerate algal growth [78]. The relationship between algal growth rates and nutrient concentrations can be explained by the Monod equation [80].

Some blue-green algae, such as *Fritillaria*, *Bacteroides*, and *Columnaris*, have the ability to fix nitrogen [81], and they can maintain the intracellular N demands by fixing atmospheric N at the absence of N in the water column. Hamilton et al. [82] and Baldia et al. [83] suggested that the ratios of mass concentration of N to P (N/P ratio) significantly affect the composition of phytoplankton community, and that lower N/P ratios can favor the dominance of cyanobacteria, leading to cyanobacterial blooms. Smith et al. [84] suggest that bloom forming cyanobacteria will dominate

when the mass ratio of total nitrogen (TN) to total phosphorus (TP) is less than 29. In addition, other recent studies have found that nitrogen removal could not solve the problem of eutrophication in lakes [85]. However, it has also been suggested that changes in N/P ratios were not a causal factor but a consequence of cyanobacterial blooms [86, 87] , while Quiros [88] argued that N/P ratios were both a causal factor and a consequence of cyanobacterial blooms.

The effect of Fe (Fe^{2+} and Fe^{3+}) ion and other trace metal ion on cyanobacterial proliferation is gradually becoming a focus of attention [89]. Fe was an essential element for electron transfer, oxygen metabolism, nitrogen uptake and utilization, and photosynthesis and respiration in the growth of phytoplankton. The deficiency of Fe ion will have serious effect on phytoplankton growth and photosynthesis [90]. Trace amount of Cu^{2+} is necessary for cyanobacterial metabolic processes, while Zn^{2+} is also a essential trace element for algal growth and metabolism. When phytoplankton are deficient in Cu^{2+} and Zn^{2+}, they can not form chlorophyll-a [36, 91, 92]. Also, Zn^{2+} plays an important role in maintaining the integrity of protein nuclei [93, 94].

(d) Dissolved inorganic carbon and pH

In water body, dissolved inorganic carbon (DIC) is the main carbon source for phytoplankton photosynthesis [95]. The concentration and composition of DIC are closely related to pH value [96], which regulates the balance between CO_2, H_2CO_3, HCO_3^-, and CO_3^{2-} in the water body.

Cyanobacteria can utilize CO_2 to lower concentrations, and some cyanobacteria can also use HCO_3^- as carbon source. A small number of eukaryotic algae also have this kind of characteristics [74]. Shapiro [97] believed that cyanobacteria can reduce the CO_2 concentration in the water to a level that only they can survive (pH is correspondingly higher), while other algae can not maintain growth in this kind of conditions, thus leading to the dominance of cyanobacteria.

Rashid et al. [98] found that the optimum pH value for the growth of *M. aeruginosa* was from 7.5 to 9.0. The optimal pH for the growth of *Arthrospira*

platensis was about 9.5 [99]. Yang et al. [100] studied the growth and photosynthesis characteristics of *M. aeruginosa*, *Phyllostachys* spp., and *Rhodophyta* in Lake Taihu at different pH values and DIC concentrations. The results showed that the effect of CO_2/pH on the three various algal species was significantly different. The optimum pH value for the growth of *M. aeruginosa* was from 8.0 to 9.0, and the photosynthetic rate could increase significantly with the increase of the value in low range. The cell growth entered a plateau at pH value of 7.0-9.0, obtaining a high photosynthetic rate. While, the photosynthetic rate of *Tetrahymena* was relatively high at various pH values (5.5-10.0), and *Rhodophyta* only obtained the maximum photosynthetic rate at pH value of around 7.0.

From the viewpoint of energy balance, the insufficiency of one chemical factor can be supplemented by another physical factor [101, 102]. The interaction of illumination and nutrient salts on algae is commonly recognized [103]. The interactions among these environmental factors will make them to jointly affect the proliferation of algae, and the relationship between these factors and cell growth is regular and can be predicted by mathematical models [104].

1.4.3 Growth kinetic models for cyanobacteria cultivation

Since the treatment of cyanobacterial blooms is still difficult and costly, there is an urgent need for the development of prediction and early warning systems for cyanobacterial blooms prevention worldwide. To estimate and evaluate cyanobacterial productivity better under various conditions, the modeling of process is necessary for the prediction based on the performance of cyanobacterial cultivation systems. Similarly, the growth kinetic model is also crucial to simulate cyanobacterial cultivation by mathematical model. In addition to numerous developed kinetic models, some studies have also proposed threshold values for indicators to provide criteria for evaluating the formation of cyanobacterial blooms.

(a) Threshold value of indicator factors

Limnologist generally recognizes that, when chlorophyll-a concentrations in a lake exceeds 10 μg L^{-1} or cyanobacterial cell density reaches 2.0 ×10^4 cells mL^{-1}, it can be called cyanobacterial blooms [50, 51].

WHO published "Guideline Values for Cyanobacteria in Freshwater" in 1999 [105], which is based on cyanobacterial biomass and algal toxin level, setting three warning frames from the guideline:

i) Vigilance level: 1 colony or 5 filaments L^{-1}

ii) Alert level I: 2×10^3 algal cells mL^{-1} or 0.2 mm^3 biovolume L^{-1}

iii) Alert level II: 1×10^5 algal cells mL^{-1}, 10 mm^3 biovolume L^{-1} or 50 μg L^{-1}

Microcystins concentration needs to be measured by chemical or bio-detection method.

Nevertheless, in actual lakes, the cyanobacterial bloom outbreak is a result of a variety of factors. Taking a single or specific impact factors to be early warning indicators does not reflect the real situation, therefore the practical significance of this method is not meaningful.

(b) Growth kinetic model and eco-mathematical model

The simulation of algae in water body is an important tool to research cyanobacterial community dynamics and to predict the timing and location of cyanobacterial bloom outbreaks. Deterministic eco-mathematical models generally focus on the physical, biological, and chemical processes affecting changes in algal communities, combined by some algebraic or differential equations. The goodness of the deterministic eco-mathematical models is that they can provide a wide variety of measurements of environmental system changes. These eco-mathematical models are generally classified as growth models.

The main nutrient related algal growth models are the Monod equation [80] and Droop equation [106]. The former equation is related to growth rate as a function of

nutrient concentration in solution. The later model proposed in 1968, stated that growth rate is related to the intracellular nutrients (nutrient cell quota).

Chalup and Laws [107] proposed a model for microalgal growth that addresses the inconsistency of growth rates related to the intracellular mass ratios of nitrogen to carbon (N/C ratios) predicted by some previous models. In this model, the relationship between the growth rate at nutrient saturation and light intensity is represented as hyperbolic, and the mass ratio of chlorophyll-a:carbon to respiration rate is linear.

Reynolds et al. [108] and Lewis et al. [109] also proposed a PROTECH (Phytoplankton responses to environmental change) model, that is a process model, simulating the dynamics of changes in phytoplankton communities in lakes and reservoirs. It can simulate the growth of up to eight species simultaneously [109]. The model has been successfully applied to more than one hundred algal species to predict dominant species in the algal community [110]. This model has been continuously developed and improved and has been widely used in the world. Elliott et al. [60] applied this model to the response of a phytoplankton community in a temperate lake to the changes of temperature and nutrient input. As a result, these two factors were found to be beneficial to the formation of *Anabaena* sp. dominance. The factors would affect the emergence timing of the maximum biomass of the bloom forming key species. Nutrient input had a greater effect on the growth of algae, and the response of the phytoplankton community to temperature changes was greatly influenced by nutrient supply. The application of eco-mathematical model make it be possible to predict change in complex ecosystem by only several initial environmental parameters, which make the prediction of cyanobacterial bloom occurrence become simple and efficient. The conclusion from prediction provides a viable method for the prevention of cyanobacterial blooms.

1.5 Perspective and purpose of this thesis

The aim in this study was to explore the effect of temperature, nutrient

concentrations, and dilution rate on *Microcystis* sp. and its main competitor, which have ecological effect on the growth of *Microcystis* sp. Based on the influencing characteristics of these environmental factors on the growth of *Microcystis* sp. and its competitor, the growth competition model can be further developed to predict the proliferation of *Microcystis* sp. and another co-existing algal simultaneously, improving the accuracy of prediction. In order to provide effective cyanobacterial treatment in Lake Tega, *Microcystis* sp. and its main competitor, the diatom *Cyclotella meneghiniana* were isolated from the lake and used as test algal strains to explore various environmental effects. By measuring and analyzing the growth characteristics of the two algae under various experimental conditions, the influencing mechanisms of temperature and nutrients were discussed. These characteristics were also utilized to estimate the mathematical relationship between the growth of algal cells and changing environmental conditions to enhance the accuracy of previous existing model. The developed model was expected to predict the dominant species succession and *Microcystis* bloom occurrence accurately. Then, depending on the developed growth competition model, the optimal environmental conditions for the competitor *Cyclotella meneghiniana* growth were discussed to suppress the *Microcystis* bloom formation.

In Chapter 2, the growth characteristics of *Microcystis* sp. and *C. meneghiniana* at different water temperatures were examined and a temperature-related term which is lacked in the interspecific growth competition model was established. The coefficients ε, reflecting temperature adaption patterns for the two species, were estimated. The interspecific dominant characteristics of the two species at low and high temperatures were also discussed under cocultivation conditions.

In Chapter 3, the nutrient uptake patterns of *Microcystis* sp. and *C. meneghiniana* at low temperature were estimated to develop the nutrient related term in the previous model and improve the deficiency between the prediction value and experimental data. The competition characteristics of the two species under N limitation with constant P concentration at low temperature were discussed and the

effective N concentration to cause dominant species succession was calculated by the developed model.

In Chapter 4, the mechanism of suppressive effect of dilution on the growth of *Microcystis* sp. and *C. meneghiniana* was examined. The broad applicability of the developed competitive model was proved by cocultivation experiments with various dilution rates. The critical dilution rate to suppress the *Microcystis* sp. growth in Lake Tega was then elucidated, which was in consistent with the field observation.

In Chapter 5, the general conclusion of this study was summarized and outlook for the future study was stated in Chapter 6.

Nomenclature

μ Growth rate or specific growth rate (day^{-1})

N Nitrate-nitrogen concentration (mg-N L^{-1})

N_0 Initial nitrate-nitrogen concentration (mg-N L^{-1})

P Phosphate-phosphorus concentration (mg-P L^{-1})

P_0 Initial phosphate-phosphorus concentration (mg-P L^{-1})

C Cell density (cells mL^{-1})

Q Cell quota (pg $cell^{-1}$)

ρ_{max} Highest uptake rate（pg $cell^{-1}$ day^{-1}）

ρ_{max}^{hi} Highest uptake rate at the beginning of cultivation (pg $cell^{-1}$ day^{-1})

ρ_{max}^{lo} Highest uptake rate at the maximum growth rate (pg $cell^{-1}$ day^{-1})

K Saturated specific cell density (cells mL^{-1})

K_μ Half-saturation constant for growth rate (mg L^{-1})

K_ρ Half-saturation constant for uptake rate (mg L^{-1}）

K_ρ^{hi} Half-saturation constant for uptake rate at the beginning of cultivation (mg L^{-1})

K_ρ^{lo} Half-saturation constant for uptake rate at the maximum growth rate (mg L^{-1})

μ_{max} Maximum growth rate at a certain nutrient concentration or temperature (day^{-1})

μ'_{max} Highest specific growth rate (day^{-1})

Q_{min} Minimum cell quota (pg $cell^{-1}$)

Q_{max} Maximum cell quota (pg $cell^{-1}$)

D Dilution rate (day^{-1})

d Daily renewal rate (day^{-1})

D_{avg} Annual average dilution rate (day^{-1})

α Inter-specific competition rate

T Environmental temperature

T_{opt} Optimum environmental temperature

Subscripts A and B, respectively, refer to two cocultured algal species (*Microcystis* sp. and *Cyclotella meneghiniana*)

Subscripts n and p, respectively, refer to nitrate-nitrogen and phosphate-phosphorus

References

[1] S.V. Avery, G. Codd, G.M. Gadd, Interactions of cyanobacteria and microalgae with caesium, Impact of heavy metals on the environment, Elsevier1992, pp. 133-182.

[2] J. Ruane, A. Sonnino, A. Agostini, Bioenergy and the potential contribution of agricultural biotechnologies in developing countries, Biomass Bioenergy, 34 (2010) 1427-1439.

[3] WHO, Addendum to the WHO guidelines for safe recreational water environments. Volume 1, Coastal and fresh waters: list of agreed updates, World Health Organization, 2009.

[4] G.A. Codd, L.F. Morrison, J.S. Metcalf, Cyanobacterial toxins: risk management for health protection, Toxicol. Appl. Pharmacol., 203 (2005) 264-272.

[5] A. Dufresne, L. Garczarek, F. Partensky, Accelerated evolution associated with genome reduction in a free-living prokaryote, Genome Biol., 6 (2005) 1-10.

[6] S. Kulasooriya, Cyanobacteria: pioneers of planet earth, Ceylon Journal of Science, 40 (2011) 71-88.

[7] J.S. Singh, A. Kumar, A.N. Rai, D.P. Singh, Cyanobacteria: a precious bio-resource in agriculture, ecosystem, and environmental sustainability, Front. Microbiol., 7 (2016) 529.

[8] P. Farrokh, M. Sheikhpour, A. Kasaeian, H. Asadi, R. Bavandi, Cyanobacteria as an eco-friendly resource for biofuel production: a critical review, Biotechnol. Prog., 35 (2019) e2835.

[9] A.M.P. Anahas, G. Muralitharan, Characterization of heterocystous cyanobacterial strains for biodiesel production based on fatty acid content analysis and hydrocarbon production, Energy Convers. Manage., 157 (2018) 423-437.

[10] M.W. Seo, Y.M. Yun, W.C. Cho, H.W. Ra, S.J. Yoon, J.G. Lee, Y.K. Kim, J.H. Kim, S.H. Lee, W.H. Eom, Methanol absorption characteristics for the removal of H_2S (hydrogen sulfide), COS (carbonyl sulfide) and CO_2 (carbon dioxide) in a pilot-scale biomass-to-liquid process, Energy, 66 (2014) 56-62.

[11] E. Christaki, P. Florou-Paneri, E. Bonos, Microalgae: a novel ingredient in nutrition, Int. J. Food Sci. Nutr., 62 (2011) 794-799.

[12] O.M. Skulberg, W.W. Carmichael, G.A. Codd, R. Skulberg, Taxonomy of toxic Cyanophyceae (cyanobacteria), Algal toxins in Seafood and Drinking water, (1993) 145-164.

[13] R. Bhateria, D. Jain, Water quality assessment of lake water: a review, Sustainable Wat. Res. Man., 2 (2016) 161-173.

[14] P.S. Salomon, S. Janson, E. Granéli, Molecular identification of bacteria associated with filaments of Nodularia spumigena and their effect on the cyanobacterial growth, Harmful Alg., 2 (2003) 261-272.

[15] S. Agusti, E.J. Phlips, Light absorption by cyanobacteria: Implications of the colonial growth form, Limnol. Oceanogr., 37 (1992) 434-441.

[16] R. Fulton, H.W. Paerl, Effects of the blue-green alga Microcystis aeruginosa on zooplankton competitive relations, Oecologia, 76 (1988) 383-389.

[17] M. Jang, K. Ha, M.C. Lucas, G. Joo, N. Takamura, Changes in microcystin production by *Microcystis* aeruginosa exposed to phytoplanktivorous and omnivorous fish, Aquat. Toxicol., 68 (2004) 51-59.

[18] W. Carmichael, The cyanotoxins, Adv. Bot. Res., Elsevier1997, pp. 211-256.

[19] I. Chorus, M. Welker, Toxic cyanobacteria in water: a guide to their public health consequences, monitoring and management, Taylor & Francis2021.

[20] Z. Chu, X. Jin, B. Yang, Q. Zeng, Buoyancy regulation of Microcystis flos-aquae during phosphorus-limited and nitrogen-limited growth, J. Plankton Res., 29 (2007) 739-745.

[21] T. Wai, T. Langer, Mitochondrial dynamics and metabolic regulation, Trends Endocrinol. Metab., 27 (2016) 105-117.

[22] Walsby, Gas vesicles, Microbiol. Rev., 58 (1994) 94-144.

[23] C.S. Reynolds, Cyanobacterial water-blooms, Adv. Bot. Res., 13 (1987) 67-143.

[24] J. Pinckney, D. Millie, B. Vinyard, H. Pearl, Environmental controls of phytoplankton bloom dynamics in the Neuse River Estuary, North Carolina, USA,

Oceanographic Literature Review, 9 (1998) 1587.

[25] Y. Inamori, N. Sugiura, N. Iwami, M. Matsumura, M. Hiroki, M.M. Watanabe, Degradation of the toxic cyanobacterium *Microcystis* viridis using predaceous micro-animals combined with bacteria, Phycol. Res., 46 (1998) 37-44.

[26] J.K. Basu, D. Bhattacharyya, T.-h. Kim, Use of artificial neural network in pattern recognition, International Journal of Software Engineering and its App., 4 (2010).

[27] A. Najah, A. El-Shafie, O.A. Karim, A.H. El-Shafie, Application of artificial neural networks for water quality prediction, Neu. Com. and App., 22 (2013) 187-201.

[28] K. Zhang, T.F. Lin, T. Zhang, C. Li, N. Gao, Characterization of typical taste and odor compounds formed by *Microcystis aeruginosa*, J. Environ. Sci., 25 (2013) 1539-1548.

[29] T. Kaloudis, T.M. Triantis, A. Hiskia, Taste and odour compounds produced by cyanobacteria, Handbook of Cyanobacterial Monitoring and Cyanotoxin Analysis; Meriluoto, J., Spoof, L., Codd, GA, Eds, (2016) 196-201.

[30] D. Drobac, N. Tokodi, J. Lujić, Z. Marinović, G. Subakov-Simić, T. Dulić, T. Važić, S. Nybom, J. Meriluoto, G.A. Codd, Cyanobacteria and cyanotoxins in fishponds and their effects on fish tissue, Harmful Alg., 55 (2016) 66-76.

[31] J. Sevrin-Reyssac, M. Pletikosic, Cyanobacteria in fish ponds, Aquaculture, 88 (1990) 1-20.

[32] A. Oberemm, J. Becker, G. Codd, C. Steinberg, Effects of cyanobacterial toxins and aqueous crude extracts of cyanobacteria on the development of fish and amphibians, Environmental Toxicology: An International Journal, 14 (1999) 77-88.

[33] M. Singh, G. Pant, K. Hossain, A. Bhatia, Green remediation. Tool for safe and sustainable environment: a review, Applied Water Science, 7 (2017) 2629-2635.

[34] B.C. Hitzfeld, S.J. Höger, D.R. Dietrich, Cyanobacterial toxins: removal during drinking water treatment, and human risk assessment, Environ. Health Perspect., 108 (2000) 113-122.

[35] A. Ghadouani, B. Pinelalloul, E.E. Prepas, Effects of experimentally induced

cyanobacterial blooms on crustacean zooplankton communities, Freshw. Biol., 48 (2003) 363-381.

[36] L. Ferber, S. Levine, A. Lini, G. Livingston, Do cyanobacteria dominate in eutrophic lakes because they fix atmospheric nitrogen?, Freshw. Biol., 49 (2004) 690-708.

[37] H. Wang, H. Wang, Mitigation of lake eutrophication: Loosen nitrogen control and focus on phosphorus abatement, Progress in Natural Science, 19 (2009) 1445-1451.

[38] H.W. Paerl, R.S. Fulton, P.H. Moisander, J. Dyble, Harmful freshwater algal blooms, with an emphasis on cyanobacteria, The Scientific World Journal, 1 (2001) 76-113.

[39] F.A. Khan, A.A. Ansari, Eutrophication: an ecological vision, The botanical review, 71 (2005) 449-482.

[40] W. Liu, R. Qiu, Water eutrophication in China and the combating strategies, Journal of Chemical Technology & Biotechnology: International Research in Process, Environmental & Clean Technology, 82 (2007) 781-786.

[41] D.M. Harper, Eutrophication of freshwaters, Springer1992.

[42] J.M.o.t. Environment, National Lake Survey Report, in: J. Ministry of the Environment (Ed.)Japan, 2009, pp. pp 3-4.

[43] R.N.H. Office, Explanatory material for the 2nd Ishitegawa dam water quality review committee, in: S.L.R. Agency (Ed.), 2015.

[44] T.J. Ballatore, V.S. Muhandiki, The case for a world lake vision, Hydrological Processes, 16 (2002) 2079-2089.

[45] C. Lopez, E. Jewett, Q. Dortch, B. Walton, H. Hudnell, Scientific Assessment of Freshwater Harmful Algal Blooms, (2008).

[46] H. Paerl, Nutrient and other environmental controls of harmful cyanobacterial blooms along the freshwater–marine continuum, Cyanobacterial harmful algal blooms: State of the science and research needs, Springer 2008, pp. 217-237.

[47] D. Roelke, Y. Buyukates, The diversity of harmful algal bloom-triggering

mechanisms and the complexity of bloom initiation, Human and Ecological Risk Assessment: An International Journal, 7 (2001) 1347-1362.

[48] H.W. Paerl, Nuisance phytoplankton blooms in coastal, estuarine, and inland waters 1, Limnol. Oceanogr., 33 (1988) 823-843.

[49] T. Zohary, A.M. Pais-Madeira, R. Robarts, K.D. Hambright, Interannual phytoplankton dynamics of a hypertrophic African lake, Archiv für Hydrobiologie, (1996) 105-126.

[50] C.-Y. Ahn, S.-H. Joung, S.-K. Yoon, H.-M. Oh, Alternative alert system for cyanobacterial bloom, using phycocyanin as a level determinant, Journal of Microbiology, 45 (2007) 98-104.

[51] H. Duan, R. Ma, X. Xu, F. Kong, S. Zhang, W. Kong, J. Hao, L. Shang, Two-decade reconstruction of algal blooms in China's Lake Taihu, Environ. Sci. Technol., 43 (2009) 3522-3528.

[52] C. Reynolds, Succession and vertical distribution of phytoplankton in response to thermal stratification in a lowland mere, with special reference to nutrient availability, The Journal of Ecology, (1976) 529-551.

[53] M.T. Dokulil, K. Teubner, Cyanobacterial dominance in lakes, Hydrobiologia, 438 (2000) 1-12.

[54] K. Ozaki, A. Ohta, C. Iwata, A. Horikawa, K. Tsuji, E. Ito, Y. Ikai, K.-i. Harada, Lysis of cyanobacteria with volatile organic compounds, Chemosphere, 71 (2008) 1531-1538.

[55] F. Garcia-Pichel, Solar ultraviolet and the evolutionary history of cyanobacteria, Orig. Life Evol. Biosph., 28 (1998) 321-347.

[56] Z. Yang, F. Kong, X. Shi, M. Zhang, P. Xing, H. Cao, Changes in the morphology and polysaccharide content of *Microcystis aeruginosa* (Cyanobacteria) during flagellate grazing 1, J. Phycol., 44 (2008) 716-720.

[57] M. Zhang, H. Duan, X. Shi, Y. Yu, F. Kong, Contributions of meteorology to the phenology of cyanobacterial blooms: implications for future climate change, Water Res., 46 (2012) 442-452.

[58] K.D. Joehnk, J. Huisman, J. Sharples, B. Sommeijer, P.M. Visser, J.M. Stroom, Summer heatwaves promote blooms of harmful cyanobacteria, Glob. Chang. Biol., 14 (2008) 495-512.

[59] Y.K. Lim, B.S. Park, J.H. Kim, S.-S. Baek, S.H. Baek, Effect of marine heatwaves on bloom formation of the harmful dinoflagellate Cochlodinium polykrikoides: Two sides of the same coin?, Harmful Algae, 104 (2021) 102029.

[60] J. Elliott, I. Jones, S. Thackeray, Testing the sensitivity of phytoplankton communities to changes in water temperature and nutrient load, in a temperate lake, Hydrobiologia, 559 (2006) 401-411.

[61] J.D. Brookes, G.G. Ganf, Variations in the buoyancy response of *Microcystis aeruginosa* to nitrogen, phosphorus and light, J. Plankton Res., 23 (2001) 1399-1411.

[62] B.W. Ibelings, L.R. Mur, A.E. Walsby, Diurnal changes in buoyancy and vertical distribution in populations of Microcystis in two shallow lakes, J. Plankton Res., 13 (1991) 419-436.

[63] J.C. Kromkamp, L.R. Mur, Buoyant density changes in the cyanobacterium Microcystis aeruginosa due to changes in the cellular carbohydrate content, FEMS Microbiol. Lett., 25 (1984) 105-109.

[64] R. Thomas, A. Walsby, Buoyancy regulation in a strain of *Microcystis*, Microbiology, 131 (1985) 799-809.

[65] D. Roelke, Y. Buyukates, Dynamics of phytoplankton succession coupled to species diversity as a system-level tool for study of *Microcystis* population dynamics in eutrophic lakes, Limnol. Oceanogr., 47 (2002) 1109-1118.

[66] G.M. Fragoso, G. Johnsen, M.S. Chauton, F. Cottier, I. Ellingsen, Phytoplankton community succession and dynamics using optical approaches, Cont. Shelf Res., 213 (2021) 104322.

[67] X. Wu, F. Kong, Effects of light and wind speed on the vertical distribution of *Microcystis aeruginosa* colonies of different sizes during a summer bloom, Int. Rev. Hydrobiol., 94 (2009) 258-266.

[68] X. Wu, F. Kong, Y. Chen, X. Qian, L. Zhang, Y. Yu, M. Zhang, P. Xing,

Horizontal distribution and transport processes of bloom-forming *Microcystis* in a large shallow lake (Taihu, China), Limnologica, 40 (2010) 8-15.

[69] R. Kurmayer, L. Deng, E. Entfellner, Role of toxic and bioactive secondary metabolites in colonization and bloom formation by filamentous cyanobacteria: Planktothrix, Harmful Algae, 54 (2016) 69-86.

[70] K.E. Havens, Cyanobacteria blooms: effects on aquatic ecosystems, Cyanobacterial harmful algal blooms: state of the science and research needs, (2008) 733-747.

[71] G.G. Ganf, Rates of oxygen uptake by the planktonic community of a shallow equatorial lake (Lake George, Uganda), Oecologia, 15 (1974) 17-32.

[72] H.W. Paerl, J. Huisman, Climate change: a catalyst for global expansion of harmful cyanobacterial blooms, Environmental microbiology reports, 1 (2009) 27-37.

[73] Z. Yang, M. Zhang, Y. Yu, X. Shi, Temperature triggers the annual cycle of *Microcystis*, comparable results from the laboratory and a large shallow lake, Chemosphere, 260 (2020) 127543.

[74] B.A. Whitton, M. Potts, The ecology of cyanobacteria: their diversity in time and space, Springer Science & Business Media2007.

[75] J. Huisman, R.R. Jonker, C. Zonneveld, F.J. Weissing, Competition for light between phytoplankton species: experimental tests of mechanistic theory, Ecology, 80 (1999) 211-222.

[76] J. Huisman, F.J. Weissing, Light-limited growth and competition for light in well-mixed aquatic environments: an elementary model, Ecology, 75 (1994) 507-520.

[77] J.R. Davis, K. Koop, Eutrophication in Australian rivers, reservoirs and estuaries–a southern hemisphere perspective on the science and its implications, Hydrobiologia, 559 (2006) 23-76.

[78] R.O. Carey, K.W. Migliaccio, Contribution of wastewater treatment plant effluents to nutrient dynamics in aquatic systems: a review, Environ. Manage., 44 (2009) 205-217.

[79] D.L. Jones, P. Cross, P.J. Withers, T.H. DeLuca, D.A. Robinson, R.S. Quilliam,

I.M. Harris, D.R. Chadwick, G. Edwardsjones, Nutrient stripping: the global disparity between food security and soil nutrient stocks, J. Appl. Ecol., 50 (2013) 851-862.

[80] J. Monod, Recherches sur la croissance des cultures bactériennes, (1942).

[81] M.B. Allen, D.I. Arnon, Studies on nitrogen-fixing blue-green algae. I. Growth and nitrogen fixation by Anabaena cylindrica Lemm, Plant Physiol., 30 (1955) 366.

[82] D.P. Hamilton, N. Salmaso, H.W. Paerl, Mitigating harmful cyanobacterial blooms: strategies for control of nitrogen and phosphorus loads, Aquat. Ecol., 50 (2016) 351-366.

[83] S. Baldia, A. Evangelista, E. Aralar, A. Santiago, Nitrogen and phosphorus utilization in the cyanobacterium *Microcystis aeruginosa* isolated from Laguna de Bay, Philippines, J. Appl. Phycol., 19 (2007) 607-613.

[84] V.H. Smith, Low nitrogen to phosphorus ratios favor dominance by blue-green algae in lake phytoplankton, Science, 221 (1983) 669-671.

[85] D.W. Schindler, R. Hecky, D. Findlay, M. Stainton, B. Parker, M. Paterson, K. Beaty, M. Lyng, S. Kasian, Eutrophication of lakes cannot be controlled by reducing nitrogen input: results of a 37-year whole-ecosystem experiment, Proceedings of the National Academy of Sciences, 105 (2008) 11254-11258.

[86] P.D. Reynolds, M. Hay, S.M. Camp, Global entrepreneurship monitor, Kansas City, Missouri: Kauffman Center for Entrepreneurial Leadership, (1999).

[87] L. Xie, P. Xie, S. Li, H. Tang, H. Liu, The low TN: TP ratio, a cause or a result of *Microcystis* blooms?, Water Res., 37 (2003) 2073-2080.

[88] R. Quirós, The relationship between nitrate and ammonia concentrations in the pelagic zone of lakes, Limnetica, 22 (2003) 37-50.

[89] J.G. Rueter, R.R. Petersen, Micronutrient effects on cyanobacterial growth and physiology, N. Z. J. Mar. Freshwater Res., 21 (1987) 435-445.

[90] S.E. Fitzwater, K.H. Coale, R.M. Gordon, K.S. Johnson, M.E. Ondrusek, Iron deficiency and phytoplankton growth in the equatorial Pacific, Deep Sea Research Part II: Topical Studies in Oceanography, 43 (1996) 995-1015.

[91] M.C. Lohan, D.W. Crawford, D.A. Purdie, P.J. Statham, Iron and zinc

enrichments in the northeastern subarctic Pacific: Ligand production and zinc availability in response to phytoplankton growth, Limnol. Oceanogr., 50 (2005) 1427-1437.

[92] D. Hindarti, A. Larasati, Copper (Cu) and Cadmium (Cd) toxicity on growth, chlorophyll-a and carotenoid content of phytoplankton Nitzschia sp, IOP Conference Series: Earth and Environmental Science, IOP Publishing, 2019, pp. 012053.

[93] D. Zhang, Z. Xu, S. Cao, K. Chen, S. Li, X. Liu, C. Gao, B. Zhang, Y. Zhou, An uncanonical CCCH-tandem zinc-finger protein represses secondary wall synthesis and controls mechanical strength in rice, Molecular plant, 11 (2018) 163-174.

[94] X. Deng, J. Yang, X. Wu, Y. Li, X. Fei, A C2H2 zinc finger protein FEMU2 is required for fox1 expression in *Chlamydomonas reinhardtii*, PLoS One, 9 (2014) e112977.

[95] K.J. Hammer, T. Kragh, K. Sand-Jensen, Inorganic carbon promotes photosynthesis, growth, and maximum biomass of phytoplankton in eutrophic water bodies, Freshw. Biol., 64 (2019) 1956-1970.

[96] M.R. Schock, D.A. Lytle, J.A. Clement, Effect of pH, DIC, orthophosphate and sulfate on drinking water cuprosolvency, National Risk Management Research Lab., Cincinnati, OH (United States), 1995.

[97] J. Shapiro, The role of carbon dioxide in the initiation and maintenance of blue-green dominance in lakes, Freshw. Biol., 37 (1997) 307-323.

[98] N. Rashid, W. Choi, K. Lee, Optimization of two-staged bio-hydrogen production by immobilized *Microcystis aeruginosa*, Biomass Bioenergy, 36 (2012) 241-249.

[99] B. Sánchez, S. Delgado, A. Blanco-Míguez, A. Lourenço, M. Gueimonde, A. Margolles, Probiotics, gut microbiota, and their influence on host health and disease, Mol. Nutr. Food Res., 61 (2017) 1600240.

[100] B. Yang, W. Cheung, J. Liu, Community mining from signed social networks, IEEE transactions on knowledge and data engineering, 19 (2007) 1333-1348.

[101] F.P. Healey, Interacting effects of light and nutrient limitation on the growth rate

of Synechococcus linearis (cyanophyceae) 1, J. Phycol., 21 (1985) 134-146.

[102] R.T. Sterner, L. Carpp, Psychomotor rehearsal: Enhancement of rotary-pursuit tracking using a massed-training procedure, Perceptual and Motor Skills, 44 (1977) 243-248.

[103] G.Y. Rhee, I.J. Gotham, The effect of environmental factors on phytoplankton growth: temperature and the interactions of temperature with nutrient limitation 1, Limnol. Oceanogr., 26 (1981) 635-648.

[104] M.E. Baird, S.M. Emsley, J.M. Mcglade, Modelling the interacting effects of nutrient uptake, light capture and temperature on phytoplankton growth, J. Plankton Res., 23 (2001) 829-840.

[105] WHO, Guideline Values for Cyanobacteria in Freshwater, World Health Organization, 1999.

[106] M.R. Droop, Vitamin B12 and marine ecology. IV. The kinetics of uptake, growth and inhibition in Monochrysis lutheri, J. Mar. Biol. Assoc. UK, 48 (1968) 689-733.

[107] E.A. Laws, M.S. Chalup, A microalgal growth model, Limnol. Oceanogr., 35 (1990) 597-608.

[108] C. Reynolds, A. Irish, J. Elliott, The ecological basis for simulating phytoplankton responses to environmental change (PROTECH), Ecol. Model., 140 (2001) 271-291.

[109] D. Lewis, J. Elliott, M. Lambert, C. Reynolds, The simulation of an Australian reservoir using a phytoplankton community model: PROTECH, Ecol. Model., 150 (2002) 107-116.

[110] D.M. Lewis, J.A. Elliott, J.D. Brookes, A.E. Irish, M.F. Lambert, C.S. Reynolds, Modelling the effects of artificial mixing and copper sulphate dosing on phytoplankton in an Australian reservoir, Lakes & Reservoirs: Research & Management, 8 (2003) 31-40.

Chapter 2 Effect of nitrogen limitation on the competition of *Microcystis* sp. and *Cyclotella meneghiniana* and improvement of growth model under low temperature

2.1 Introduction

The frequency of cyanobacterial bloom occurrence in freshwater has increased worldwide with the progress of eutrophication and rise in water temperature [1-3], resulting in serious water management problems [4]. Among several bloom-forming cyanobacterial species, the genus *Microcystis* has been usually observed to be dominant in the phytoplankton community [5, 6]. There have been many studies focusing on the influence of environmental factors on the growth of *Microcystis*, including nutrient concentration, light intensity, and temperature [7-9]. In order to predict *Microcystis* blooms and explore the method to inhibit them, several simulation models have been proposed [10-12]. Among the models, Chujo et al. [12] have recently developed a prediction model on the interspecific competition to predict the cell density of *Microcystis* and one of its competitor, the diatom *Cyclotella.* The model combined with the Droop model and the Lotka-Volterra model could accurately predict the cell density for both species under various nutrient concentrations and dilution rates with elapsed time, thereby predicting the probability of the *Microcystis* bloom occurrence. However, due to the lack of a temperature-related term in the model, the prediction could be performed only under a constant temperature of 25^{o}C.

Water temperature is an important factor, which can directly affect algal growth by altering their metabolic processes and nutrient uptake rate [13, 14]. It can also affect the cell size and volume [15, 16], then influence the dominance in the phytoplankton community. The occurrence of *Microcystis* blooms in field generally

has an annual seasonal cycle, mainly due to different water temperatures [17]. Lake Tega (35° 51′ N, 140° 02′ E) is a eutrophic freshwater lake with the worst water quality from 1974 to 2000 in Japan [18]. Before a large volume of water was transferred from the Tone River to this lake in 2000, *Microcystis* blooms broke out frequently from June to September, when the monthly average water temperature was in the range of 23°C to 30°C. After the water transfer in 2000, the monthly average water temperature in these months did not change very much, ranging from 25°C to 30°C. In comparison, from December to February, there was no record of *Microcystis* blooms and the average water temperature was between 3°C and 15°C [18]. Although the previously developed competition model could accurately predict the growth of *Microcystis* at a certain temperature, it is difficult to apply the model to actual lakes with changing water temperature, like Lake Tega, due to the lack of the temperature-related term.

In order to develop the temperature-related term, the temperature-dependent growth characteristics of *Microcystis* need to be understood. Ganf [19] has found that the preferable temperature range of *Microcystis* spp. growth was from 24°C to 34°C. Paerl and Huisman [20] also suggested that *Microcystis* spp. presented the maximal growth rate at 25°C or higher, and the increase in cells was always observed between 20°C and 30°C [21]. Moreover, the competition for nutrients and/or light among *Microcystis* and other phytoplankton (as competitors) was also affected by temperature, which would affect their inhibitory effect on the growth of *Microcystis* [13, 22, 23]. Thus, the temperature-dependent growth characteristics of the competitors are also important. Sugimoto et al. [24] have summarized the dominant algal species in Lake Tega from 1998 to 2014. It showed that after water transfer in 2000, *Cyclotella* (Thalassiosirales) has completely replaced the dominant position of *Microcystis*. Furthermore, the average biovolume ratio of *Microcystis* to *Cyclotella* in summer has changed from 47:9 at the highest before 2000, to 9:1561 in the last five years [18]. Thus, *Cyclotella* has been a major interspecific competitor against *Microcystis* in Lake Tega. The optimum temperature for the growth of *Cyclotella*

meneghiniana Kützing was suggested as 25°C by Shafik et al. [15] , and it could also grow within the temperature ranging from 10°C to 30°C. The above-mentioned studies have suggested several temperature-dependent growth characteristics of *Microcystis* and *Cyclotella*. Nevertheless, the relationship between the growth characteristics of the two species and temperatures has not been understood in detail. Due to this problem, the functional term regarding temperature can not be established.

This study aimed to examine the growth characteristics of *Microcystis* and *Cyclotella* at different water temperatures and establish a temperature-related term that is lacking in the previous interspecific competition model. In order to investigate the temperature-dependent growth patterns, *Microcystis* sp. and *C. meneghiniana* isolated from Lake Tega were used in batch monoculture experiments at different temperatures in laboratory. Based on the growth patterns obtained from monoculture experiments, the highest specific growth rate related to temperature and the corresponding temperature for each species were suggested. The coefficient ε reflecting the extent of the biovolume change affected by temperature has also been estimated for two species. Furthermore, cocultivation experiments of *Microcystis* sp. and *C. meneghiniana* were conducted at different temperatures to explore the inhibitory effect of coexisting species on *Microcystis*, and the interspecific dominant characteristics of the two species at low and high temperatures were discussed.

2.2 Materials and methods

2.2.1 Test algae and culture conditions

Microcystis sp. and *C. meneghiniana* isolated from Lake Tega using the capillary pipette technique [12] were used as the test algal species in this study. The cell shape of *Microcystis* sp. was assumed to be spherical. Cell diameter of *Microcystis* sp. was ca. 2-7 μm (2.7 μm as the mean value, n = 60) and the average volume of a cell was calculated to be 9.73 μm^3. On the other hand, the cell shape of *C. meneghiniana* was

observed by a scanning electron microscope (JSM-6510A, JEOL, Japan). The *C. meneghiniana* cell shape was cylindrical with an average diameter and height of 8.8 μm and 4.0 μm (n = 68), respectively. Thus, an average volume was obtained to be 243.35 μm^3. The cell size for both species was not largely changed within the experimental temperature range in the present study. Therefore, the average single-cell volume of both species was regarded as constant.

Each isolated species was separately inoculated into a 300 mL Erlenmeyer flask containing 100 mL fresh Wright's cryptophyte (WC) media [25] and subcultured. The solution pH was adjusted to 8.0 by adding 0.5 M hydrochloric acid and/or 0.5 M sodium hydroxide. Initial concentrations of nitrate-nitrogen (NO_3-N [below N]) and phosphate-phosphorus (PO_4-P [below P]) were 14.0 mg-N L^{-1} and 1.55 mg P L^{-1} by dissolving sodium nitrate ($NaNO_3$) and dipotassium hydrogen phosphate (K_2HPO_4), respectively. The carbon source was supplied by sodium hydrogen carbonate ($NaHCO_3$). The necessary element, silicon (Si), for the growth of diatom was adjusted to 11 mg L^{-1} by providing sodium metasilicate (Na_2SiO_3). The Si concentration was referred to the concentration in the Tone River water [18].

All the media were autoclaved at 121°C for 20 minutes to keep them sterile, and the inoculation of both species for subculture was performed in a clean bench to minimize bacterial contamination. The subculture was performed in an incubator (MTI-202, EYELA, Japan) at 25°C under a light intensity of 10,000 lux, measured by a light meter (LX-1102, Lutron, America), with 14 hours light / 10 hours dark cycle, and each flask was manually shaken three times a day. An aliquot of the subculture was transferred to the fresh autoclaved WC medium every 2 or 3 weeks.

2.2.2 Growth characteristics of *C. meneghiniana* and *Microcystis* sp. at different temperatures

Monoculture experiments under different temperatures were conducted to

explore the growth characteristics of *Microcystis* sp. and *C. meneghiniana*.

Considering the temperature range of Lake Tega in summer (*Microcystis* bloom outbreak period) as well as the preferable temperature range for the growth of *Microcystis* species (**Table 2-1**) and *C. meneghiniana*, the temperature of monoculture experiments for *Microcystis* sp. was set at 10°C, 20°C, 25°C, 30°C, 35°C, and 40°C. As for *C. meneghiniana*, it was set at 10°C, 20°C, 25°C, 30°C, and 35°C. Both species need to be precultured to adapt to different temperatures before the monoculture experiment, so as to eliminate the impact of sudden changes in the temperature. Each species was separately inoculated in 100 mL WC medium in a 300 mL Erlenmeyer flask and the initial cell density was adjusted to 1.0×10^4 cells mL^{-1}. The culture flasks were put into different temperature rooms of the same incubator. The preculture lasted for 7 days, after which each species was adapted to different temperatures. The other experimental conditions were the same as those in the subculture.

Table 2-1. Preferable temperature range of different *Microcystis* species.

Species	Temperature (°C)	Light intensity (μmol photons m^{-2} s^{-1})	Reference
M. aeruginosa	24-34	field study	Ganf (1974)
Microcystis spp.	28.8-30.5	20-33	Krüger and Eloff (1978)
M. wesenbergii	25-35	60	Imai et al. (2009)
M. aeruginosa	20-30	60	Imai et al. (2009)
M. ichthyoblabe	30-36	30-40	Mowe et al. (2015)
M. aeruginosa	27.5	169	You et al. (2018)

In the monoculture experiment, the precultured *Microcystis* sp. and *C. meneghiniana* at different temperatures were inoculated in 200 mL sterilized WC medium in a 300 mL Erlenmeyer flask and cultivated at the same temperature for the preculture. To eliminate the influence of the initial biovolume on the growth of each species, the initial cell densities of *Microcystis* sp. and *C. meneghiniana* were adjusted to 1.0×10^4 and 4.0×10^2 cells mL^{-1}, respectively, which were equivalent to the same

biovolume of around 1.0×10^5 μm^3 mL^{-1}. The other experimental conditions were the same as those in the subculture. Each experiment at different temperatures was conducted in triplicates.

The cell densities at 20°C and 25°C for both species were measured every half or one week. When the experimental temperatures were 30°C and 35°C, the cell density for *Microcystis* sp. was measured every two or three days, while for *C. meneghiniana* it was measured every one or two days. At 10°C, it was measured every five or eight days for both species. Measurement of *Microcystis* sp. cell density at 40°C was performed every one or two days. When the cell density increased logarithmically, the algal growth was regarded to enter logarithmical phase. When the cell density tended to be constant after the logarithmical phase, the algal growth was regarded to enter stationary phase. If the cell density decreased persistently in the following phase, the algal growth was supposed to enter decline phase. Batch monoculture experiments continued until the cells were saturated and/or became constant. The biovolume occupied by saturated cells at a certain temperature would be determined as the biovolume in saturation.

The specific growth rate (μ, day^{-1}), defined as the maximal daily growth rate at a certain temperature, is one of the important indicators to evaluate the growth characteristics for *Microcystis* sp. and *C. meneghiniana*. It was obtained at different temperatures from Eq. (1):

$$\mu = \frac{\ln C_2 - \ln C_1}{t_2 - t_1}, \quad (1)$$

where, C_1 and C_2 are the biovolume (μm^3 mL^{-1}) at t_1 (day) and t_2 (day), respectively. Both t_1 and t_2 are taken as the two time points at the period, which the maximal growth rate can be obtained at a certain temperature.

The highest temperature-dependent growth rate could be obtained from the peak point of the correlation curve of specific growth rates versus temperature drawn in Eq. (2), which was suggested by Ratkowsky et al. [26]:

$$\sqrt{\mu} = b\,(T - T_{min})\,\{1 - \exp[c(T - T_{max})]\}. \quad (2)$$

The parameter b is a constant of regression coefficient in the low temperature range and the c is the fit coefficient in the high temperature range. The estimated values were rounded to three decimal places. The temperature is expressed as T (°C) in Eq. (2) and the T_{min} (°C) and T_{max} (°C) are the extreme temperatures when the square root of the growth rate catches zero. When the value of T_{min} was over the freezing point of water, it could be a realizable temperature condition. Otherwise, it is just a conceptual temperature without metabolic significance [26].

The influential function term related to temperature on the algal biovolume can be presented in Eq. (3) proposed by Sugimoto et al. [27]:

$$f(T) = \left\{ \frac{T}{T_{optc}} \exp\left(1 - \frac{T}{T_{optc}}\right) \right\}^{\varepsilon}, \quad (3)$$

where, T (°C) and T_{optc} (°C) are the cultivation temperature and the optimum cultivation temperature depending on biovolume. The coefficient ε indicates the extent of the biovolume change affected by temperature.

The function f (T) was drawn using the biovolume in saturation at each temperature, and the ε values for each species were calculated by fitting the approximation curve of f (T) to biovolume and determined by taking the highest coefficient of determination (R^2). The higher is the value of the coefficient ε, the more the growth of each species biovolume will be affected by temperature, i.e. more sensitive to temperature. The value of T_{optc} was evaluated by the Gaussian regression formula presented in Eq. (4) as suggested by Tonner et al. [28]:

$$V_S = l \exp\left\{ -\left[\frac{(T-m)}{n} \right]^2 \right\}, \quad (4)$$

where, V_S (μm^3 mL^{-1}) is the biovolume in saturation of an algal species at a certain temperature, and l, m, and n are the correlation coefficients. When V_S reaches the maximum, the corresponding temperature can be determined as T_{optc}.

2.2.3 Cocultivation experiment of *C. meneghiniana* and *Microcystis* sp. at different temperatures

In order to explore the growth characteristics of two species when they grow together under various temperatures and the inhibition effect of *C. meneghiniana* on *Microcystis* sp. growth, the cocultivation experiments between *Microcystis* sp. and *C. meneghiniana* were conducted.

The experimental temperatures were set at 20^{o}C (low-temperature group) and 30^{o}C (high-temperature group). Both precultured species were cultivated together in 200 mL sterilized WC medium in a 300 mL flask. The initial cell densities were 1.0×10^{4} cells mL^{-1} for *Microcystis* sp. and 4.0×10^{2} cells mL^{-1} for *C. meneghiniana*, which occupied the same biovolume of around 1.0×10^{5} μm^{3} mL^{-1}. The other experimental conditions for both low-temperature and high-temperature groups were the same as the monoculture experiment. Each experiment was conducted in triplicates.

2.2.4 Measurements and statistical analyses

The culture flask was shaken uniformly, and 1 mL culture medium was taken out as a test sample. Then it was diluted appropriately and added to a plankton counting plate (MPC-200, Matsunami Glass Industry, Japan). An optical microscope (ECLIPSE E100, Nikon, Japan) was used to measure the cell density of samples. The biovolume was obtained by multiplying cell numbers with the average single-cell volume. The results of measurement for the same experimental group were presented as [average value] ± [standard deviation].

Regression analyses were conducted by software Origin 8.0 (Originlab Corporation, U.S.A.). Kruskal-Wallis test was performed via SPSS Statistics (IBM, U.S.A.), to measure the differences of experimental data at different temperatures.

When $p < 0.05$, the results were determined to be significantly different.

2.3 Results

2.3.1 Biovolume change of *C. meneghiniana* in monoculture experiments at different temperatures

The changes in the biovolume of *C. meneghiniana* during the growth period at different temperatures are shown in **Fig. 2-1**. The experimental results showed that *C. meneghiniana* could grow within the set experiment temperatures ranging from 10°C to 35°C.

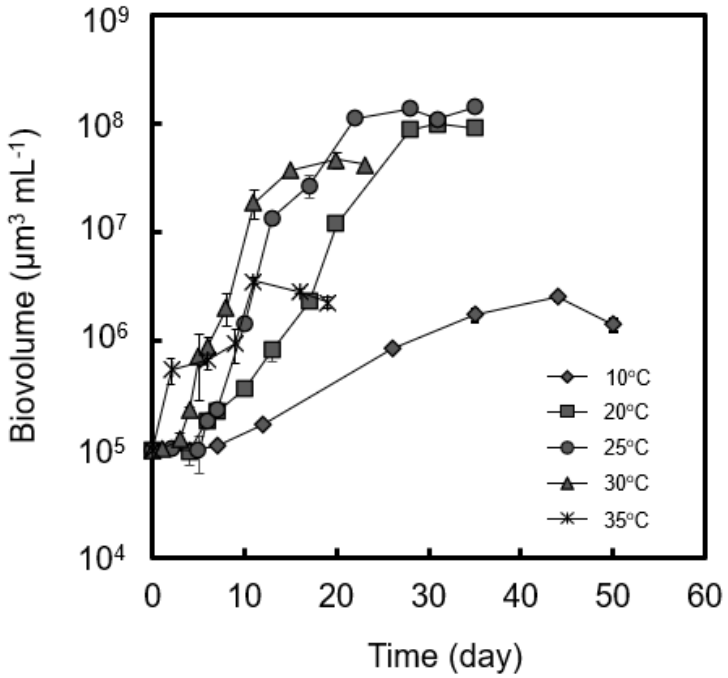

Fig. 2-1 Changes in biovolume of *C. meneghiniana* at different temperatures. Error bars present the standard deviations

From the growth curve, it can be observed that the biovolume of *C. meneghiniana* at 10°C did not increase as quickly as that of the other experimental groups. The biovolume reached saturation with $2.5\times10^6 \pm 2.1\times10^5$ μm³ mL^{-1} on day 44, and it decreased to $1.4\times10^6 \pm 2.0\times10^5$ μm³ mL^{-1} on day 50. On the other hand, the

biovolume at 30°C and 35°C reached saturation quickly on day 20 and day 16, respectively. Meanwhile, in the experimental groups at 20°C and 25°C, both biovolumes reached saturation on day 35.

Although the logarithmic phase in the 30°C experimental group was shorter than that in the 20°C and 25°C groups, the biovolume in saturation in the 30°C group was twice or three times lower than that in the above two groups. The maximum biovolume at 30°C was $4.6\times10^7 \pm 7.8\times10^6$ μm^3 mL^{-1}, and it was $9.7\times10^7 \pm 2.4\times10^6$ μm^3 mL^{-1} at 20°C and $1.4\times10^8 \pm 9.5\times10^6$ μm^3 mL^{-1} at 25°C. As for the 20°C and 25°C groups, the biovolume at 20°C was always higher than that at 25°C in the logarithmic phase. However, in the subsequent stationary phase, there was not much difference in the biovolume between the two groups ($p > 0.05$).

In comparison with other groups, the growth period of *C. meneghiniana* was quite short at 35°C. *C. meneghiniana* has entered the decline phase on day 19 and the biovolume in saturation was only $2.8\times10^6 \pm 1.6\times10^5$ μm^3 mL^{-1} measured on day 16.

2.3.2 Biovolume change of *Microcystis* sp. in monoculture experiments at different temperatures

The changes in the biovolume of *Microcystis* sp. during the culture experiment at different temperatures are shown in **Fig. 2-2**. It indicates that *Microcystis* sp. was more suitable to grow in the higher temperature groups of 25°C, 30°C and 35°C rather than the lower temperature groups of 10°C and 20°C.

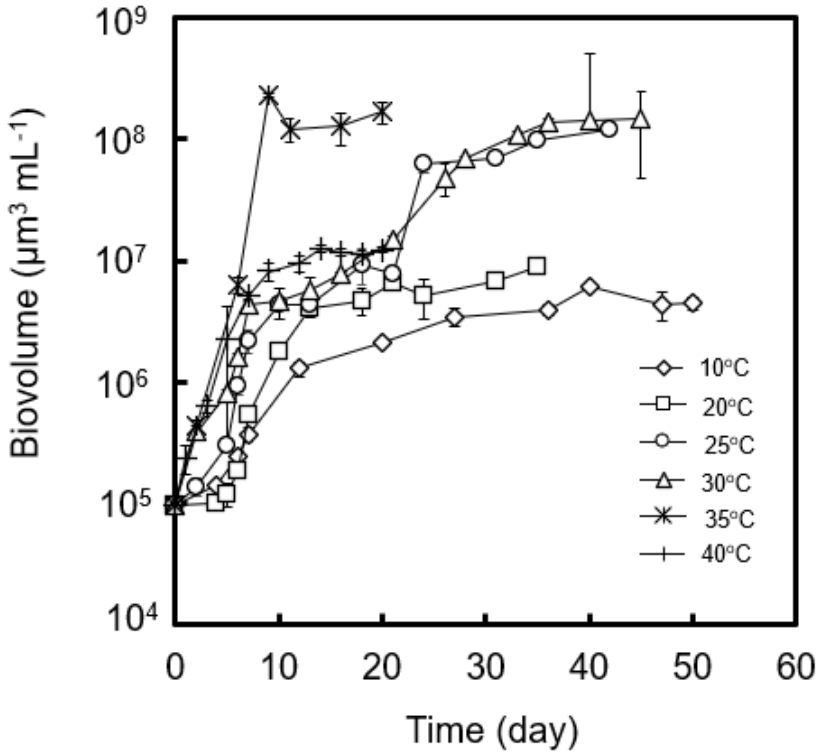

Fig. 2-2 Changes in biovolume of *Microcystis* sp. at different temperatures. Error bars represent the standard deviations

Microcystis sp. entered the logarithmic phase quickly after the beginning of the experiment at 30°C, 35°C and 40°C. During the logarithmic phase in the 35°C group, *Microcystis* sp. continued to grow and entered the stationary phase quickly within 11 days. The maximal biovolume at this temperature was recorded to be $2.3\times10^8 \pm 6.1\times10^6$ μm^3 mL^{-1} on day 9. Although *Microcystis* sp. in the 40°C group also entered the stationary phase quickly within 12 days, the maximal biovolume only reached $1.2\times10^7 \pm 6.8\times10^5$ μm^3 mL^{-1} on day 14, which was one order of magnitude lower than that in the 35°C group. Compared to the 35°C and 40°C groups, the logarithmic phase at 30°C lasted for a longer time, and *Microcystis* sp. continued to grow and entered the stationary phase at day 36. The maximal biovolume was $1.5\times10^8 \pm 9.8\times10^7$ μm^3 mL^{-1} in this group. At 25°C, *Microcystis* sp. reached the maximal biovolume of $1.2\times10^8 \pm 4.0\times10^6$ μm^3 mL^{-1}, which was less than that at 30°C, but still in the same order of magnitude.

However, when it comes to the 10°C and 20°C groups, the biovolume growth has

been suppressed compared to the higher temperature groups. In these two groups, the biovolume almost did not increase in the first 5 days. When it entered the logarithmic phase, the biovolume in the 20°C group was similar to that in the 25°C group ($p > 0.05$). However, the logarithmic phase at 20°C did not last for a long period, then *Microcystis* sp. entered the stationary phase quickly at day 18, after which the biovolume almost no longer increased. The maximum biovolume in the 20°C group was $8.8\times10^6 \pm 1.5\times10^5$ μm^3 mL^{-1}, which was about two orders of magnitude lower than that in the 25°C and 30°C groups.

In the 10°C group, the logarithmic phase was short and the growth curve began to flatten from day 12. The biovolume did not reach saturation until day 50 with the value of $4.4\times10^6 \pm 5.0\times10^5$ μm^3 mL^{-1}, which was only two orders of magnitude higher than that of the initial value.

2.3.3 Determination of growth parameters of *C. meneghiniana* and *Microcystis* sp. at different temperatures

Table 2-2 pointed out the specific growth rate, μ, calculated by Eq. (1) for both species at different temperatures. The minimum and maximal specific growth rate values of *C. meneghiniana* obtained from monoculture experiments were 0.10 ± 0.003 day^{-1} at 10°C and 0.63 ± 0.012 day^{-1} at 30°C, while those of *Microcystis* sp. were 0.15 ± 0.003 day^{-1} at 10°C and 0.62 ± 0.013 day^{-1} at 35°C.

Table 2-2. Specific growth rates of *C. meneghiniana* and *Microcystis* sp. at different temperatures.

	Specific growth rate, μ (day^{-1})	
Temperature (°C)	*C. meneghiniana*	*Microcystis* sp.
10	0.10±0.003	0.15±0.003
20	0.35±0.003	0.44±0.003
25	0.62±0.029	0.43±0.008
30	0.63±0.012	0.49±0.002
35	0.21±0.019	0.62±0.013
40	-	0.43±0.008

The μ values at each temperature for *C. meneghiniana* were substituted into Eq. (2) for linear regression analysis to obtain the coefficients. Then, the correlation curve of growth rate and temperature could be drawn as shown in **Fig. 2-3** with a dashed line and the fitting formula is expressed as:

$$\sqrt{\mu} = 0.031\ (T + 0)\ \{1 - \exp[0.272(T - 37)]\}. \quad (5)$$

According to the correlation curve, the highest temperature-dependent growth rate for *C. meneghiniana* was estimated to be 0.64 day^{-1}, and its corresponding temperature was 29°C. Coefficient of determination (R^2) was 0.98, which indicated that the correlation curve describes 98% variability of growth rate.

Similarly, the same procedure was adapted to *Microcystis* sp. to obtain each parameter. In **Fig. 2-3**, the correlation curve (R^2 = 0.88) was drawn in a solid line, and the fitting formula is indicated below:

$$\sqrt{\mu} = 0.015\ (T + 20)\ \{1 - \exp[0.561(T - 43)]\}. \quad (6)$$

The highest temperature-dependent growth rate and the corresponding temperature for *Microcystis* sp. was obtained as 0.65 day^{-1} and 37°C, respectively. Both the correlation curves for each species were fitted well ($p < 0.05$).

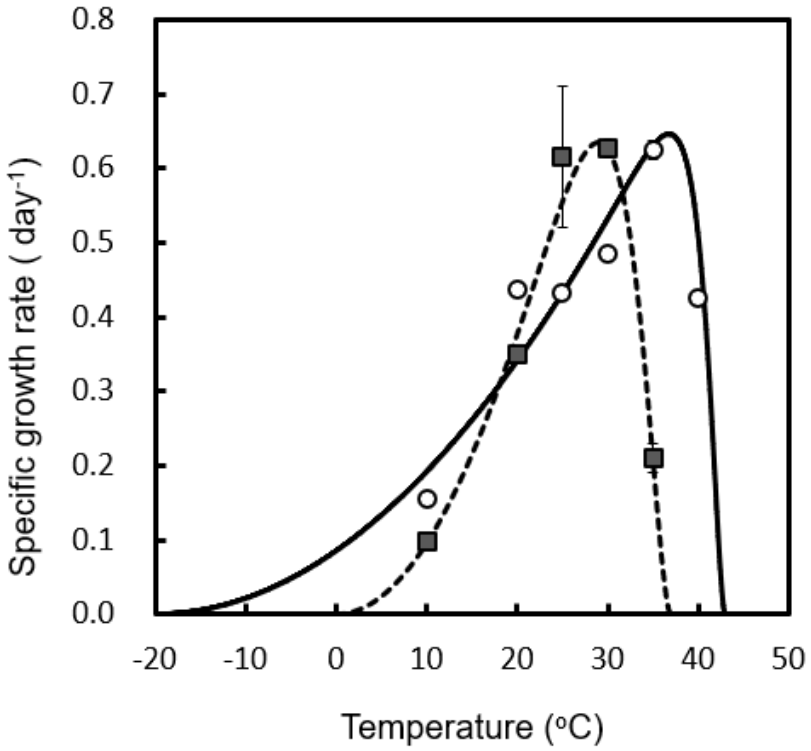

Fig. 2-3 Specific growth rates for *C. meneghiniana* (filled square) and *Microcystis* sp. (open circle) as a function of temperature. Dashed curve presents the calculated specific growth rate by Eq. (2) for *C. meneghiniana* and solid curve presents that for *Microcystis* sp. Error bars represent the standard deviations

The biovolume values of *C. meneghiniana* and *Microcystis* sp. in saturation at different temperatures are depicted in **Fig. 2- 4**.

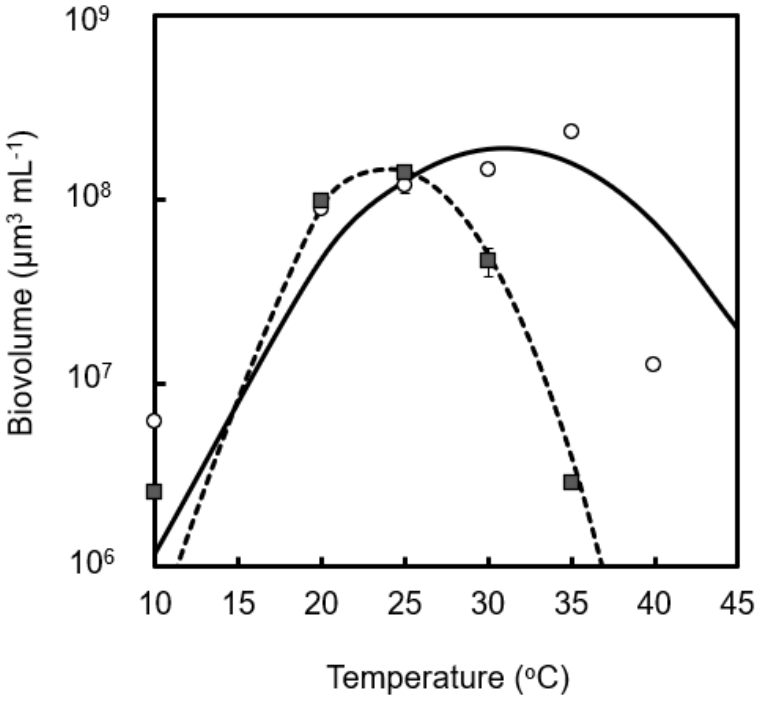

Fig. 2-4 The biovolume of *C. meneghiniana* (filled square) and *Microcystis* sp. (open circle) in saturation in different monoculture experiment groups. Dashed curve presents the correlated curve fitted by Eq. (3) for *C. meneghiniana* and solid curve presents that for *Microcystis* sp. Error bars represent the standard deviations

The biovolume values of *C. meneghiniana* were fitted to Eq. (4) by regression analysis to evaluate the coefficients and obtained the fitting formula as:

$$V_S = 1.48 \times 10^8 \exp\left\{-\left[\frac{(T-24)}{5.8}\right]^2\right\}. \quad (7)$$

The correlation curve for *C. meneghiniana* was depicted by dashed line in **Fig. 2-4** which can fit the biovolume well ($R^2 = 0.99$). Based on Eq. (7), when T was 24°C, V_S reached the maximal value to be 1.5×10^8 μm^3 mL^{-1}. Thus, T_{optc} for *C. meneghiniana* was determined as 24°C.

In the same way, the fitting formula for *Microcystis* sp. was derived to be:

$$V_S = 1.91 \times 10^8 \exp\left\{-\left[\frac{(T-31)}{9.4}\right]^2\right\}. \quad (8)$$

The correlation curve for *Microcystis* sp. was drown in solid line in **Fig. 2-4** with R^2 = 0.65. It portrayed that *Microcystis* sp. reached the maximal biovolume of 1.9×10^8 μm^3

mL^{-1} at 31°C, which temperature can be determined to be T_{optc} for *Microcystis* sp.

Using the maximum biovolume data for *C. meneghiniana* and *Microcystis* sp., the relationship between $f(T)$ and temperature is represented in **Fig. 2-5**.

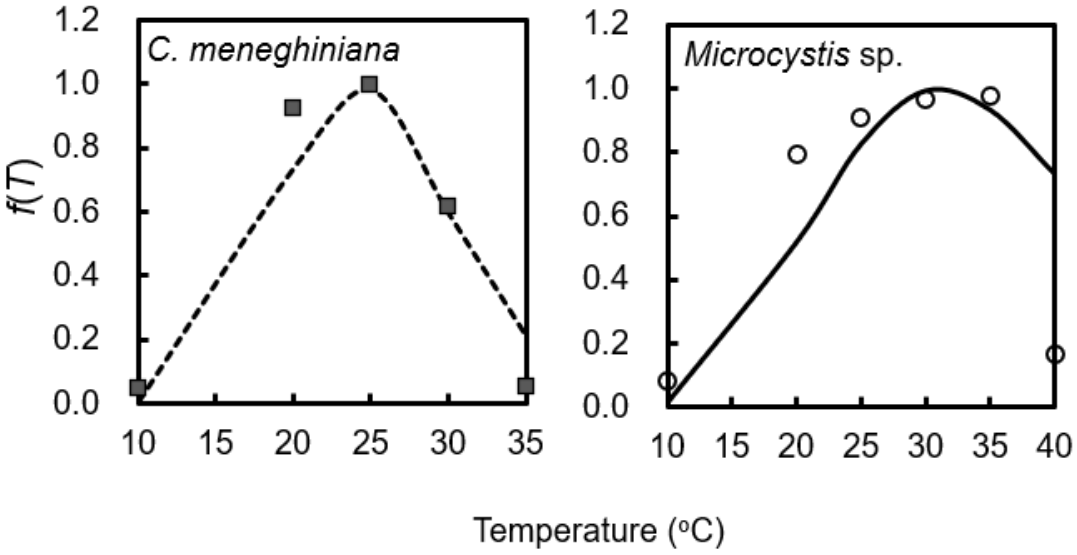

Fig. 2-5 The function term related to temperature ($f(T)$) and the correlation function term on the biovolume in saturation of *C. meneghiniana* (filled square) and *Microcystis* sp. (open circle). Dashed- and solid- curves present the approximation curve ($f(T)$) for *C. meneghiniana* and *Microcystis* sp., respectively

The ε values for *C. meneghiniana* and *Microcystis* sp. were calculated to be 19.4 (R^2 = 0.94, $p < 0.05$) and 8.7 (R^2 = 0.82, $p < 0.05$) and the corresponding approximation curves were depicted as dashed and solid line, respectively.

Since the coefficient ε and T_{optc} for the two species have been determined, the temperature related term $f(T)$ for *C. meneghiniana* was established as:

$$f(T) = \left\{\frac{T}{24}\exp\left(1-\frac{T}{24}\right)\right\}^{19.4}, \quad (9)$$

that for *Microcystis* sp. was:

$$f(T) = \left\{\frac{T}{31}\exp\left(1-\frac{T}{31}\right)\right\}^{8.7}. \quad (10)$$

2.3.4 Dominant characteristics of *Microcystis* sp. and *C. meneghiniana* in cocultivation experiment at different temperatures

Fig. 2-6 depicts the growth characteristics of *C. meneghiniana* and *Microcystis* sp. in the low- and high-temperature groups in the cocultivation experiment.

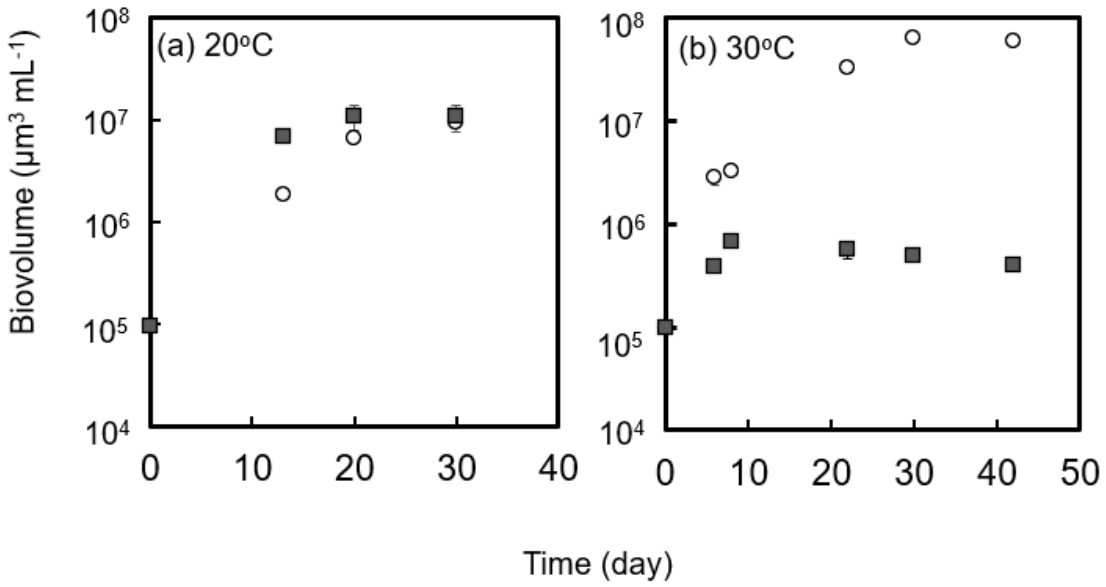

Fig. 2-6 Biovolume of *C. meneghiniana* (filled square) and *Microcystis* sp. (open circle) in cocultivation experiments at (a) 20°C and (b) 30°C with elapsed time. Error bars represent the standard deviations

The biovolume occupied by *C. meneghiniana* was not much different from that by *Microcystis* sp. in the low temperature group (20°C) during the whole cultivation period (p = 0.317). The biovolume of *C. meneghiniana* reached saturation with $1.1\times10^7 \pm 3.2\times10^6$ μm^3 mL^{-1} on day 30, while that of *Microcystis* sp. was $9.5\times10^6 \pm 5.2\times10^5$ μm^3 mL^{-1}. Compared to *Microcystis* sp., the biovolume of *C. meneghiniana* always slightly took advantage in the cultivation period. In the high-temperature group, the dominant species, defined as the species occupying the largest biovolume among a phytoplankton community, was opposite; *C. meneghiniana* showed low

biovolume throughout the cultivation period, whereas *Microcystis* sp. grew well and dominated until the end of the experiment. In the cocultivation experiment at 30°C, *Microcystis* sp. had a longer logarithmic growth phase than the monoculture experiment and entered the stational phase on day 30 with the biovolume of $6.5\times10^7 \pm 5.3\times10^6$ μm^3 mL^{-1} in saturation. Meanwhile, the biovolume of *C. meneghiniana* had already declined and entered the decline phase from day 22. The biovolume values in saturation for both *Microcystis* sp. and *C. meneghiniana* were lower than those in the monoculture at 30°C, which indicated the inhibition effect of the two species to each other.

2.4 Discussion

Changes in water temperature have different effects on cyanobacteria and diatoms [29-31]. In this study, *C. meneghiniana* and *Microcystis* sp. isolated from Lake Tega showed different temperature-dependent growth characteristics and sensitivities. Based on their growth characteristics, the highest temperature-dependent growth rates of the two species were obtained. The present study also suggested the optimum temperature and coefficient ε values for each species. These values are required to establish a temperature-related term for the development of the algal prediction model.

The higher sensitivity of temperature, which indicates the growth rate curve was steeper, for *C. meneghiniana* could be observed in low temperature ranges. The simulation results showed that *C. meneghiniana* and *Microcystis* sp. reach their highest growth rate at 29°C and 37°C, respectively. The simulation curves in **Fig. 2-3** displayed that the increase in the μ value with temperature change for *C. meneghiniana* at temperatures lower than 29°C was greater than that of *Microcystis* sp. at temperatures lower than 37°C. The higher regression coefficient b (b = 0.031) in low temperature range of Eq. (2) for *C. meneghiniana* could support this result. On the contrary, as for *Microcystis* sp. at the temperature higher than 37°C, the μ value

decreased more sharply with the rise in temperature until up to $T_{max,}$ compared with that for *C. meneghiniana* at the temperature higher than 29°C. The higher regression coefficient c (c = 0.561) in high temperature range for *Microcystis* sp. would cause this difference in growth rate of the two species.

The curves in **Fig. 2-3** also displayed that the conceptual growth temperature range determined by T_{min} and T_{max} for *C. meneghiniana* was narrower (0°C-37°C) than that for *Microcystis* sp. (-20°C-43°C), which implies the temperature-sensitivity of *C. meneghiniana*. However, the values of T_{min} for each species were lower than or equal to the freezing point of water. That is, the T_{min} values for *C. meneghiniana* and *Microcystis* sp. were 0°C and -20°C, respectively, indicating that these values have no biological significance [26]. The wide growth temperature range of *Microcystis* has also been discussed in several studies. Krüger and Eloff [32] suggested that the upper temperature limit of *Microcystis* was between 35°C to 40°C, which is consistent with our simulated result that the highest growth rate of *Microcystis* sp. was evaluated at 37°C. On the other hand, the persistence of *Microcystis* blooms could be still observed even below 10°C in Lake Taihu, China [33]. The temperature-sensitive characteristics of *C. meneghiniana* has been mentioned by Xu, Jiang, Juneau and Qiu [34] as well. The growth rate only increased in the temperature range between 14°C and 20°C, and Mitrovic, Hitchcock, Davie and Ryan [29] portrayed that the growth rate has decreased at 28°C.

The μ can only reflect the growth speed during the logarithmic phase, and it is hard to evaluate the subsequent growth trend. Moreover, Lehman, Boyer, Satchwell and Waller [35] examined the effect of temperature on the growth of *M. aeruginosa* by the maximum cell density in different seasons in field. Thus, the algal growth should be evaluated by not only the single index of growth rate, but also algal yield such as the biovolume in saturation, which is an essential index for evaluation at different temperatures.

The coefficient ε in Eq. (3) can further corroborate the sensitivity related to temperature for each species. The ε value for *C. meneghiniana* was obtained to be

19.4, which was more than twice higher than that (ε = 8.7) for *Microcystis* sp. It conveyed that the biovolume of *C. meneghiniana* in saturation was more sensitive to the change in temperature than *Microcystis* sp.

The previously developed competition model [12] could be presented by the following equation:

$$\frac{dC}{dt} = f(N, P, D), \tag{11}$$

where, *C* and *t* are the cell density and time, respectively. The *f* (*N, P, D*) means the function of nutrient (nitrogen and phosphorus) concentrations and dilution rate (*D*). With the established additional term *f* (*T*) for *C. meneghiniana* and *Microcystis* sp. in Eq. (9) and Eq. (10), the lack of temperature-related term in the previous competition model could be expected to be modified.

The result of cocultivation experiment at 20°C displayed that, compared with *Microcystis* sp., *C. meneghiniana* maintained a higher cell density during the 30 days experimental period. Even if *C. meneghiniana* dominated only with a weak advantage, it has still suppressed the dominance of *Microcystis* sp. Furthermore, the biovolume of *Microcystis* sp. in saturation at 20°C was nearly 10 times lower than that in the monoculture experiment at the same temperature, indicating that *C. meneghiniana* could inhibit the growth of *Microcystis* sp. effectively. These results are consistent with the field observation in Lake Tega when the temperature is lower than 20°C, where there were nearly no *Microcystis* blooms [18].

At higher temperatures (≥ 30°C), the growth of *C. meneghiniana* has been highly inhibited. The weakness against high temperature for the genus *Cyclotella* was mentioned by Butterwick, Heaney and Talling [36] as well. They highlighted that *C. pseudostelligera* could sustain a number of cells at 20°C and 25°C, but no growth occurred at 30°C. Shafik, Herodek, Vörös, Présing and Kiss [15] also portrayed the weak growth of the genus *Cyclotella* at temperatures higher than 25°C. Furthermore, as shown in **Fig. 2-6**, *C. meneghiniana* almost did not proliferate in the cocultivation experiment at 30°C, while *Microcystis* sp. had higher value in biovolume. McQueen and Lean [37] and Robarts and Zohary [38] proposed that cyanobacteria, especially

the genus *Microcystis*, will dominate at temperatures above 25°C, which was consistent with the results obtained in the present study.

Ultimately, no matter based on temperature effect on the specific growth rate or biovolume, *C. meneghiniana* always showed higher sensitivity to temperature in experimental results. If treatment measures for *Microcystis* blooms were taken at lower temperature seasons, the inhibitory effect would be more significant. In Lake Tega, the treatment measures should be taken before June, when the monthly average temperature is lower than 23°C [18].

Although the present study simulated the natural light cycle (light and dark circle), the light intensity given to different experimental groups was all the same. In the case of a natural lake, as the seasonal temperature changes, the light intensity must also change. As one of the important factors influencing algal growth, the light intensity will definitely have a significant effect on the growth, affecting the formation of *Microcystis* blooms [9, 39, 40]. In the future study, temperature and light intensity can be combined to study their influences on the coculture of *C. meneghiniana* and *Microcystis* sp.

2.5 Summary

The results of monoculture experiments for *C. meneghiniana* and *Microcystis* sp. at various temperatures showed different responses. Compared with *Microcystis* sp., *C. meneghiniana* had superior growth in low temperature conditions (10°C and 20°C), while *Microcystis* sp. grew better at high temperatures (25°C, 30°C, and 35°C). As demonstrated by the growth rate prediction as a function of temperature, *Microcystis* sp. had the highest temperature-dependent growth rate of 0.65 day^{-1} at 37°C, meanwhile that of *C. meneghiniana* was 0.64 day^{-1} at 29°C. The coefficient ε value reflecting the extent of the biovolume change affected by temperature for *C. meneghiniana* was 19.4 and that for *Microcystis* sp. was 8.7, indicating that *C. meneghiniana* was more sensitive to temperature compared to *Microcystis* sp. These

characteristics related to temperature would affect the dominance of the two species when they grow together, thereby affecting the formation of *Microcystis* blooms. *C. meneghiniana* dominated in the low temperature group (20^{o}C) in the cocultivation experiment, while in the high temperature group (30^{o}C) *C. meneghiniana* was remarkably inhibited by *Microcystis* sp. The dominant characteristics were consistent with the results of monoculture experiments and the predictions of growth rate characteristics. These characteristics can be used to establish the temperature-related term that enhances the accuracy of the previously developed interspecific competition model, so as to construct more effective methods to inhibit *Microcystis* blooms.

References

[1] P.M. Visser, J.M. Verspagen, G. Sandrini, L.J. Stal, H.C. Matthijs, T.W. Davis, H.W. Paerl, J. Huisman, How rising CO_2 and global warming may stimulate harmful cyanobacterial blooms, Harmful Algae, 54 (2016) 145-159.

[2] P. Lehman, T. Kurobe, S. Lesmeister, D. Baxa, A. Tung, S.J. Teh, Impacts of the 2014 severe drought on the *Microcystis* bloom in San Francisco Estuary, Harmful Algae, 63 (2017) 94-108.

[3] Z. Duan, X. Tan, K. Parajuli, S. Upadhyay, D. Zhang, X. Shu, Q. Liu, Colony formation in two *Microcystis morphotypes*: Effects of temperature and nutrient availability, Harmful Algae, 72 (2018) 14-24.

[4] H. Imai, K.-H. Chang, M. Kusaba, S.-i. Nakano, Temperature-dependent dominance of *Microcystis* (Cyanophyceae) species: *M. aeruginosa* and *M. wesenbergii*, J. Plankton Res., 31 (2009) 171-178.

[5] M.J. Harke, M.M. Steffen, C.J. Gobler, T.G. Otten, S.W. Wilhelm, S.A. Wood, H.W. Paerl, A review of the global ecology, genomics, and biogeography of the toxic cyanobacterium, *Microcystis* spp., Harmful Algae, 54 (2016) 4-20.

[6] L. Sampognaro, K. Eirín, G.M. de la Escalera, C. Piccini, A. Segura, C. Kruk, Experimental evidence on the effects of temperature and salinity in morphological traits of the *Microcystis aeruginosa* complex, J. Microbiol. Methods, 175 (2020) 105971.

[7] S. Ninio, A. Lupu, Y. Viner-Mozzini, T. Zohary, A. Sukenik, Multiannual variations in *Microcystis* bloom episodes–Temperature drives shift in species composition, Harmful Algae, 92 (2020) 101710.

[8] Y. Amano, K. Takahashi, M. Machida, Competition between the cyanobacterium *Microcystis aeruginosa* and the diatom *Cyclotella* sp. under nitrogen-limited condition caused by dilution in eutrophic lake, J. Appl. Phycol., 24 (2012) 965-971.

[9] J.C. Nzayisenga, X. Farge, S.L. Groll, A. Sellstedt, Effects of light intensity on growth and lipid production in microalgae grown in wastewater, Biotechnology for

Biofuels, 13 (2020) 1-8.

[10] N. Fujimoto, R. Sudo, N. Sugiura, Y. Inamori, Nutrient-limited growth of *Microcystis aeruginosa* and *Phormidium tenue* and competition under various N: P supply ratios and temperatures, Limnol. Oceanogr., 42 (1997) 250-256.

[11] M. Mikawa, K. Sugimoto, Y. Amano, M. Machida, F. Imazeki, Competitive growth characteristics between *Microcystis aeruginosa* and *Cyclotella* sp. accompanying changes in river water inflow and their simulation model, Phycol. Res., 64 (2016) 123-132.

[12] M. Chujo, J. Li, T. Datta, Y. Amano, M. Machida, A competitive growth model for the simulation of cyanobacterial blooms under eutrophic conditions, Environ. Eng. Sci., 38 (2021) 15-23.

[13] A.M.d.A. Gomes, M. Lürling, Temperature effect on exploitation and interference competition among *Microcystis aeruginosa*, *Planktothrix agardhii* and, *Cyclotella meneghiniana*, The Scientific World Journal, 2015 (2015).

[14] M.A. Mowe, C. Porojan, F. Abbas, S.M. Mitrovic, R.P. Lim, A. Furey, D.C. Yeo, Rising temperatures may increase growth rates and microcystin production in tropical *Microcystis* species, Harmful Algae, 50 (2015) 88-98.

[15] H. Shafik, S. Herodek, L. Vörös, M. Présing, K. Kiss, Growth of *Cyclotella meneghiniana* Kutz. I. Effects of temperature, light and low rate of nutrient supply, Annales de Limnologie-International Journal of Limnology, EDP Sciences, 1997, pp. 139-147.

[16] T. Zohary, T. Fishbein, M. Shlichter, L. Naselli-Flores, Larger cell or colony size in winter, smaller in summer–a pattern shared by many species of Lake Kinneret phytoplankton, Inland Waters, 7 (2017) 200-209.

[17] I. Schlegel, W. Scheffler, Seasonal development and morphological variability of *Cyclotella ocellata* (Bacillariophyceae) in the eutrophic Lake Dagow (Germany), Int. Rev. Hydrobiol., 84 (1999) 469-478.

[18] Chiba Prefectural Government, Water quality for lakes in Chiba prefecture, Chiba city, Chiba Prefectural Government, 2019.

[19] G.G. Ganf, Rates of oxygen uptake by the planktonic community of a shallow equatorial lake (Lake George, Uganda), Oecologia, 15 (1974) 17-32.

[20] H.W. Paerl, J. Huisman, Climate change: a catalyst for global expansion of harmful cyanobacterial blooms, Environmental microbiology reports, 1 (2009) 27-37.

[21] Z. Yang, M. Zhang, Y. Yu, X. Shi, Temperature triggers the annual cycle of *Microcystis*, comparable results from the laboratory and a large shallow lake, Chemosphere, 260 (2020) 127543.

[22] P. Zhang, C. Zhai, X. Wang, C. Liu, J. Jiang, Y. Xue, Growth competition between *Microcystis aeruginosa* and *Quadrigula chodatii* under controlled conditions, J. Appl. Phycol., 25 (2013) 555-565.

[23] L. Lei, J. Dai, Q. Lin, L. Peng, Competitive dominance of *Microcystis aeruginosa* against *Raphidiopsis raciborskii* is strain-and temperature-dependent, Knowledge & Management of Aquatic Ecosystems, (2020) 36.

[24] K. Sugimoto, Y. Negishi, Y. Amano, M. Machida, F. Imazeki, Roles of dilution rate and nitrogen concentration in competition between the cyanobacterium *Microcystis aeruginosa* and the diatom *Cyclotella* sp. in eutrophic lakes, J. Appl. Phycol., 28 (2016) 2255-2263.

[25] R.R. Guillard, C.J. Lorenzen, Yellow-green algae with chlororhyllide c 1,2, J. Phycol., 8 (1972) 10-14.

[26] D. Ratkowsky, R. Lowry, T. McMeekin, A. Stokes, R. Chandler, Model for bacterial culture growth rate throughout the entire biokinetic temperature range, J. Bacteriol., 154 (1983) 1222-1226.

[27] R. Sugimoto, K. Kitagawa, S. Nishi, H. Honda, M. Yamada, S. Kobayashi, J. Shoji, S. Ohsawa, M. Taniguchi, O. Tominaga, Phytoplankton primary productivity around submarine groundwater discharge in nearshore coasts, Mar. Ecol. Prog. Ser., 563 (2017) 25-33.

[28] P.D. Tonner, C.L. Darnell, B.E. Engelhardt, A.K. Schmid, Detecting differential growth of microbial populations with Gaussian process regression, Genome Res., 27 (2017) 320-333.

[29] S.M. Mitrovic, J.N. Hitchcock, A.W. Davie, D.A. Ryan, Growth responses of *Cyclotella meneghiniana* (Bacillariophyceae) to various temperatures, J. Plankton Res., 32 (2010) 1217-1221.

[30] X. Liu, X. Lu, Y. Chen, The effects of temperature and nutrient ratios on *Microcystis* blooms in Lake Taihu, China: an 11-year investigation, Harmful Algae, 10 (2011) 337-343.

[31] J. You, K. Mallery, J. Hong, M. Hondzo, Temperature effects on growth and buoyancy of *Microcystis aeruginosa*, J. Plankton Res., 40 (2018) 16-28.

[32] G. Krüger, J. Eloff, The effect of temperature on specific growth rate and activation energy of *Microcystis* and *Synechococcus* isolates relevant to the onset of natural blooms, Journal of the Limnological Society of Southern Africa, 4 (1978) 9-20.

[33] J. Ma, B. Qin, H.W. Paerl, J.D. Brookes, N.S. Hall, K. Shi, Y. Zhou, J. Guo, Z. Li, H. Xu, The persistence of cyanobacterial (*Microcystis* spp.) blooms throughout winter in Lake Taihu, China, Limnol. Oceanogr., 61 (2016) 711-722.

[34] K. Xu, H. Jiang, P. Juneau, B. Qiu, Comparative studies on the photosynthetic responses of three freshwater phytoplankton species to temperature and light regimes, J. Appl. Phycol., 24 (2012) 1113-1122.

[35] P. Lehman, G. Boyer, M. Satchwell, S. Waller, The influence of environmental conditions on the seasonal variation of *Microcystis* cell density and microcystins concentration in San Francisco Estuary, Hydrobiologia, 600 (2008) 187-204.

[36] C. Butterwick, S. Heaney, J. Talling, Diversity in the influence of temperature on the growth rates of freshwater algae, and its ecological relevance, Freshw. Biol., 50 (2005) 291-300.

[37] D. McQueen, D. Lean, Influence of water temperature and nitrogen to phosphorus ratios on the dominance of blue-green algae in Lake St. George, Ontario, Can. J. Fish. Aquat. Sci., 44 (1987) 598-604.

[38] R.D. Robarts, T. Zohary, Temperature effects on photosynthetic capacity, respiration, and growth rates of bloom-forming cyanobacteria, N. Z. J. Mar. Freshwater Res., 21 (1987) 391-399.

[39] C. Sorokin, R.W. Krauss, The Effects of Light Intensity on the Growth Rates of Green Algae, Plant Physiol., 33 (1958) 109.

[40] R. Foy, C. Gibson, R. Smith, The influence of daylength, light intensity and temperature on the growth rates of planktonic blue-green algae, British Phycological Journal, 11 (1976) 151-163.

Chapter 3 Growth competition model improvement overcome the overestimation of nutrient uptake under low temperature

3.1 Introduction

The occurrence of harmful cyanobacterial blooms recently has kept rising with the eutrophication problem globally [1, 2]. Cyanobacterial blooms can cause various water quality problems, including unpleasant odor and taste in potable water and toxin productions [3]. Among coexisting species in phytoplankton community, the dominance of beneficial algae can suppress the outbreak of harmful cyanobacterial blooms [4]. It is therefore vital to understand the growth characteristics of algae to predict their proliferation in advance, and thereby develop efficient treatment to suppress the harmful cyanobacterial blooms by promoting the algal species successions. There are many environmental factors affecting the successions of dominant species. As one of them, nutrient concentrations were considered to be an important factor [5, 6]. Various nutrient uptake tendencies which will affect interspecific competition leading to species succession [7-9]. Understanding the patterns of nutrient uptake by algae is essential to predict the proliferation of cyanobacteria and its coexisting species.

The relationship between nutrient concentrations and algal growth is commonly characterized by Monod model, Michaelis-Menten model, and Droop model. These models describe the growth rate as a function of dissolved and intracellular nutrient concentrations [10-12]. Meanwhile, the limitation of applicability of these models has also been frequently noticed by several studies. Sommer [13] mentioned the doubtable applicability of Monod model in the early stage of algal growth, in which the cell would uptake extra nutrients for the subsequent growth stage. This kind of excessive uptake can lead the Monod model to invalidate. Moreover, although the applicability of the Monod model was extensively warranted under steady state conditions such as

chemostat culture system, it occasionally failed because the model was empirically derived and can not fit exactly growth patterns for all species [14, 15]. The inappropriacy of the Michaelis-Menten model has been also discussed by Lee et al. [16]. They investigated the uptake kinetics of *Microcystis aeruginosa* for different categories of nitrogen sources: although the *M. aeruginosa* adsorption kinetics of urea could be well described with the Michaelis-Menten model, the adsorption kinetic of ammonium (NH_4^+) and nitrate (NO_3^-) were hard to be endorsed to fit accurately by this model. In the Droop model, the measured intracellular nutrient concentrations are necessary as an independent variable, and the techno difficulties of the measurements have considered an obstacle to evaluate the accuracy of model prediction [14, 17]. There have been some studies focused on the revision of these classical models to improve the accuracy of algal prediction and species succession [14, 18, 19]. However, these modifications were derived depending on the growth and uptake patterns of one and/or some certain algal species measured in experiments. Therefore, whether the modified models could be utilized to predict the growth and nutrient uptake of some algae in various actual lakes still need to be verified experimentally.

In Lake Tega (35° 51′ N, 140° 02′ E), Japan, the water quality was the worst from 1974 to 2000. The nitrogen and phosphorus concentrations were emphasized as the major nutrients that limit algal proliferation and affect the lake trophic status [1, 20, 21]. The total nitrogen (TN) and total phosphorus (TP) concentrations in lake water have been recorded in the range from 4.0-5.3 mg L^{-1} and 0.21-0.33 mg L^{-1} during 1995-1999, respectively [22], and the lake water was always plagued by cyanobacterial blooms (mainly the genus *Microcystis*). However, after a large amount of water transferred from the Tone River to Lake Tega, whose water quality was better than Lake Tega, the genus *Cyclotella* (Thalassiosirales) has become the dominant algal species instead of *Microcystis* [23] since 2000. The TN and TP concentrations has decreased to 2.01 mg L^{-1} and 0.14 mg L^{-1} in average in year 2017-2022, and the biovolume ratio of *Microcystis* to *Cyclotella* was evolved from 47:9 at the highest in year 1999 to 9:1561 in average in year 2017-2022 [24]. In order to predict the algal species succession and investigate the appropriate environmental condition for

Microcystis suppression, Chujo et al. [3] developed a competition growth model combined with the Droop [25] and the Lotka-Volterra model by estimating the growth patterns of *Microcystis* sp. and its main competitor *Cyclotella meneghiniana* in semi-continuous experiments. This model was utilized to predict the cell density and growth trend for both *Microcystis* sp. and *C. meneghiniana* under different nitrate-nitrogen (NO_3-N [hereafter N]) and phosphate-phosphorus (PO_4-P [hereafter P]) concentrations and dilution rates at any time point. Nevertheless, the predicted values of nutrient uptake amounts always displayed overestimation compared with experimental results.

In this model, the relationship between the dissolved nutrient concentrations and growth rates was always taken to follow the Michaelis-Menten hyperbolic relationship, which may cause the overestimation. Even with the discrepancy in predicted values of the nutrient uptake, the model could be still utilized effectively to predict the growth trend of *Microcystis* sp. and *C. meneghiniana* at 25^{o}C in Lake Tega, where the cyanobacterial blooms were frequently observed. However, when it comes to the lower temperature of 20^{o}C, the deficiency was accentuated and made the cell density prediction lose validity. This discrepancy would cause the predicted results to not always fit the actual data well. However, cyanobacterial blooms have also been seen in June in Lake Tega, when the average temperature was 21.5^{o}C (Chiba Prefectural Government 2019). It means that the lake still suffers the risk of cyanobacterial bloom appearance under low temperature.

In order to improve this deficiency, it was aimed to explore a new nutrient uptake term and introduce it to the previous model, to improve the overestimation of cyanobacterial cells under low temperature during a long term cultivation. Batch monoculture experiments were conducted for *Microcystis* sp. and *C. meneghiniana* at low temperature of 20^{o}C in laboratory to investigate the growth and nutrient uptake patterns. Based on the results obtained from monoculture experiments, the relationship between dissolved nutrient concentrations and growth rate in long term cultivation was estimated. Cocultivation experiments between *Microcystis* sp. and *C. meneghiniana* were also conducted at 20^{o}C under different N concentrations and

dilution rates to explore the effect of these factors on the interspecific competition and species succession. Furthermore, a new species interaction coefficient between the two algal species was derived to improve the previous model as demonstrated by the cocultivation experiments. The applicability of the developed model was tested by comparing the new prediction values with experimental values. The coefficient of determination (R^2) for prediction was calculated and compared with the previous one which was calculated from the previous model, to test the accuracy of the new predicted values. Under the utilization of the developed model, the efficient nitrogen concentrations and dilution rates to suppress *Microcystis* sp. proliferation in Lake Tega was suggested.

3.2 Materials and methods

3.2.1 Experimental algae and culture conditions

The algal species used in this chapter were *Microcystis* sp. and *C. meneghiniana* as test algae, which were collected and isolated from Lake Tega, Japan [3]. The size of both species was remarkably different, and the average cell volumes for *Microcystis* sp. and *C. meneghiniana* were 9.73 μm^3 and 243.35 μm^3, respectively [24]. And the changes in individual algal cell's size during cultivation did not change the dominant species, which took larger total biovolume, between co-cultivated algal species. Therefore, the single-cell volume for both species were assumed to be invariant.

For subculture, each isolated alga was separately inoculated into sterilized 100 mL of Wright's cryptophyte (WC) medium [26] in a 300 mL Erlenmeyer flask separately. The WC medium used here was all sterilized by autoclaving at 121^oC for 20 minutes before inoculation, and 0.5 M hydrochloric acid and/or sodium hydroxide was used to accommodate the pH of medium to 8.0. The sodium nitrate ($NaNO_3$) and dipotassium hydrogen phosphate (K_2HPO_4) were dissolved to adjust the initial N and

P concentrations to 14.0 mg-N L^{-1} and 1.55 mg-P L^{-1}, respectively. Sodium hydrogen carbonate ($NaHCO_3$) and sodium metasilicate (Na_2SiO_3) were also added as the carbon source and silicon source. As the necessary element for proliferation of *C. meneghiniana*, the silicon (Si) concentration in media was adjusted to 11 mg-Si L^{-1} referring to the silicon (Si) concentration in Tone River water [22].

The subculture cultivation was incubated in an incubator (MTI-202, EYELA, Japan) under 25°C. After light meter (LX-1102, Lutron, America) measurement, the light intensity was remained to be 10000 lux. The turnover cycle of light was 14 hours-light and 10 hours-dark. Every 2 or 3 weeks, the sub-cultured *Microcystis* sp. and *C. meneghiniana* were reinoculated in fresh sterilized medium. Sampling and inoculation were all performed in a clean bench to prevent bacterial contamination.

3.2.2 Growth characteristics and nutrient uptake patterns of *Microcystis* sp. and *C. meneghiniana*

Batch monoculture experiments for *Microcystis* sp. and *C. meneghiniana* at the low temperature of 20°C were conducted to explore the nutrient uptake and growth characteristics for both two species at the low temperature of 20°C.

Before the monoculture experiment, both species were precultured at 20°C for 7 days to adapt them to the cultivation temperature. In the preculture, nitrogen- and phosphorus- free WC medium was used to deplete the intracellular N and P content. The two species were separately inoculated in 100 mL WC medium in a 300 mL Erlenmeyer flask. The initial cell density for both species were 1.0×10^4 cells mL^{-1}. Cultivation conditions were the same as those in subculture.

In the monoculture experiment, the precultured *Microcystis* sp. and *C. meneghiniana* were inoculated into 200 mL WC medium in a 300 mL Erlenmeyer flask at 20°C. The initial cell densities of *Microcystis* sp. and *C. meneghiniana* were adjusted to 1.0×10^4 and 4.0×10^2 cells mL^{-1}, respectively. The inoculation with the different cell density was needed to adjust the same biovolume of around 1.0×10^5 μm^3 mL^{-1}, which could eliminate the effect of initial biovolume on the growth of each

species. Each experimental group was conducted. in triplicates. Other experimental conditions were the same as those in the subculture experiment.

In order to measure the growth characteristics of the two species, the cell densities in each flask were measured every 3 or 5 days. Batch monoculture experiments continued until the cell densities were saturated and/or constant. The dissolved N and P concentrations of medium in each flask were measured every 7 days to obtain the nutrient uptake characteristics for both two species. The measurement of nutrient concentration also continued until the cell densities became saturation.

Growth characteristics and nutrient uptake of the two species were obtained by measuring cell densities and dissolved nutrient concentrations in monoculture experiments with the following equations. The growth rate (μ, day^{-1}) was calculated in Eq. (1), which is an important indicator to evaluate the algal growth characteristics.

$$\mu = \frac{\ln C_2 - \ln C_1}{t_2 - t_1}, \quad (1)$$

where, C_1 and C_2 are the cell densities (cells mL^{-1}) at day t_2 and t_1 (days) respectively.

The maximum specific growth rate μ_{max} (day^{-1}) and the half saturation constant $K\mu$ (mg L^{-1}) was obtained following the Monod equation in Eq. (2) with various nutrient concentrations (S, mg L^{-1}):

$$\mu = \mu_{max} \frac{S}{K_\mu + S}. \quad (2)$$

The assimilated nutrients by algal cell defined as cell quota Q (pg cell^{-1}) was determined by the nutrient concentration quotient change and relating cell density C as shown in Eq. (3):

$$Q = \frac{S_0 - S}{C}, \quad (3)$$

where, S_0 (mg L^{-1}) is the initial nutrient concentration.

The minimum amount of cell quota $Q_{\min}$ (pg cell^{-1}) was calculated by the conventional quota type control developed from Droop equation by John and Flynn [27]:

$$\mu = \mu'_{max} \frac{Q - Q_{min}}{(Q - Q_{min}) + K_Q}, \quad (4)$$

where, μ'_{max} (day^{-1}) is the cell quota depending on the maximum growth rate, and the K_Q is the half saturations constant on cell quota concentration. Similarly, the maximum amount of cell quota Q_{max} (pg cell^{-1}) could be derived with μ_{max} from Eq. (4), which also obeys the following equation [28]:

$$\mu_{max} = \mu'_{max} \frac{Q_{max} - Q_{min}}{(Q_{max} - Q_{min}) + K_Q}, \quad (5)$$

The nutrient uptake rate from cultivation nutrient ρ (pg cell^{-1} day^{-1}) can be estimated by the change in nutrient concentrations change ΔS (mg L^{-1}) caused by cell growth with elapsed time Δt (day) like shown in Eq. (6):

$$\rho = \frac{\Delta S}{C \Delta t}. \quad (6)$$

In some certain short term cultivation period, such as the beginning of cultivation experiments, the relationship between nutrient uptake rate and nutrient concentrations can be simulated using the Michaelis-Menten equation:

$$\rho = \rho_{max} \frac{S}{S + K_\rho}, \quad (7)$$

where K_ρ is the half-saturation constant for nutrient uptake. ρ_{max}^{lo} was estimated at the period of biovolume density reaching saturated and K_ρ^{lo} is the corresponding half-saturation constant, while ρ_{max}^{hi} and K_ρ^{hi} were obtained at the start of experiment.

Sunda, Shertzer and Hardison [14] have proved that the nutrient uptake rate was not only affected by the dissolved nutrient concentrations in long term cultivation. The nutrient uptake rate of cell will change to zero at a certain nutrient concentration, but the concentration will not always be zero. Meanwhile, from the experiments results, it can be observed when growth rate μ trends to decrease, the nutrient uptake rate ρ will decrease with it. Lim et al. [29] have derived the change of growth rate with various cell density:

$$\frac{\mathrm{d}C}{\mathrm{d}t} = \mu_c C[1 - \frac{\mathrm{C}}{K_C}], \quad (8)$$

where K_C is the saturated cell density limited by environmental capacity. Therefore, combine the effect of cell density on the nutrient uptake rate, the cultivation nutrient uptake rate in long-term can be limited by cell density as Eq. (9):

$$\rho = \rho_{max} \frac{S}{S + K_\rho}(1 - \frac{C}{K_C}), \quad (9)$$

Furthermore, Morel [28] indicated that the maximum nutrient uptake rate in long-term cultivation is related to intracellular nutrient contents (cell quota), and the ρ_{max} and K_ρ are decided following Eq. (10) and (11):

$$\rho_{max} = {\rho_{max}}^{hi} - ({\rho_{max}}^{hi} - {\rho_{max}}^{lo}) \frac{Q - Q_{min}}{(Q_{max} - Q_{min})} \quad (10)$$

$$K_\rho = {K_\rho}^{hi} - ({K_\rho}^{hi} - {K_\rho}^{lo}) \frac{Q - Q_{min}}{(Q_{max} - Q_{min})} \quad (11)$$

3.2.3 Cocultivation experiment for *Microcystis* sp. and *C. meneghiniana*

In order to explore the growth and nutrient uptake characteristics of *Microcystis* sp. and *C. meneghinina* and their interaction when they were cultured together under low temperature, cocultivation experiments were conducted.

The experimental conditions for cocultivation experiments were prepared in different groups as shown in **Table 3-1**. The experimental temperatures were controlled to be in low temperature of 20°C. Since nitrogen is the key nutrient element to cause eutrophication and cyanobacterial blooms, the N concentrations in cocultivation experiments was set to be 0.5, 1, 5 and 10 mg L^{-1} to measure the nutrient effect on species competition under low temperature. Different daily renewal rates *d* (% day^{-1}) were also set to be 5% and 15% to explore the completed effect combined with nutrient change.

The experiments were cultivated in stable incubator with semi-continuous culture system. To derive the corresponding dilution rate *D* (% day^{-1}) of *d* in continues culture system as actual lake, the Eq. (12) [30] was used:

$$D = \ln \frac{100}{100 - d} \times 100. \quad (12)$$

After precultured, both *Microcystis* sp. and *C. meneghiniana* were inoculated in 200 mL sterilized and N adjusted WC medium in a 300 mL flask. In order to exclude the effect of initial biovolume, the initial cell density for *Microcystis* sp. was 1.0×10^4 cells mL^{-1} and that for *C. meneghiniana* was 4.0×10^2 cells mL^{-1}, which occupied the

same biovolume of around 1.0×10^5 $\mu m^3\,mL^{-1}$. Other experimental conditions in each group were the same as those in monoculture experiments. The cell densities and dissolved nutrient concentrations were measured directly, and the measuring frequency was also the same as that of monoculture experiments. The other parameters were derived with the above-mentioned equations.

Table 3-1 Conditions of cocultivation experiments

Group	Light intensity (lx)	Temperature (°C)	Nitrate concentrations (mg/L)	Phosphate concentrations (mg/L)	Daily renewal rate (%)
1	10000	20	0.5	1.55	5
2			1.0		
3			5.0		
4			10.0		
5			0.5		15
6			1.0		
7			5.0		
8			10.0		

To measure the effect of *Microcystis* sp. and *C. meneghiniana* on each other, the interspecific reaction rate (α) was calculated by the Lotka-Volterra equation in Eq. (13) and (14):

$$K_{\mathrm{A}} = C_{A'} + \alpha_{\mathrm{AB}} C_{B'}\,, \tag{13}$$

$$K_{\mathrm{B}} = C_{\mathrm{B}''} + \alpha_{B\mathrm{A}} C_{\mathrm{A}''}\,, \tag{14}$$

where K_{A} (cells mL^{-1}) and K_{B} (cells mL^{-1}) are the environmental capacity of *Microcystis* sp. and *C. meneghiniana*, respectively. This parameter was determined by the maximum cell densities of a species in one flask in monoculture experiments. When the cell density of *Microcystis* sp. reached saturation in cocultivation

experiment, the cell densities of *Microcystis* sp. and *C. meneghiniana* are $C_{A'}$ (cells mL^{-1}) and $C_{B'}$ (cells mL^{-1}) respectively, and the corresponding α_{AB} represent the effect of *C. meneghiniana* growth on *Microcystis* sp. Similarly, $C_{B''}$ (cells mL^{-1}) and $C_{A''}$ (cells mL^{-1}) are the cell density of *C. meneghiniana* and *Microcystis* sp., respectively, when the saturated cell density of *C. meneghiniana* was reached in cocultivation experiment with *Microcystis* sp., and α_{BA} reflects the effect from *Microcystis* sp.

3.2.4 Growth competition model

Based on the previous developed model [3], a new growth competition model was established by the improvement of nutrient uptake term (**Table 3-2**), which can apply to only the excessive nutrient uptake prediction of algal cell in long term cultivation. Since the growth rate μ was decided by the cell quota of assimilated nutrients [25], the limiting nutrient for growth was decided by the relationship between the ratio of Q_N:Q_P and the optimal N:P ratio, which was determined from the ratio of Q_{Nmin}:Q_{Pmin}. When the value of Q_N:Q_P is higher than the optimal N:P ratio, the growth limiting nutrient is P. In contrast, the growth of algal cell is limited by N when the value of Q_N:Q_P is lower than the optimal N:P ratio.

The calculation for the model followed a fourth-order form of the Runge-Kutta method, and the time step was set as Δt = 0.01 day. The growth predictions for both of the two species were simulated under the same conditions in cocultivation experiments as shown in **Table 3-1**, to investigate the accuracy of model prediction. After the verification of the accuracy, the growth of *Microcystis* sp. was simulated under various N concentrations and daily renewal rates with a sufficient P concentration, based on which the effective treatments to control *Microcystis* blooms were discussed.

Table 3-2 Model equations used in this chapter

State variable	Model of each state variable
N concentration	$\frac{dN}{dt} = -C_A \frac{\rho_{NA,max} N}{K_{NA}+N}(1-\frac{C_A}{K_{CA}}) - C_B \frac{\rho_{NB,max} N}{K_{NB}+N}(1-\frac{C_B}{K_{CB}}) + D(N_0 - N)$
P concentration	$\frac{dP}{dt} = -C_A \frac{\rho_{PA,max} P}{K_{PA}+P}(1-\frac{C_A}{K_{CA}})(1-\frac{Q_{PA}}{Q_{PA,max}}) - C_B \frac{\rho_{PB,max} P}{K_{PB}+P}(1-\frac{C_B}{K_{CB}}) + D(P_0 - P)$
Cell quota of assimilated N of *Microcystis* sp.	$\frac{dQ_{NA}}{dt} = \frac{\rho_{NA,max} N}{K_{NA}+N}\left(1-\frac{C_A}{K_{CA}}\right) - \left[\mu'_{NA,max}\left(\frac{Q_{NA}-Q_{NA,min}}{Q_{NA}-Q_{NA,min}+K_{QNA}}\right), \mu'_{PA,max}\left(\frac{Q_{PA}-Q_{PA,min}}{Q_{PA}-Q_{PA,min}+K_{QPA}}\right)\right]^{*}\left(1-\frac{C_A{}' - \alpha_{AB} C_B{}'}{K_A}\right) Q_{NA}$
Cell quota of assimilated N of *C.meneghiniana*	$\frac{dQ_{NB}}{dt} = \frac{\rho_{NB,max} N}{K_{nB}+N}(1-\frac{C_B}{K_{CB}}) - \left[\mu'_{NA,max}\left(\frac{Q_{NA}-Q_{NA,min}}{Q_{NA}-Q_{NA,min}+K_{QNA}}\right), \mu'_{pA,max}\left(\frac{Q_{PA}-Q_{PA,min}}{Q_{PA}-Q_{PA,min}+K_{QPA}}\right)\right]^{**}(1-\frac{C_B{}'' - \alpha_{BA} C_A{}''}{K_B}) Q_{NB}$
Cell quota of assimilated P of *Microcystis* sp.	$\frac{dQ_{PA}}{dt} = \frac{\rho_{PA,max} P}{K_{PA}+P}(1-\frac{C_A}{K_{CA}})(1-\frac{Q_{PA}}{Q_{PA,max}}) - \left[\mu'_{NA,max}\left(1-\frac{Q_{NA,min}}{Q_{NA}}\right), \mu'_{PA,max}\left(1-\frac{Q_{PA,min}}{Q_{PA}}\right)\right]^{*}(1-\frac{C_A{}' - \alpha_{AB} C_B{}'}{K_A}) Q_{PA}$
Cell quota of assimilated P of *C.meneghiniana*	$\frac{dQ_{PB}}{dt} = \frac{\rho_{PB,max} P}{K_{PB}+P}(1-\frac{C_B}{K_{CB}}) - \left[\mu'_{NB,max}\left(\frac{Q_{NB}-Q_{NB,min}}{Q_{NB}-Q_{NB,min}+K_{QNB}}\right), \mu'_{pB,max}\left(\frac{Q_{PB}-Q_{PB,min}}{Q_{PB}-Q_{PB,min}+K_{QPB}}\right)\right]^{**}(1-\frac{C_B{}'' - \alpha_{BA} C_A{}''}{K_B}) Q_{PB}$
Cell density of *Microcystis* sp.	$\frac{dC_A}{dt} = \left\{\left[\mu'_{NA,max}\left(\frac{Q_{NA}-Q_{NA,min}}{Q_{NA}-Q_{NA,min}+K_{QNA}}\right), \mu'_{pA,max}\left(\frac{Q_{PA}-Q_{PA,min}}{Q_{PA}-Q_{PA,min}+K_{QPA}}\right)\right]^{*}\left(1-\frac{C_A{}' - \alpha_{AB} C_B{}'}{K_A}\right) - D\right\} C_A$
Cell density of *C.meneghiniana*	$\frac{dC_B}{dt} = \left\{\left[\mu'_{NB,max}\left(\frac{Q_{NB}-Q_{NB,min}}{Q_{NB}-Q_{NB,min}+K_{QNB}}\right), \mu'_{pB,max}\left(\frac{Q_{PB}-Q_{PB,min}}{Q_{PB}-Q_{PB,min}+K_{QPB}}\right)\right]^{**}\left(1-\frac{C_B{}'' - \alpha_{BA} C_A{}''}{K_B}\right) - D\right\} C_B$

***In case of *Microcystis* sp.,**

If the Q_{nA}:Q_{pA} ratio is higher than the optimum N:P ratio (= 2.7): $\mu'_{pA,max}\left(\frac{Q_{pA}-Q_{pA,min}}{Q_{pA}-Q_{pA,min}+K_{QpA}}\right)$

if not: $\mu'_{NA,max}\left(\frac{Q_{NA}-Q_{NA,min}}{Q_{NA}-Q_{NA,min}+K_{QNA}}\right)$

****In case of *C. meneghiniana*,**

If the Q_{nB}:Q_{pB} ratio is higher than the optimum N:P ratio (= 3.4): $\mu'_{pB,max}\left(\frac{Q_{pB}-Q_{pB,min}}{Q_{pB}-Q_{pB,min}+K_{QpB}}\right)$ if not:

$\mu'_{NB,max}\left(\frac{Q_{NB}-Q_{NB,min}}{Q_{NB}-Q_{NB,min}+K_{QNB}}\right)$

3.2.5 Measurements and statistical analysis

An optical microscope (ECLIPSE E100, Nikon, Japan) was used to measure the cell density by counting appropriately diluted test sample in a plankton counting plate (MPC-200, Matsunami Glass Industry, Japan). The biovolume was obtained by multiplying cell numbers with the average single-cell volume. The results of triplicate for the same experimental group were presented as [average value] ± [standard deviation].

Regression analyses were conducted by software Python 3.10.6. Kruskal-Wallis test was performed using SPSS Statistics (IBM, America) to measure the differences of experimental data at different experimental groups. Coefficient of determination (R^2) was calculated to measure the prediction accuracy. When $p < 0.05$, the results were determined to be significantly different.

3.3 Results

3.3.1 Growth and nutrient uptake characteristics of *Microcystis* sp. and *C. meneghiniana* under low temperature

The change of biovolume and dissolved nutrient (N and P) concentrations of the two species in cultivation were shown in **Fig. 3-1**. The different growth and nutrient adsorption characteristics of *Microcystis* sp. and *C. meneghiniana* at low temperature can be observed from the curves in this figure.

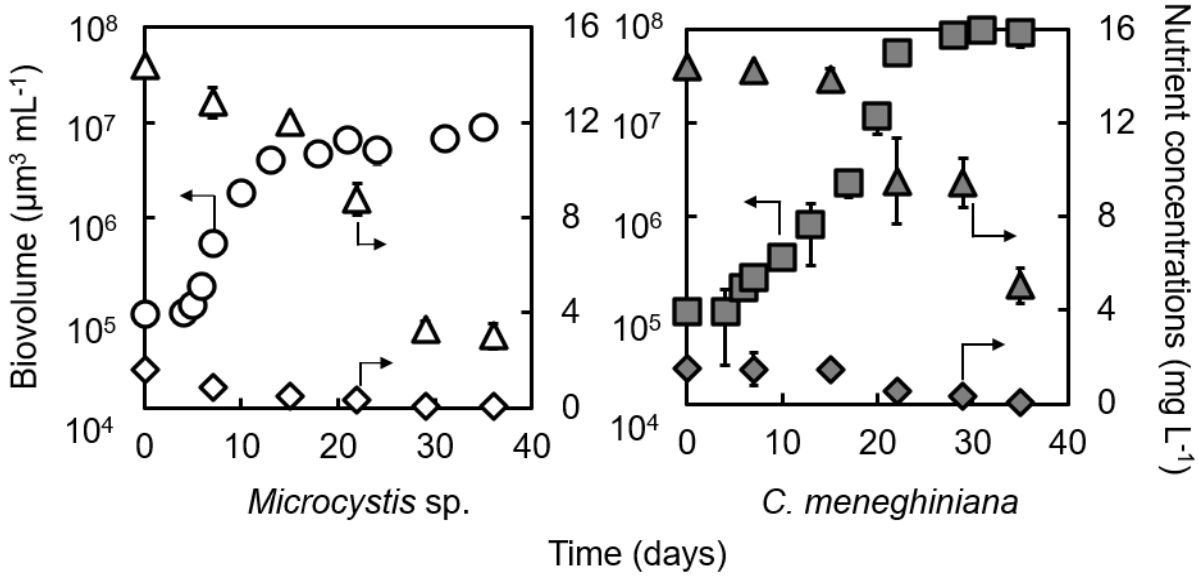

Fig. 3-1 Growth curves of *Microcystis* sp. and *Cyclotella meneghiniana* and nutrient concentrations change in monoculture experiments. The open circle presents the cell densities for *Microcystis* sp. and the filled square presents that for *Cyclotella meneghiniana*. The open and filled triangle presents the nitrate concentrations in the monoculture experiment for *Microcystis* sp. and *Cyclotella meneghiniana*, respectively. The open and filled diamond presents the phosphate concentrations in the monoculture experiment for *Microcystis*

sp. and *Cyclotella meneghiniana*, respectively.

At 20°C, the growth of *Microcystis* sp. cell entered into the exponential growth phase from day 3 and lasted until day 13 with the highest growth rate μ of 0.882 ± 0.030 day^{-1}. The cell density finally reached saturation, which determined as K_A, at day 35 occupying the biovolume of $1.01\times10^7 \pm 1.21\times10^6$ μm^3 mL^{-1}. The concentration of P decreased faster at the first measured time point (day 7 and day 14) than that in the following phase, and it decreased to 0.050 ± 0.002 mg mL^{-1} at the end of experiment (day 36). Meanwhile, the N concentration decreased to the final concentration of 3.021 ± 0.001 mg mL^{-1} at day 36.

C. meneghiniana entered into the exponential growth phase from day 4 at the same conditions, and the phase lasted to day 20 with the highest growth rate μ of 0.681± 0.121 day^{-1}. At day 31, the cell density reached saturation with the biovolume of $9.734\times10^7 \pm 1.09\times10^6$ μm^3 mL^{-1}, that is K_B, the environmental capacity of *C. meneghiniana*. Therefore, the interaction coefficient α_{AB} in 20°C was calculated to be 0.175, while α_{BA} was 1.334. Both the concentrations of N and P decreased with cell growth to 5.05 ± 0.17 mg mL^{-1} and 0.06 ± 0.0035 mg mL^{-1}, respectively, at the end of experiment.

Other growth and uptake parameters for *Microcystis* sp. and *C. meneghiniana* were then calculated and summarized in **Table 3-3**. The μ_{max} related to dissolved N concentration for *Microcystis* sp. was 6 times as high as that for *C. meneghiniana*, while the cell quota limiting growth rate of *Microcystis* sp. was nearly the same as that of *C. meneghiniana*. The low maximum N uptake rate ρ_{max}^{lo} for *Microcystis* sp. was only one-tenth of that for *C. meneghiniana*, but the ρ_{max}^{hi} obtained from the beginning of experiment for the two species were not much different.

Table 3-3 Parameters for the competition growth model which referred to last chapter

Parameter	*Microcystis* sp.	*C. meneghiniana*	*Microcystis* sp.	*C. meneghiniana*
	Nitrogen		Phosphorus	
Growth parameters				
μ_{max} (day^{-1})	0.267	0.381	0.383	1.170
K_μ (mg L^{-1})	7.62	1.22	4.64	2.59
Cell quota parameters				
μ'_{max} (day^{-1})	0.426	0.650	1.761	1.322
Q_{max} (pg cell^{-1})	2.483	1.399	1.878	3.612
Q_{min} (pg cell^{-1})	0.425	0.121	1.569	0.357
K_Q (mg L^{-1})	1.225	0.908	1.107	0.417
Uptake parameters				
ρ_{max}^{hi} (pg cell^{-1} day^{-1})	2.95	4.68	1.11	0.74
K_ρ^{hi} (mg L^{-1})	18.9	14.3	0.13	1.63
ρ_{max}^{lo} (pg cell^{-1} day^{-1})	0.348	3.216	0.267	0.232
K_ρ^{lo} (mg L^{-1})	10.5	14.2	0.4	0.04

When it come to the P related parameters, the $\mu_{\max}$ for *C. meneghiniana* was 3 times as high as that for *Microcystis* sp. The maximum and minimum cell quota of P for *C. meneghiniana* was twice higher than those of N. However, the Q_{max} of P for *Microcystis* sp. was nearly the same as that of N. The ρ_{max}^{lo} and ρ_{max}^{hi} for the two species were almost same.

Based on the change in the measured cell densities and nutrients concentrations, the nutrient uptake rate of N and P for the two species was calculated and shown in **Fig.3-2**. The calculated data were displayed with all measured data instead of the average value to show the changing trend more clearly. The nutrient uptake rate for

both *Microcystis* sp. and *C. meneghiniana* decreased with reduction of dissolved nutrient concentration. Each curves were depicted by the previous growth model [3] under the same experimental conditions. The coefficient of determination (R^2) for experimental and simulated value for *Microcystis* sp. was 0.374, while that for *C. meneghiniana* was 0.457. As for P uptake rate for the two species, the R^2 for *Microcystis* sp. was 0.181, and for *C. meneghiniana* was 0.076. These results imply that the P uptake was not well simulated by the previous model.

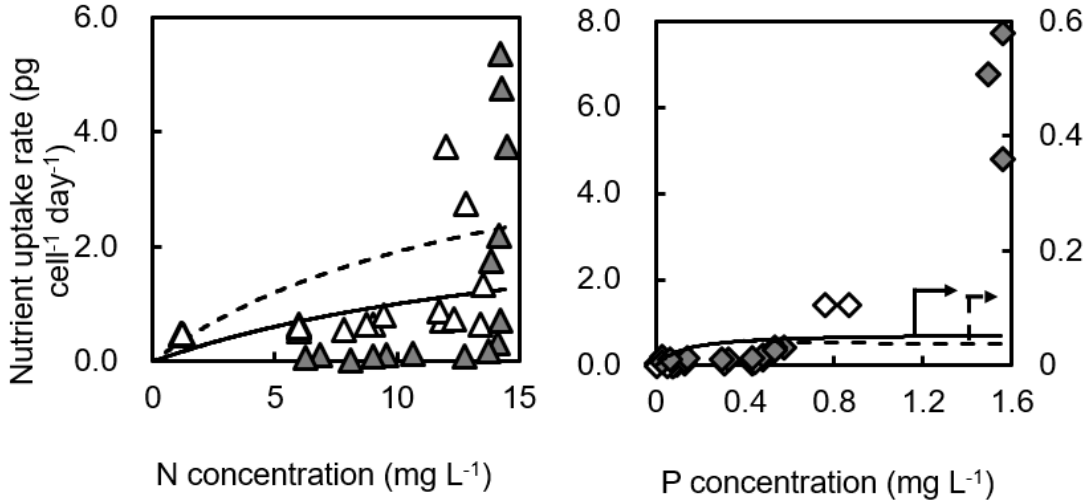

Fig. 3-2 Measured nutrient uptake rate ρ of *Microcystis* sp. and *C. meneghiniana* and Michaelis-Menten model simulated curves. The open and filled triangle presents the measured nitrate uptake rate for *Microcystis* sp. and *C. meneghiniana* respectively. The open and filled diamond presents the measured phosphate uptake rate for *Microcystis* sp. and *C. meneghiniana* respectively. Solid lines are the simulated values for *Microcystis* sp. and dashed lines are those for *C. meneghiniana*.

3.3.2 Competitive growth patterns and growth prediction

Cell proliferation of *Microcystis* sp. and *C. meneghiniana* under different daily renewal rate and N concentrations as shown in **Table 3-1** was presented in **Fig. 3-3**. The curves in the same figure were the simulated results from the modified growth competition model.

It was displayed that the dominant species all were *Cyclotella meneghiniana* in

all the experimental groups under 20°C. In the experimental group with N= 0.5 mg-N L^{-1} and *d* = 5%, the highest growth rate for *Microcystis* sp. was only 0.322 ± 0.021 day^{-1} and the saturated biovolume was $9.87\times10^5 \pm 1.04\times10^4$ μm^3 mL^{-1} at day 25. When the *d* raised to 15%, the growth of *Microcystis* sp. was relatively inhibited, and the saturated biovolume was $1.69\times10^5 \pm 0.92\times10^4$ μm^3 mL^{-1}. Compared with the previous competition model, the simulated results by modified model were closer to the experimental data. The R^2 for the new simulated curve and experimental data was 0.63, while that for the previous one was 0.88. In the *d* = 15% group, although the R^2 for the previous model was 0.53, the value in the modified model prediction increased up to 0.71. In contrast, the growth of *C. meneghiniana* was more vigorous compared with that of *Microcystis* sp. Even the increase in daily renewal rate also did not cause obvious effect. Compared to the previous simulated results, the R^2 in the two groups was both improved. The R^2 at *d* = 5% raised from 0.81 to 0.90 and also raised from 0.87 to 0.94 in *d* = 15%.

The inhibited effect of dilution on the growth of *Microcystis* sp. was portrayed in all the other groups with the daily renewal rate of *d* = 15%. *Microcystis* sp. in these groups almost could not proliferate and the cell density only increased less than one order of magnitude. In the groups with low renewal rate of *d* = 5%, the growth of *Microcystis* sp. was promoted by increasing N concentrations. The saturated biovolume of *Microcystis* sp. increased up to $1.02\times10^7 \pm 0.71\times10^6$ μm^3 mL^{-1} in the groups with 10 mg-N mL^{-1}, which is two orders of magnitude higher compared with the initial biovolume. The modified competition model has predicted the proliferation accurately (R^2 = 0.97).

Compared with *Microcystis* sp., the growth of *C. meneghiniana* was not affected obviously by dilution. Even in the groups with N concentrations higher than 1.0 mg-N L^{-1}, the growth under the conditions with *d* = 15% was more vigorous compared with that in *d* = 5% groups. The accuracy of simulated curves prediction was higher in those groups under *d* = 15%.

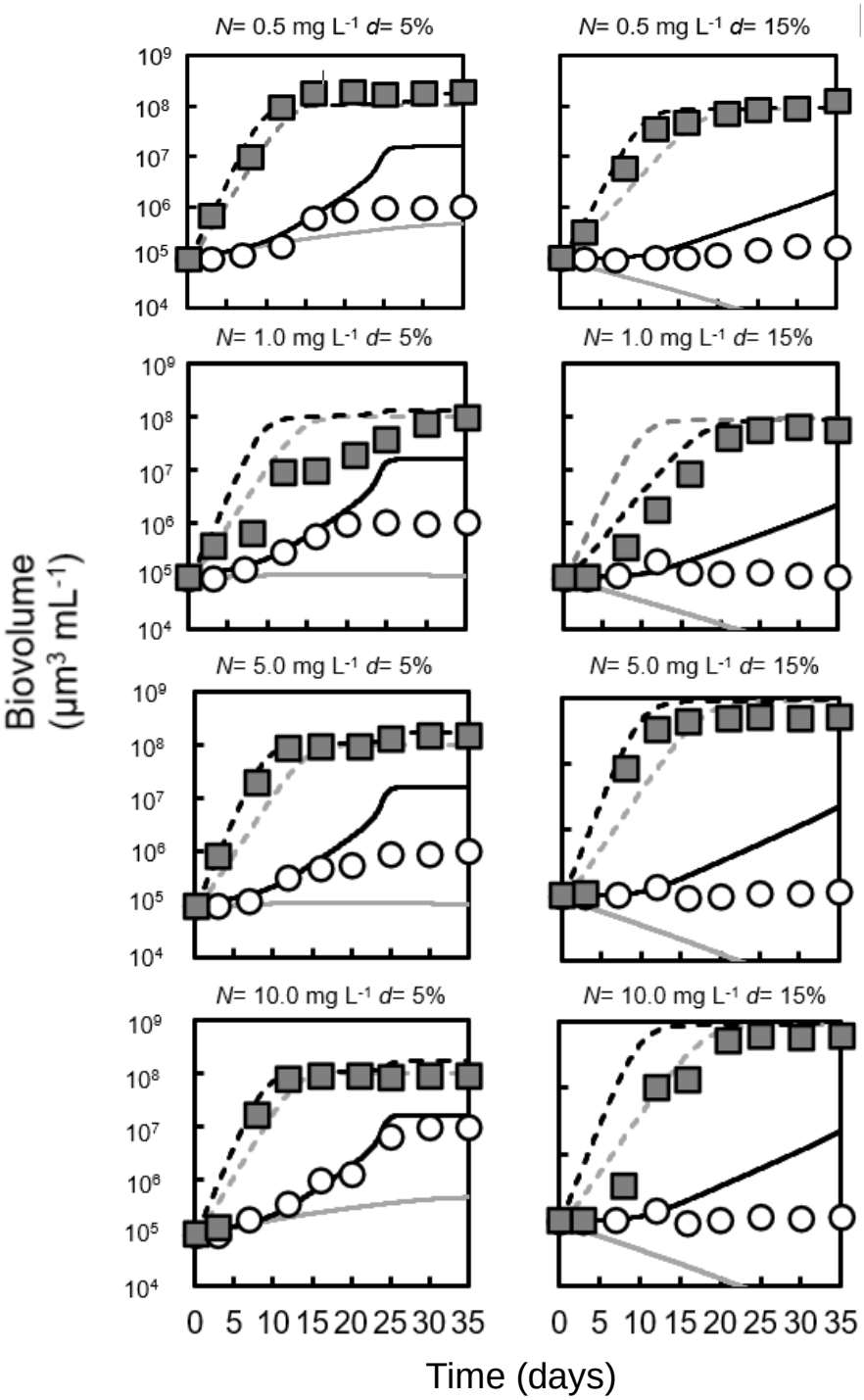

Fig. 3-3 Simulated cocultivated growth patterns of *Microcystis* sp. and *Cyclotella meneghiniana* under various conditions. The open circles are the experimental measured biovolume of *Microcystis* sp. and the filled squares are those of *Cyclotella meneghiniana*. The grey solid and dashed curves are the predicted biovolume for *Microcystis* sp. and *Cyclotella meneghiniana* by the previous growth model. Meanwhile, the black solid and dashed curves are the predicted biovolume for *Microcystis* sp. and *Cyclotella* by the modified growth model.

3.3.3 Competitive nutrient uptake patterns

The change of nutrient concentration in cocultivation experiments and the simulated curves are presented in **Fig. 3-4**. Compared with the previous prediction curves, the simulated curves by modified growth model were more accurate.

It was portrayed that the overestimation in the amount of nutrient uptake caused by the previous model still demonstrated in low temperature of 20^{o}C. However, the modified growth model in which combined a new nutrient adsorption term has improved the problem. This kind of accurate prediction especially could be observed in the P concentration change. The P concentrations predicted by modified growth model were closer to the experimental value compared with the previous prediction, and all the R^2 values of new predicted and experimental data in all experimental groups were higher than 0.9. Although the accuracy of new prediction for N was not so accurate as it for P prediction, it still could describe the changing trend well and more accurately compared with the previous (higher R^2).

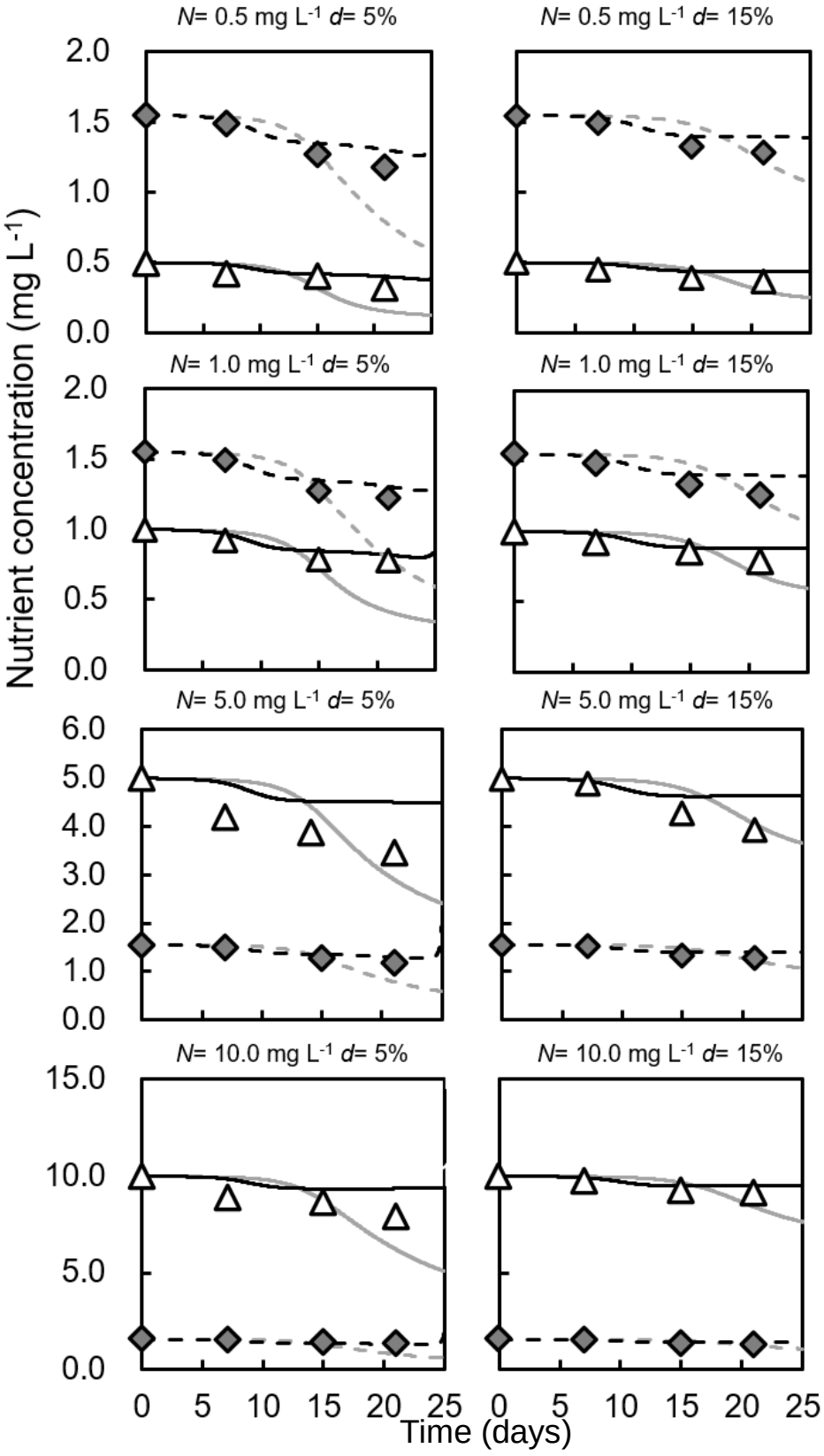

Fig 3-4 Nutrient concentrations change in cocultivation experiments under different conditions. The open triangles are the experimental measured N concentrations, and the filled diamond are the experimental measured P concentrations. The grey solid and dashed curves are the simulated values of N and P concentrations by the previous growth model. Meanwhile, the black solid and dashed curves are the simulated values of N and P concentrations

by the new growth model.

3.3.4 Predictions of *Microcystis* sp. growth with various nutrient concentrations and dilution rates

Since the effectivity of the model has been recognized, the *Microcystis* sp. cell densities at day 35 under various N concentrations and daily renewal rate, and constant P concentration of 1.55 mg-P L^{-1} were predicted using the competition model improved in this study. The simulated results were summarized in **Fig. 3-5**, which is an aerial view of the 3-dimensional graph. Depending on the algal bloom alert principle [31], when the cell densities higher than 1.0×10^5 cells mL^{-1}, it can be decided the bloom has formed. With the cell densities of 3.0×10^4 -1.0×10^5 cells mL^{-1}, though the algae did not form blooms, it has been a threat to the lake. This area will be colored to be white. The black area means that the algal cell densities were lower than 3.0×10^4 cells mL^{-1}. Furthermore, the grey area means that the cell could not proliferate and lead to the densities was lower than the initial cell densities (1.0×10^4 cells mL^{-1}). It was observed that when *d* is higher than 3%, the growth of *Microcystis* sp. was severely inhibited within the set N concentrations, compared with it in the condition with no dilution. On the other hand, when the initial N concentration is lower than 0.31, the growth of *Microcystis* sp. was suppressed and the saturated cell densities did not reach 3.0×10^4 cells mL^{-1}.

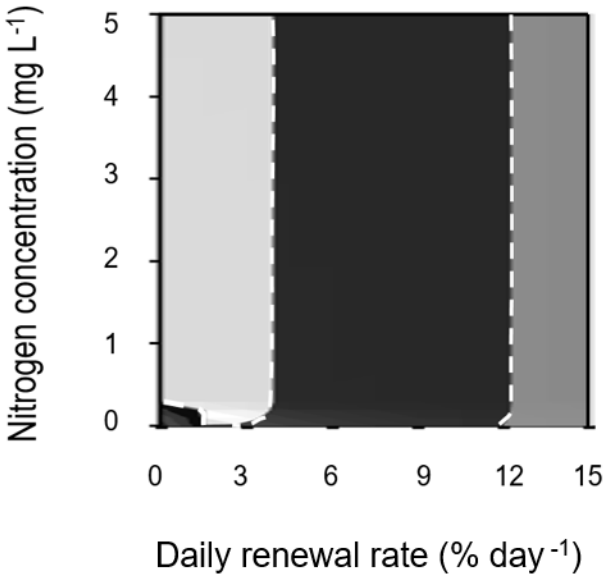

Fig. 3-5 Contour figure of simulated *Microcystis* sp. cell densities at day 35 under various initial nitrate concentrations and daily renewal rates (aerial view). Every different area was divided by white dashed lines. White area: the cell densities in the range of 30,000 - 100,000 cells mL^{-1}; black area: the cell densities in the range of 10,000 - 30,000 cells mL^{-1}; grey area: the cell densities less than 10,000 cells mL^{-1}.

3.4 Discussion

The nutrient uptake kinetic of the cyanobacteria does not always follow the Michaelis-Menten models in long term cultivation [14, 32, 33]. In this study the overestimation of the previous growth model has been ameliorated depend on the growth characteristics and nutrient uptake rate of *C. meneghiniana* and *Microcystis* sp. isolated from Lake Tega, Japan.

The inaccurate nutrient concentration prediction by the previous growth model was mainly caused by the nutrient adsorption term ρ. The predicted curves in **Fig. 3-2** displayed obvious deficiency compared with measured data ($p < 0.05$), especially under the high nutrient conditions. The nutrient uptake rates for N and P for both the two species decreased sharply at the first two measured point which means at the start of experiment. This kind of enhanced nutrient uptake of algae at the early phase of algal growth has been focused and discussed by many studies [34-36], which could not be simulated by Michaelis-Menten. With the growth of cell, the nutrient uptake

activity tend to stabilize, at when the uptake characteristics followed the Michaelis-Menten equation, which was consistent with curve fitting result in **Fig. 3-2**. However, at the end of experiment when the nutrient concentration decreasing to 0, the deficiency of prediction result occurred again. Ahn et al. [37] have observed the phosphate uptake rate of green algae was inversely proportional to the cell density, and Mallick and Rai [38] also have proved the inversely proportional nitrate uptake rate with increasing cell density. These patterns of nutrient uptake in experiments were unanimous. When the cell densities gradually reach the environmental capacity of the incubator, the rate of nutrient adsorb began to decrease. Thus, after adding the cell density relating item into the previous nutrient adsorption term, the overestimation of nutrient adsorption has been refined. As results of that, the accuracy of the modified model for nutrient concentration prediction has been improved as shown in **Fig. 3-4.**

Fujimoto et al. [39] measured the cell quota and related growth rate of *M. aeruginosa* under 20^{o}C with nitrogen and phosphorus limitation. They measured the μ'_{max} by Droop model, and μ'_{max} of nitrogen is 0.84 ± 0.09 day^{-1} and that of phosphorus is 0.46 ± 0.03 day^{-1}. Compared with the value in this study, it was twice (μ'_{max} for N: 0.426 ± 0.013 day^{-1}) and one quarter (1.76 ± 0.01 day^{-1}). The difference between the measured values were caused by the simulating model and species difference. Since the accuracy of prediction on the change of nutrient concentrations in various experiments were proved, the simulating model used in this study could be recognized useful.

Although the modified model can predict the growth and nutrient concentrations change accurately so far, the sources of nitrogen and phosphorus in experiments were only nitrate and phosphate. In actual water environments, there are many types of nitrogen such as ammonium and organic nitrogen, which can affect the cell nutrient uptake [16, 40], the difference in uptake ability of various nutrient source will lead to deficiency in the model prediction. To improve the accuracy of prediction value, these uptake kinetics should be further explored in following study.

3.5 Conclusion

The enhance of the original nutrient uptake term has improved the prediction result of the cocultivation experiment accuracy severely. As a result of that, the overestimation of nutrient uptake also has been reduced by modified the nutrient uptake term. Under 20^{o}C temperature and limitation of nitrogen, the filed isolated *Cyclotella meneghiniana* can dominate the growth of *Microcystis* sp. totally within the setting experimental conditions. Based on the model predict result, under 20^{o}C temperature, when N concentration was lower than 0.31 mg-N L^{-1} and daily renewal rate was higher than 3%, the growth of Microcystis would be suppressed most severely. To control the environment under the condition like that, the risk of cyanobacteria bloom break will be suppressed efficiently.

References

[1] H.W. Paerl, Mitigating harmful cyanobacterial blooms in a human-and climatically-impacted world, Life, 4 (2014) 988-1012.

[2] S.B. Watson, C. Miller, G. Arhonditsis, G.L. Boyer, W. Carmichael, M.N. Charlton, R. Confesor, D.C. Depew, T.O. Höök, S.A. Ludsin, The re-eutrophication of Lake Erie: Harmful algal blooms and hypoxia, Harmful Algae, 56 (2016) 44-66.

[3] M. Chujo, J. Li, T. Datta, Y. Amano, M. Machida, A competitive growth model for the simulation of cyanobacterial blooms under eutrophic conditions, Environ. Eng. Sci., 38 (2021) 15-23.

[4] U. Tillmann, Interactions between planktonic microalgae and protozoan grazers 1, J. Eukaryot. Microbiol., 51 (2004) 156-168.

[5] F. Recknagel, ANNA–Artificial Neural Network model for predicting species abundance and succession of blue-green algae, Hydrobiologia, 349 (1997) 47-57.

[6] A. Fadel, A. Atoui, B.J. Lemaire, B. Vinçon-Leite, K. Slim, Environmental factors associated with phytoplankton succession in a Mediterranean reservoir with a highly fluctuating water level, Environ. Monit. Assess., 187 (2015) 1-14.

[7] C. Reynolds, Succession and vertical distribution of phytoplankton in response to thermal stratification in a lowland mere, with special reference to nutrient availability, The Journal of Ecology, (1976) 529-551.

[8] D. Dubey, V. Dutta, Nutrient enrichment in lake ecosystem and its effects on algae and macrophytes, Environmental concerns and sustainable development, (2020) 81-126.

[9] S.I. Passy, C.A. Larson, Succession in stream biofilms is an environmentally driven gradient of stress tolerance, Microb. Ecol., 62 (2011) 414-424.

[10] L. Michaelis, M.L. Menten, Die kinetik der invertinwirkung, Biochem. z, 49 (1913) 352.

[11] J. Monod, Recherches sur la croissance des cultures bactériennes, (1942).

[12] M.R. Droop, Vitamin B12 and marine ecology. IV. The kinetics of uptake, growth and inhibition in Monochrysis lutheri, J. Mar. Biol. Assoc. UK, 48 (1968) 689-

733.

[13] U. Sommer, A comparison of the Droop and the Monod models of nutrient limited growth applied to natural populations of phytoplankton, Funct. Ecol., (1991) 535-544.

[14] W. Sunda, K. Shertzer, D. Hardison, Ammonium uptake and growth models in marine diatoms: Monod and Droop revisited, Mar. Ecol. Prog. Ser., 386 (2009) 29-41.

[15] M.R. Droop, 25 years of algal growth kinetics a personal view, Res. Process. (1983).

[16] J. Lee, A.E. Parker, F.P. Wilkerson, R.C. Dugdale, Uptake and inhibition kinetics of nitrogen in Microcystis aeruginosa: results from cultures and field assemblages collected in the San Francisco Bay Delta, CA, Harmful Algae, 47 (2015) 126-140.

[17] S. Ghaffar, R.J. Stevenson, Z. Khan, Effect of phosphorus stress on Microcystis aeruginosa growth and phosphorus uptake, PLoS One, 12 (2017) e0174349.

[18] O. Levenspiel, The Monod equation: a revisit and a generalization to product inhibition situations, Biotechnol. Bioeng., 22 (1980) 1671-1687.

[19] B.P. English, W. Min, A.M. Van Oijen, K.T. Lee, G. Luo, H. Sun, B.J. Cherayil, S. Kou, X.S. Xie, Ever-fluctuating single enzyme molecules: Michaelis-Menten equation revisited, Nat. Chem. Biol., 2 (2006) 87-94.

[20] J.J. Elser, E.R. Marzolf, C.R. Goldman, Phosphorus and nitrogen limitation of phytoplankton growth in the freshwaters of North America: a review and critique of experimental enrichments, Can. J. Fish. Aquat. Sci., 47 (1990) 1468-1477.

[21] J.M. Abell, D. Özkundakci, D.P. Hamilton, Nitrogen and phosphorus limitation of phytoplankton growth in New Zealand lakes: implications for eutrophication control, Ecosystems, 13 (2010) 966-977.

[22] Chiba Prefectural Government, Water quality for lakes in Chiba prefecture, Chiba city, Chiba Prefectural Government, 2019.

[23] K. Sugimoto, Y. Negishi, Y. Amano, M. Machida, F. Imazeki, Roles of dilution rate and nitrogen concentration in competition between the cyanobacterium *Microcystis aeruginosa* and the diatom *Cyclotella* sp. in eutrophic lakes, J. Appl. Phycol., 28 (2016) 2255-2263.

[24] J. Li, Y. Amano, M. Machida, Temperature-dependent growth characteristics and dominance trends of the cyanobacterium Microcystis sp. and the diatom Cyclotella meneghiniana, Hydrobiologia, (2022) 1-12.

[25] M. Droop, Some thoughts on nutrient limitation in algae 1, J. Phycol., 9 (1973) 264-272.

[26] R.R. Guillard, C.J. Lorenzen, Yellow-green algae with chlororhyllide c 1,2, J. Phycol., 8 (1972) 10-14.

[27] E.H. John, K.J. Flynn, Modelling phosphate transport and assimilation in microalgae; how much complexity is warranted?, Ecol. Model., 125 (2000) 145-157.

[28] F.M. Morel, Kinetics of nutrient uptake and growth in phytoplankton 1, J. Phycol., 23 (1987) 137-150.

[29] A.S. Lim, H.J. Jeong, T.Y. Jang, S.H. Jang, P.J. Franks, Inhibition of growth rate and swimming speed of the harmful dinoflagellate Cochlodinium polykrikoides by diatoms: implications for red tide formation, Harmful Algae, 37 (2014) 53-61.

[30] D. Tilman, S.S. Kilham, Phosphate and silicate growth and uptake kinetics of the diatoms *Asterionella formosa* and *Cyclotella meneghiniana* in batch and semicontinuous culture., J. Phycol., 12 (1976) 375-383.

[31] WHO, Addendum to the WHO guidelines for safe recreational water environments. Volume 1, Coastal and fresh waters: list of agreed updates, World Health Organization, 2009.

[32] M. Woźniak, K.M. Bradtke, M. Darecki, A. Krężel, Empirical model for phycocyanin concentration estimation as an indicator of cyanobacterial bloom in the optically complex coastal waters of the Baltic Sea, Remote Sensing, 8 (2016) 212.

[33] F.J. Gordillo, M.J. Dring, G. Savidge, Nitrate and phosphate uptake characteristics of three species of brown algae cultured at low salinity, Mar. Ecol. Prog. Ser., 234 (2002) 111-118.

[34] M. Halpern, A. Bar-Tal, M. Ofek, D. Minz, T. Muller, U. Yermiyahu, The use of biostimulants for enhancing nutrient uptake, Advances in agronomy, 130 (2015) 141-174.

[35] D.L. Sutherland, J. Burke, P.J. Ralph, Flow-way water depth affects algal

productivity and nutrient uptake in a filamentous algae nutrient scrubber, J. Appl. Phycol., 32 (2020) 4321-4332.

[36] L. Xin, H. Hong-Ying, G. Ke, S. Ying-Xue, Effects of different nitrogen and phosphorus concentrations on the growth, nutrient uptake, and lipid accumulation of a freshwater microalga Scenedesmus sp, Bioresour. Technol., 101 (2010) 5494-5500.

[37] C.Y. Ahn, A.S. Chung, H.M. Oh, Diel rhythm of algal phosphate uptake rates in P-limited cyclostats and simulation of its effect on growth and competition J. Phycol., 38 (2002) 695-704.

[38] N. Mallick, L. Rai, Influence of culture density, pH, organic acids and divalent cations on the removal of nutrients and metals by immobilized Anabaena doliolum and Chlorella vulgaris, World J. Microbiol. Biotechnol., 9 (1993) 196-201.

[39] N. Fujimoto, R. Sudo, N. Sugiura, Y. Inamori, Nutrient-limited growth of *Microcystis aeruginosa* and *Phormidium tenue* and competition under various N: P supply ratios and temperatures, Limnol. Oceanogr., 42 (1997) 250-256.

[40] B. Shipley, P. Keddy, The relationship between relative growth rate and sensitivity to nutrient stress in twenty-eight species of emergent macrophytes, The Journal of Ecology, (1988) 1101-1110.

Chapter 4 Effective dilution rate to suppress the risk of *Microcystis* blooms in Lake Tega, based on a competitive growth simulation model

4.1 Introduction

The severe impact of cyanobacterial blooms in eutrophic lakes on water quality has caused a lot of environmental problems worldwide in recent decades. Many treatment methods to remove cyanobacterial blooms such as pump suction, bubble floatation, chemical coagulation and so on, have been carried out and examined in several studies [1-4]. Water transfer is one of the effective treatment methods among them, which not only can suppress the formation of cyanobacterial blooms but also ameliorate the water quality. The transferred water can wash the algae away and dilute or enrich the nutrient concentrations to inhibit or promote algal growth [5, 6]. Although there have been many studies focusing on the inhibitory effect of water transfer on cyanobacterial blooms, the limited experience in some certain lakes could not be applied to other lakes worldwide.

From 1974 to 2000, the lake ranked with the worst water quality in Japan was Lake Tega (35° 51′ N, 140° 02′ E) [7], where suffered from cyanobacterial blooms (mainly the genus *Microcystis*) frequently in summer. In order to improve the deteriorated water quality, a water conveyance channel was constructed in 2000 to convey a large amount of water (maximum volume: 8.6×10^5 m^3 day^{-1}) from the Tone River to Lake Tega. After water conveyance, the highest total nitrogen (TN) concentration in Lake Tega has decreased to 2.2 mg-N L^{-1} in the last five years from 5.3 mg-N L^{-1} in the 1990s. Simultaneously, the highest concentration of total phosphorus (TP) in the last five years has dropped to nearly one-half of the highest value in the 1990s [7]. The dominant algal species changed into diatoms (mainly the genus *Cyclotella*) in summer instead of *Microcystis*, which reduced the frequency of

Microcystis blooms occurrence [6].

In order to explore the effect of water transfer on the growth and dominant species shift from *Microcystis* to *Cyclotella*, Sugimoto et al. [6] have concluded that the dilution rate of up to 36% per day or more was effective to control *M. aeruginosa* growth according to the result of competition experiments with *Cyclotella* sp. However, the inhibitory effect of water transfer on the growth of *M. aeruginosa* was still not considered when the dilution rate was lower than 36%. Afterward, domination characteristics for each species under various nitrate-nitrogen (NO_3-N): phosphate-phosphorus (PO_4-P) mass ratios and dilution rates were predicted by Mikawa et al. [8] based on their algal growth simulation model. The effective dilution rate to suppress the growth of *M. aeruginosa* was proposed at 20% per day by a simulated result in the study. However, the predicted cell densities were always overestimated compared with experimental values due to the defect of the simulation model. In order to modify the overestimation problem in their model, Chujo et al. [9] introduced an additional growth limitation term from Lotka-Volterra model into the previous model to develop an improved simulation model. The developed simulation model could present a more accurate prediction of the growth patterns of *Microcystis* sp. and *C. meneghiniana*, which were isolated from Lake Tega, in cocultivation experiments under high nitrogen and phosphorus concentrations.

Although Chujo's model has been confirmed to work under eutrophic nutrient concentrations [9], the accuracy of the model simulation has been still unclear under the condition with the combination of one nutrient is limited and another one is enough. In Chapter 3, the model has been improved to make the prediction result more accurate. Maberly et al. [10] have estimated the nutrient concentrations of 17 freshwater meres in Shropshire and Cheshire, England. They found that some meres contained high nitrogen and limited phosphorus, while the nutrient concentration conditions in some other meres were opposite. Takamura et al. [11] reported that the concentration of nitrogen exceeded that of phosphorus by 20 times after 1986 in Lake Kasumigaura, Japan. The dominant algae had shifted from *Microcystis* spp. to *Planktothrix agardhii* at that time, which was related to the phosphorus limitation and

the disparity between nitrogen and phosphorus concentrations. To reveal a more accurate dilution rate that can effectively suppress *Microcystis* blooms in such actual lakes, it should be examined whether the developed model in Chapter 3 is practical under various combinations of nutrient concentration. Otherwise, the predicted values by the model would not be applicable to *Microcystis* bloom suppression.

In this study, the aim was exploring the mechanism of suppressive effect of dilution on the growth of two different species and examining the broad applicability of the developed model. Then, indicate an effective dilution rate to suppress *Microcystis* blooms in Lake Tega. For exploring the mechanism of the dilution suppressive effect, a cocultivation experiment of two algal species, *Microcystis* sp. and *C. meneghiniana*, was conducted in phosphorus-limited and nitrogen-enough conditions under various dilution rates. Based on the model, the growth curves were simulated, and the accuracy of simulated data was tested by comparing with the experimental data. After the accuracy was verified, the growth of the two algal species under simultaneous changes of various nitrogen, phosphorus concentrations, and daily renewal rates (used instead of dilution rate in semi-continuous culture system) was simulated based on the model. The simulated values could evaluate an effective dilution rate, which suppresses *Microcystis* blooms effectively under various nitrogen and phosphorus concentrations. The outcome was compared with the field observation of *Microcystis* growth in Lake Tega under different dilution rates to discuss the optimum way to suppress *Microcystis* blooms.

4.2 Materials and methods

4.2.1 Test algae and culture conditions

Microcystis sp. and *C. meneghiniana* in Lake Tega water were isolated [12] and used as test algae in this study. The average single cell volume of the two species was measured to be 9.73 μm^3 for *Microcystis* sp. and 243.35 μm^3 for *C. meneghiniana*.

Wright's cryptophytes (WC) medium [13] at pH 8.0 that can cultivate both cyanobacteria and diatoms [14] was selected as culture medium. Sodium nitrate ($NaNO_3$) and dipotassium hydrogen phosphate (K_2HPO_4) were used to adjust the initial nitrate-nitrogen (N) and phosphate-phosphorus (P) concentrations of the culture medium to be 14 mg-N L^{-1} and 1.55 mg-P L^{-1}, respectively. Silicate-silicon (Si) concentration in the medium supplied by sodium metasilicate (Na_2SiO_3) was raised from 2.8 mg-Si L^{-1} to 11 mg-Si L^{-1}, which is the same as the concentration in the Tone River water. Carbon source was provided by sodium hydrogen carbonate ($NaHCO_3$). The medium was autoclaved at 121ºC for 20 minutes in all experiments.

For subculture, *Microcystis* sp. and *C. meneghiniana* were separately cultivated in WC medium in a 300 mL Erlenmeyer flask. Each flask was incubated in an incubator (MTI-202, EYELA, Japan) at the temperature of 25ºC, and the light intensity was adjusted to 10,000 lux using a light meter (LX-1102, Lutron, America). The light-dark cycle was set as 14 hours-light and 10 hours-dark. The two sub-cultured species were inoculated to fresh medium every two or three weeks. All the operations of inoculation and sampling were conducted in a clean bench to minimize bacterial contamination.

4.2.2 Semi-continuous competition experiments for *Microcystis* sp. and *C. meneghiniana*

Semi-continuous competition experiments were conducted with various dilution rates under the limited phosphorus and enough nitrate concentrations, to investigate the combined effect of these conditions on *Microcystis* sp. and *C. meneghiniana*.

Prior to the competition experiment, both species were precultured in nitrogen- and phosphorus-free medium for 7 days to deplete intracellular N and P, thereby eliminating the effect of intracellular nutrients. After the preculture, both species were inoculated together in 200 mL sterilized medium in a 300 mL Erlenmeyer flask for semi-continuous competition experiments. The initial cell

density of *Microcystis* sp. was adjusted to 1.0×10^4 cells mL^{-1} and that of *C. meneghiniana* was 3.98×10^2 cells mL^{-1} to make the two species' cell volume equivalent to the same volume of 10^5 μm^3.

In actual lakes, there was continuous water inflow from river, which could be modeled as a continuous culture system. The dilution rate (*D*, %) was used to represent the continuous inflow of the water per day. In this study, the culture medium was diluted with fresh medium once a day instead of the continuous water inflow, which should be modeled as a semi-continuous culture system. The daily renewal rate (*d*, %) was used to describe the medium replacement in this culture system. The daily renewal rate in the semi-continuous culture system can be converted to the dilution rate by the following equation [15] :

$$D = \ln\frac{100}{100-d}\times 100. \quad (1)$$

The daily renewal rates of the competition experiment were set as 0%, 5% and 15%. An appropriate volume of culture medium was removed and as soon an equal volume of fresh medium was added to each flask once a day. In addition to the different daily renewal rates, the P concentration of each group was limited to 0.1 mg-P L^{-1}, which was the same as the minimum P concentration in Lake Tega in the last five years [7]. The initial N concentration of 14 mg-N L^{-1} was adequate for the growth of both species [14]. The cell density was measured every 2-5 days and continued until it tended to be constant. The nutrient concentrations were measured once a week. The experiments with different dilution rates were conducted in triplicate. All the experimental results were presented as [the mean value] ± [standard deviation].

4.2.3 Measurements and statistical analyses

The cell density of samples was measured by directly counting cell in a plankton counting plate (MPC-200, Matsunami Glass Industry, Japan) using an optical microscope (ECLIPSE E100, Nikon, Japan) after appropriately diluted. The entire cell volume of each species in the flask was calculated by multiplying single

cell volume and cell density for each, and it was defined as the biovolume. The following Eq. (2) was employed to calculate the average growth rate (μ, day^{-1}) at a certain growth period:

$$\mu = \frac{\ln C_2 - \ln C_1}{t_2 - t_1}, \quad (2)$$

where C_1 and C_2 are the cell densities at time points t_1 (day) and t_2(day), respectively.

Concentrations of N were measured by ion chromatography (ICS-1100, Nippon Dionex, Japan), and molybdenum blue method (Japanese Standard Association, 2016) was used to measure P concentration. The solution pH was monitored by a pH meter (D-51, Horiba, Japan).

Differences in experimental parameters of *Microcystis* sp. and *C. meneghiniana* in each condition were analyzed by a one-way analysis of variance (ANOVA) with a post hoc comparison being performed with Turkey's test, via SPSS Statistics (Ver. 23, IBM Corporation, USA). The results were judged to be a significant difference at $p < 0.05$.

4.2.4 Mathematical model and simulation

In order to predict the cell densities of *Microcystis* sp. and *C. meneghiniana* when they grow together and the trends of the appearance of *Microcystis* blooms under various nutrient concentrations and daily renewal rates, the model constructed by Chujo et al. [9] was used. The equations of the model are tabulated in **Table 4-1**.

Table 4-1 Model equations used in this study

State variable	Modeling of each state variable
N concentration	$\frac{dN}{dt} = -C_A \frac{\rho_{nA,max} N}{K_{nA} + N}(1 - \frac{C_A}{K_{CA}}) - C_B \frac{\rho_{nB,max} N}{K_{nB} + N}(1 - \frac{C_B}{K_{CB}}) + D(N_0 - N)$
P concentration	$\frac{dP}{dt} = -C_A \frac{\rho_{pA,max} P}{K_{pA} + P}(1 - \frac{C_A}{K_C})(1 - \frac{Q_{pA}}{Q_{pA,max}}) - C_B \frac{\rho_{pB,max} P}{K_{pB} + P}(1 - \frac{C_B}{K_{CB}}) + D(P_0 - P)$
Cell quota of assimilated N of *Microcystis* sp.	$\frac{dQ_{nA}}{dt} = \frac{\rho_{nA,max} N}{K_{nA} + N}(1 - \frac{C_A}{K_{CA}}) - \left[\mu'_{nA,max}\left(\frac{Q_{nA} - Q_{nA,min}}{Q_{nA} - Q_{nA,min} + K_{QnA}}\right), \mu'_{pA,max}\left(\frac{Q_{pA} - Q_{pA,min}}{Q_{pA} - Q_{pA,min} + K_{QpA}}\right)\right]^{*}(1 - \frac{C_A' - \alpha_{AB} C_B'}{K_A})Q_{nA}$
Cell quota of assimilated N of *C.meneghiniana*	$\frac{dQ_{nB}}{dt} = \frac{\rho_{nB,max} N}{K_{nB} + N}(1 - \frac{C_B}{K_{CB}}) - \left[\mu'_{nA,max}\left(\frac{Q_{nA} - Q_{nA,min}}{Q_{nA} - Q_{nA,min} + K_{QnA}}\right), \mu'_{pA,max}\left(\frac{Q_{pA} - Q_{pA,min}}{Q_{pA} - Q_{pA,min} + K_{QpA}}\right)\right]^{**}(1 - \frac{C_B'' - \alpha_{BA} C_A''}{K_B})Q_{nB}$
Cell quota of assimilated P of *Microcystis* sp.	$\frac{dQ_{pA}}{dt} = \frac{\rho_{pA,max} P}{K_{pA} + P}(1 - \frac{C_A}{K_{CA}})(1 - \frac{Q_{pA}}{Q_{pA,max}}) - \left[\mu'_{nA,max}\left(1 - \frac{Q_{nA,min}}{Q_{nA}}\right), \mu'_{pA,max}\left(1 - \frac{Q_{pA,min}}{Q_{pA}}\right)\right]^{*}(1 - \frac{C_A' - \alpha_{AB} C_B'}{K_A})Q_{pA}$
Cell quota of assimilated P of *C.meneghiniana*	$\frac{dQ_{pB}}{dt} = \frac{\rho_{pB,max} P}{K_{pB} + P}(1 - \frac{C_B}{K_{CB}}) - \left[\mu'_{nB,max}\left(\frac{Q_{nB} - Q_{nB,min}}{Q_{nB} - Q_{nB,min} + K_{QnB}}\right), \mu'_{pB,max}\left(\frac{Q_{pB} - Q_{pB,min}}{Q_{pB} - Q_{pB,min} + K_{QpB}}\right)\right]^{**}(1 - \frac{C_B'' - \alpha_{BA} C_A''}{K_B})Q_{pB}$
Cell density of *Microcystis* sp.	$\frac{dC_A}{dt} = \left\{\left[\mu'_{nA,max}\left(\frac{Q_{nA} - Q_{nA,min}}{Q_{nA} - Q_{nA,min} + K_{QnA}}\right), \mu'_{pA,max}\left(\frac{Q_{pA} - Q_{pA,min}}{Q_{pA} - Q_{pA,min} + K_{QpA}}\right)\right]^{*}\left(1 - \frac{C_A' - \alpha_{AB} C_B'}{K_A}\right) - D\right\}C_A$
Cell density of *C.meneghiniana*	$\frac{dC_B}{dt} = \left\{\left[\mu'_{nB,max}\left(\frac{Q_{nB} - Q_{nB,min}}{Q_{nB} - Q_{nB,min} + K_{QnB}}\right), \mu'_{pB,max}\left(\frac{Q_{pB} - Q_{pB,min}}{Q_{pB} - Q_{pB,min} + K_{QpB}}\right)\right]^{**}\left(1 - \frac{C_B'' - \alpha_{BA} C_A''}{K_B}\right) - D\right\}C_B$

***In case of *Microcystis* sp.,**

If the Q_{nA}:Q_{pA} ratio is higher than the optimum N:P ratio (= 2.71): $\mu'_{pA,max}\left(\frac{Q_{pA} - Q_{pA,min}}{Q_{pA} - Q_{pA,min} + K_{QpA}}\right)$

if not: $\mu'_{nA,max}\left(\frac{Q_{nA} - Q_{nA,min}}{Q_{nA} - Q_{nA,min} + K_{QnA}}\right)$

****In case of *C. meneghiniana*,**

If the Q_{nB}:Q_{pB} ratio is higher than the optimum N:P ratio (= 3.38): $\mu'_{pB,max}\left(\frac{Q_{pB} - Q_{pB,min}}{Q_{pB} - Q_{pBmin} + K_{QpB}}\right)$

if not: $\mu'_{nB,max}\left(\frac{Q_{nB} - Q_{nB,min}}{Q_{nB} - Q_{nB,min} + K_{QnB}}\right)$

The accuracy of a previous model [16] tended to decrease under high nutrient concentrations. In the previous model, the limiting nutrient was determined as the relationship between the mass ratio of minimum cell quota of assimilated N:P (the optimum N:P ratio) and the external dissolved N:P mass ratio. While in the Chujo's model, the relationship between the mass ratio of cell quota of assimilated N:P (Q_n:Q_p) and the optimum N:P ratio was taken to determine the limiting nutrient (as shown in the tag of **Table 4-1**).

The model equations were calculated via a fourth-order form of the Runge-Kutta method with the time step of $\Delta t = 0.01$ day, using Microsoft Excel. The values

of each constant parameter in the equations taken to calculate were shown in **Table 4-2**, which were obtained from monoculture experiments in the study of Chujo, Li, Datta, Amano and Machida [17]. Furthermore, to investigate the accuracy of the model simulation under combined nutrient concentration, the growth curves of both species were simulated under the same experimental condition as the semi-continuous competition experiments mentioned above.

Table 4-2 Parameters for the competition growth model which referred to last chapter

Parameter	*Microcystis* sp.	*C. meneghiniana*	*Microcystis* sp.	*C. meneghiniana*
	Nitrogen		Phosphorus	
Growth parameters				
μ_{max} (day^{-1})	0.267	0.381	0.383	1.170
K_{μ} (mg L^{-1})	7.62	1.22	4.64	2.59
Cell quota parameters				
μ'_{max} (day^{-1})	0.426	0.650	1.761	1.322
Q_{max} (pg cell^{-1})	2.483	1.399	1.878	3.612
Q_{min} (pg cell^{-1})	0.425	0.121	1.569	0.357
K_Q (mg L^{-1})	1.225	0.908	1.107	0.417
Uptake parameters				
ρ_{max}^{hi} (pg cell^{-1} day^{-1})	2.95	4.68	1.11	0.74
K_{ρ}^{hi} (mg L^{-1})	18.9	14.3	0.13	1.63
ρ_{max}^{lo} (pg cell^{-1} day^{-1})	0.348	3.216	0.267	0.232
K_{ρ}^{lo} (mg L^{-1})	10.5	14.2	0.4	0.04

In the investigation of effective dilution rate, the growth of both species was simulated under various nutrient concentrations and dilution rates based on the Chujo's model. The initial N and P concentrations were ranged from 0 to 5.0 mg-N L^{-1} and 0 to 0.5 mg-P L^{-1}, respectively, reflecting the nutrient concentration in Lake

Tega. The daily renewal rate (*d*) was increased from 0% to 20% with a 2.5% interval for each step. Since the two species always reached saturation within around 20 days [17], the cell density in day 30 was used as the final result for prediction.

4.3 Results

4.3.1 Growth characteristics of *Microcystis* sp. and *C. meneghiniana* at different daily renewal rates under phosphorus limited condition

Growth characteristics for *Microcystis* sp. and *C. meneghiniana* in P limited culture experiment are shown in **Fig. 4-1**. The simulated growth curves of both species are also depicted in the same figure.

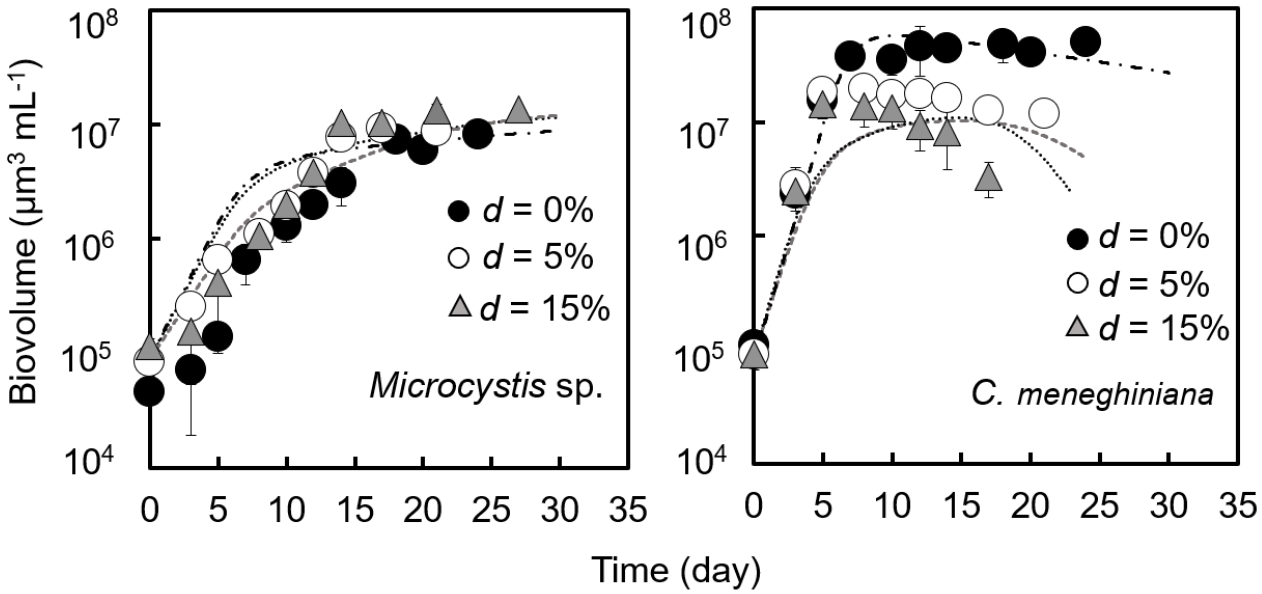

Fig. 4-1 Biovolume of *Microcystis* sp. and *C. meneghiniana* under limited phosphorus and sufficient nitrogen concentration with various daily renewal rates of *d* = 0% (black filled circle), *d* = 5% (open circle), and *d* = 15% (grey filled triangle), and the simulated competitive growth curves of two species. Dotted-dashed line indicates the simulated cell volume of Microcystis sp. under *d* = 0%, dashed line indicates that under *d* = 5%, dotted line indicates that under *d* = 15%.

In all daily renewal rates (d) experimental groups, the biovolume of both species has reached saturation within 25 days. At d = 0%, the biovolume of *Microcystis* sp. was $8.13\times10^6 \pm 1.76\times10^6$ μm^3 L^{-1} at day 24, and after that, the biovolume remained constant within 7 days. For the other two experimental groups (d = 5% and 15%), there was no significant discrepancy in the biovolume ($p > 0.05$). In the d = 5% group, the biovolume in saturation was obtained at day 17 as $9.31\times10^6 \pm 1.29\times10^6$ μm^3 L^{-1} and that for the 15% group was $1.31\times10^7 \pm 1.17\times10^6$ μm^3 L^{-1} at day 21. The average growth rate of *Microcystis* sp. in the logarithmic phase of the three groups was also similar ($p > 0.05$). The value was 0.313 ± 0.007 day^{-1} in the d = 0% group, and 0.318 ± 0.005 day^{-1} in the d = 5% group. When the daily renewal rate increased to 15%, the average growth rate in the logarithmic phase was obtained to be 0.291 ± 0.002 day^{-1}.

On the other hand, the growth of *C. meneghiniana* was affected obviously by the daily renewal rate under phosphorus limitation. *C. meneghiniana* has reached saturation at day 7 with the biovolume of $3.76\times10^7 \pm 1.01\times10^6$ μm^3 L^{-1} in the d = 10% group and remained stationary until the end of the experiment. In comparison, the growth of *C. meneghiniana* at d = 15% has entered the death phase directly after it reached saturation at day 5. Moreover, the biovolume in this group at the end of the experiment was $2.18\times10^6 \pm 1.01\times10^6$ μm^3 L^{-1}, which decreased by nearly one order of magnitude compared with that in the d = 5% group. As a result of the competition experiments, the dominant species, defined as the species which take the most biovolume in the flask, was always *Microcystis* sp. in each group. The obvious effect of the daily renewal rate was also reflected in the growth rate of *C. meneghiniana*. At the beginning of the experiment (from day 0 to day 5), although the differences in growth rate among each group were not obvious ($p > 0.05$), the average growth rates of the three groups displayed different characteristics after the logarithmic phase. From day 12 to day 18, the average growth rate in the d = 0% group was 0.005 ± 0.001 day^{-1}, and then the growth rate of *C. meneghiniana* gradually changed to 0 until

the end of the experiment. On the contrary, in the groups of d = 5% and d = 15%, the average growth rate has become negative after the logarithmic phase.

From the result of nutrient analysis as shown in **Fig. 4-2**, it was observed that the dilution had scant effect on the change in nutrient concentrations in the competition experiments. The differences in the N and P concentrations among each group were not significant ($p > 0.05$), and the decline of both nutrient concentrations were mainly attributed to the growth of two species as the competition experiment progressed. The concentration of P dropped rapidly during the logarithmic phase of the two species and remained at 0.012 ± 0.002 mg-P L^{-1} and 0.016 ± 0.004 mg-P L^{-1} at d = 0% and d = 15%, while the N concentration remained at 9.25 ± 0.39 mg-N L^{-1} and 8.62 ± 0.22 mg-N L^{-1} at d = 0% and d = 15%, respectively. These values portrayed that the nutrient concentrations were similar at the end of the competition experiments, despite the differences in daily renewal rates.

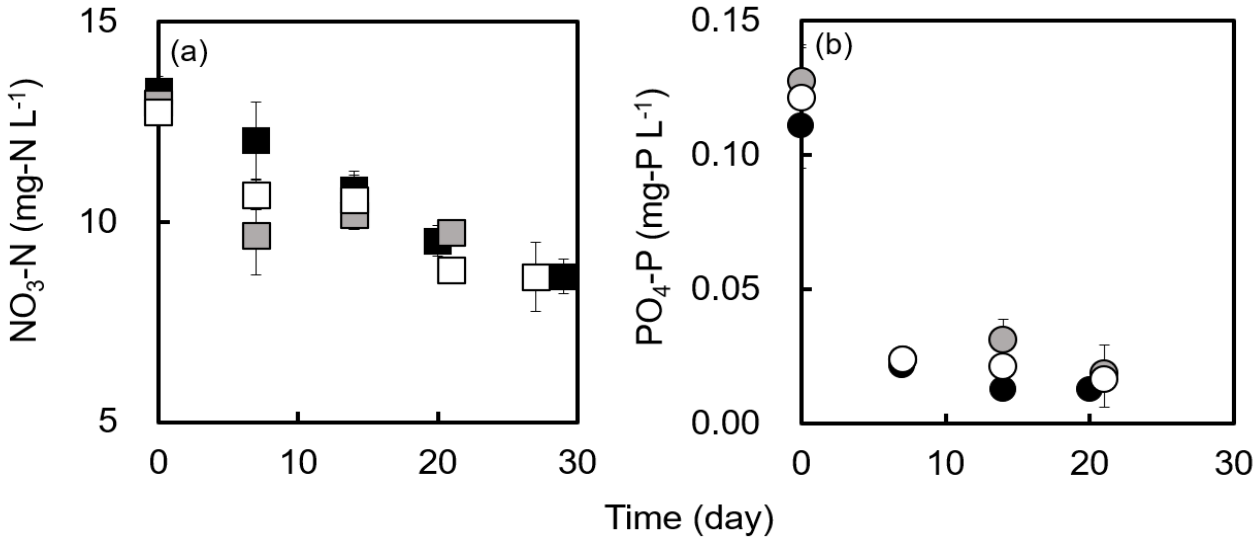

Fig. 4-2 Nutrient concentration in competition experiments.

(a) Nitrogen concentrations change in experiments under various dilution rates of d = 0% (black filled square), d = 5% (grey filled square) and d = 15% (open square).

(b) Phosphorus concentrations change in experiments under various dilution rates of d = 0% (black filled circle), d = 5% (grey filled circle) and d = 15% (open circle).

4.3.2 Accuracy of competitive growth simulation model under limited P concentration

The simulated growth curves in **Fig. 4-1** displayed that the simulated data could well correspond with the experimental growth patterns for *Microcystis* sp. In the d = 0% group, the trend of experimental cell growth data and simulated curve changing trend have coherence. The two simulated growth curves in the d = 5% and d = 15% group almost coincided with each other, which is consistent with the fact that there was not a significant difference in experimental data between the two groups ($p > 0.05$). The coefficient of determination (R^2) for the simulated curve at d = 0% was 0.827 and the values at d = 5% and d = 15% were 0.894 and 0.915, respectively. Thus, the feasibility of Chujo's model under limited phosphorus and sufficient nitrogen conditions could be verified. It would be used to predict the growth of *Microcystis* sp. under various nutrient conditions including phosphorus deficiency. Similarly, the simulated values also matched with the experimental patterns in the growth of *C. meneghiniana* at d = 0% under low P concentration (R^2 = 0.973). Although a little discrepancy between simulated and experimental biovolume were observed at d = 5% and 15%, the model can still be valid to simulate the growth trend of *C. meneghiniana.*

4.3.3 Prediction of *Microcystis* blooms under various dilution rates

Since the accuracy of the model was verified, the cell density of *Microcystis* sp. was predicted under the same N and P concentrations and daily renewal rate as those in Lake Tega before (d = 5%) and after (d = 15%) water transfer. The estimated *Microcystis* sp. cell densities in saturation were 2.72×10^6 cells mL^{-1} (before water transfer) and 1.36×10^6 cells mL^{-1} (after water transfer), respectively. Based on these values, it could be assumed that, when the estimated cell density was more than 2.72×10^6 cells mL^{-1}, there is a high possibility of *Microcystis* blooms

occurrence, while the cell density of less than 1.36×10^6 cells mL^{-1} implies that blooms would occur hardly. The plane view of contour figures in **Fig. 4-3** shows the predicted values at various daily renewal rates and different nutrient concentrations. The black area was taken as the bloom occurrence area where the predicted cell densities were equal to or more than 2.72×10^6 cells mL^{-1}. The dark-grey area was taken as the non-bloom occurrence area where the predicted cell densities were equal to or less than 1.36×10^6 cells mL^{-1}. The light-grey area between the black and dark-grey area implies the state that suffers the risk of bloom appearance although the blooms has not still occurred. Solid lines and dashed lines were used to indicate the boundary of the bloom occurrence area and non-bloom occurrence area, respectively.

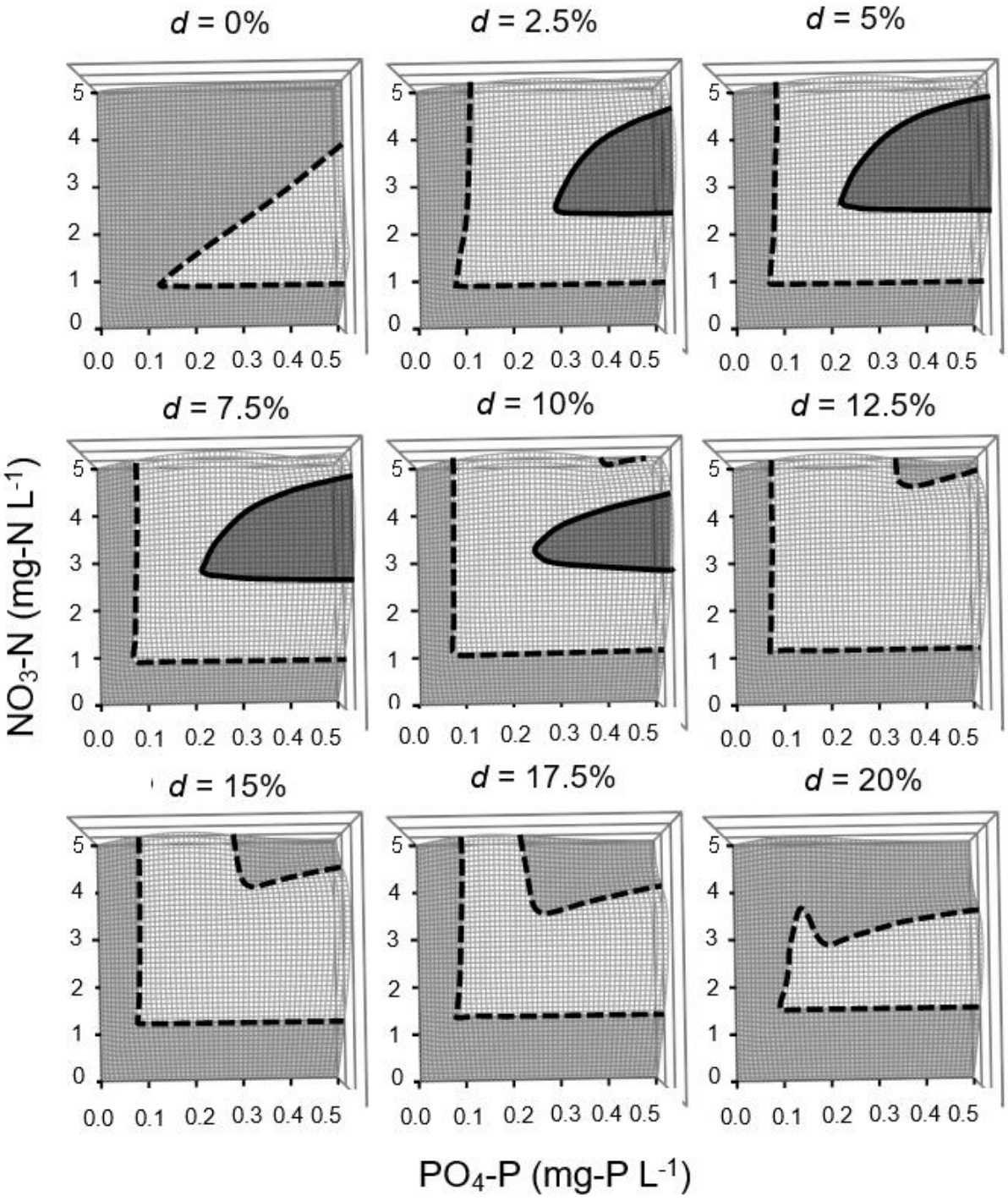

Fig. 4-3 Contour figures of simulated *Microcystis* sp. cell density at day 30 under various daily renewal rates at plane view. Black area and dark-grey area indicate bloom occurrence and non-bloom occurrence area, respectively. Light-grey area suffers a high risk of bloom appearance although has still non-bloom occurrence yet.

When the daily renewal rate changed from 0% to 5%, the bloom area was

obviously enlarged. However, as the daily renewal rate gradually increased from 5%, the bloom area gradually decreased. At the same time, the non-bloom occurrence area increased. It could be anticipated that the *Microcystis* bloom area would disappear at a certain dilution rate. In particular, it can be found in the figures that when the renewal rate was equal to or higher than 12.5%, the bloom area no longer existed. Based on Eq. (1), the dilution rate D was 13.3% when the renewal rate was 12.5%.

The data from Chiba Prefectural Government [7] was used to calculate the annual average of dilution rate (D_{avg}) and the cell densities of *Microcystis* sp. in every month of each year in Lake Tega. The results are displayed in **Fig. 4-4**. The field observation data indicated that when the dilution rate was above 13.3%, *Microcystis* sp. was hard to proliferate, and the cell density was less than 3×10^3 cells mL^{-1}. This trend apparently corresponds to the predicted data as shown in **Fig. 4-3**. Thus, the dilution rate D = 13.3% could be considered to suppress *Microcystis* blooms effectively.

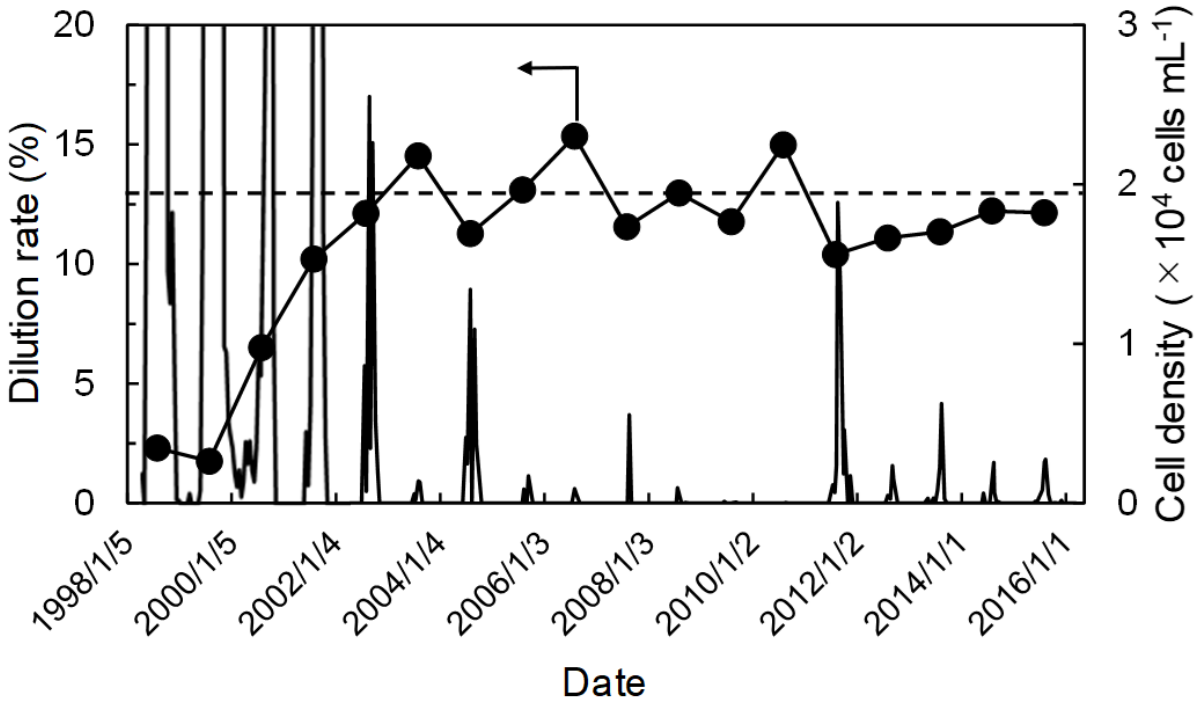

Fig. 4-4 Monthly cell density of *M. aeruginosa* and annual average dilution rates in Lake Tega. A dashed line indicates 13.3% of the dilution rate.

4.4 Discussion

Semi-continuous competition experiments showed that the growth of *C. meneghiniana* isolated from Lake Tega was greater affected by the replacement of medium (dilution) than that of *Microcystis* sp. under phosphorus limitation. Meanwhile, the dilution still had a suppressive effect on the growth of *Microcystis* sp. The simulation results for the competitive growth elucidated that the lowest dilution rate to suppress *Microcystis* blooms was D = 13.3%, which is consistent with the field observation results in Lake Tega.

In semi-continuous competition experiments, *Microcystis* sp. showed better adaptability than *C. meneghiniana* under the phosphorus limited condition. The growth parameters obtained from monoculture experiments of the two species in the previous study [17] as shown in **Table 4-2** indicate that the maximum cell quota (Q_{max}) of *C. meneghiniana* for N and P ($Q_{max,n}$ = 104 pg cell^{-1}, $Q_{max,p}$ = 5.08 pg cell^{-1}) were nearly 20 times higher than those of *Microcystis* sp. ($Q_{max,n}$ = 5 pg cell^{-1}, $Q_{max,p}$ = 0.28 pg cell^{-1}), whereas the uptake rate ρ_{max}^{hi} for N was only twice that of *Microcystis* sp. This indicates that the deficiency of phosphorus would influence the growth of *C. meneghiniana* more than *Microcystis* sp., and that *Microcystis* sp. would grow more advantageously with adequate nutrients, excluding the effect of other factors such as temperature and dilution. Based on the changes of nutrient concentration as shown in **Fig. 4-2**, there should be no remarkable differences in cell densities of both species in each group. However, *C. meneghiniana* cell densities decreased sharply with the increase in daily renewal rate. Thus, it could be considered that the number of *C. meneghiniana* cells washed away everyday was greater than that grown under the phosphorus limitation. Furthermore, the fluctuation of phosphorus concentration caused by water transfer has been proven that it can not lead to the shift of dominant species and suppress the formation of *Microcystis* blooms. [18]. This was consistent with our results in the semi-continuous competition experiment.

Tatsumoto, Amano, Machida, Aikawa, Fujimura, George, Berk and Taki [19] indicated that the ignition loss of the Lake Tega sediment was measured to be ca. 16%

and the upper 20 cm of the sediment was supposed to contribute to nutrient elution, which may provide nutrient constantly after water transfer. Water pH is also an important influential factor of the nutrient release from sediment, although the release of ammonium-nitrogen increases with pH and the release of nitrate-nitrogen has no obvious relation with pH [20]. The release of phosphorus will decrease with increasing pH until 7.0, and increase with rising pH after higher than 8.0 [21]. Furthermore, the contribution of different ratios of various nitrogen sources to the growth of *Microcystis* sp. has also been observed by several studies [22, 23]. In the north part of Lake Taihu, China, when the molar ratio of ammonium to nitrate was below 1, *Microcystis* blooms tended to be dominant during summer [24]. Therefore, methods of controlling the internal pollution, adjusting the nutrient concentrations, and controlling the pH of the water body were essential for the prevention and management of cyanobacterial (*Microcystis*) blooms and should be developed in the future.

As for the simulated results shown in **Fig. 4-3**, the prediction of *Microcystis* sp. growth displayed a decrease at the daily renewal rates of lower than 5%, and the cyanobacteria blooms were nearly impossible to occur when the daily renewal rate was 0%. However, in reality, the smaller the daily renewal rate is, the more possibility the cyanobacterial blooms occurrence should be [25]. The discrepancy would be due to a shortcoming with the nutrient uptake term of the Chujo's model. According to the equations of the model (**Table 4-1**), the value of the uptake rate term ρ_{max} was always obtained when the nutrient concentration was adequate. However, it could not always reach the maximum value and would decrease with algal growth as well as nutrient concentration decline in the competition process. As a result of the shortcoming, the simulated nutrient concentrations always decreased exponentially when the cell densities of *Microcystis* sp. increase exponentially. In comparison, in reality, when the cell density increased exponentially with initial sufficient nutrients, the decrease in nutrient concentration was only proportionally reduced. [17, 26]. For this reason, the predicted nutrients uptake of *Microcystis* sp. after the logarithmic phase would be overestimated.

However, when the two species were grown together under eutrophic conditions, *C. meneghiniana* showed a very advantage in nutrient uptake over *Microcystis* sp. as shown in our previous study [17]. At the daily renewal rate of 0%, both the experimental and the simulation results indicated that the nutrient was almost exclusively occupied by *C. meneghiniana*, which led to the suppression of the proliferation of *Microcystis* sp. This mechanism provided a reasonable explanation and support for the predicted cell density of *Microcystis* sp. at d = 0%. Nevertheless, there was still a gap between the experimental and predicted values of the *C. meneghiniana* cell densities when it was under relatively scarce nutrient concentration. With the objective of improving the accuracy of the simulation model, the amelioration of the uptake rate term and other environmental factors such as temperature and light intensity should be focused on in the future study.

4.5 Conclusion

The replacement water (medium) restricted both the growth of *C. meneghiniana* and *Microcystis* sp. in competition experiments. Especially, the restricted effect was more significant on the growth of *C. meneghiniana* compared with that of *Microcystis* sp. under the nutrient condition with the combination of limited P and sufficient N. The difference was caused by the more excellent ability of nutrient uptake of *Microcystis* sp., and *C. meneghiniana* was easier to flow away. The broad accuracy of the new developed competition growth model in various nutrient concentrations was also verified based on the prediction curves and competition experiments results. The minimum effective dilution rate (D) to suppress *Microcystis* bloom in Lake Tega was estimated to be 13.3% by this model, which was in consistent with the field observation in Lake Tega. Since the accuracy of the new developed model in broad nutrient concentration range has been verified, it can be a powerful tool to apply for the management of *Microcystis* bloom in many actual lakes with complex nutrient conditions.

References

[1] A. Türkmen, Y. Kütük, Effects of chemical fertilizer, algea compost and zeolite on green bean yield., Turkish JAF Sci.Tech., 5 (2017) 289-293.

[2] K. Cottingham, H. Ewing, M. Greer, C. Carey, K. Weathers, Cyanobacteria as biological drivers of lake nitrogen and phosphorus cycling., Ecosphere, 6 (2015) 1-19.

[3] T.T. Bui, S.-N. Nam, M. Han, Micro-bubble flotation of freshwater algae: a comparative study of differing shapes and sizes, Sep. Sci. Technol., 50 (2015) 1066-1072.

[4] W. Farnham, C. Murfin, A. Critchley, S. Morrell, Distribution and control of the brown alga Sargassum muticum, International Seaweed Symposium (Xth), De Gruyter, 2019, pp. 277-282.

[5] Y. Amano, K. Takahashi, M. Machida, Competition between the cyanobacterium *Microcystis aeruginosa* and the diatom *Cyclotella* sp. under nitrogen-limited condition caused by dilution in eutrophic lake., J. Appl. Phycol., 24 (2012) 965-971.

[6] K. Sugimoto, Y. Negishi, Y. Amano, M. Machida, F. Imazeki, Roles of dilution rate and nitrogen concentration in competition between the cyanobacterium *Microcystis aeruginosa* and the diatom *Cyclotella* sp. in eutrophic lakes, J. Appl. Phycol., 28 (2016) 2255-2263.

[7] Chiba Prefectural Government, Water quality for lakes in Chiba prefecture, Chiba city, Chiba Prefectural Government, 2019.

[8] M. Mikawa, T. Datta, Y. Amano, M. Machida, Dominant characteristics between Microcystis aeruginosa and Cyclotella sp. accompanying dilution process in eutrophic lake, Water, Air, Soil Pollut., 228 (2017) 174.

[9] M. Chujo, J. Li, T. Datta, Y. Amano, M. Machida, A competitive growth model for the simulation of cyanobacterial blooms under eutrophic conditions, Environ. Eng. Sci., 38 (2021) 15-23.

[10] S.C. Maberly, J.-A. Pitt, P.S. Davies, L. Carvalho, Nitrogen and phosphorus limitation and the management of small productive lakes, Inland Waters, 10 (2020) 159-172.

[11] N. Takamura, A. Otsuki, M. Aizaki, Y. Nojiri, Phytoplankton species shift accompanied by transition from nitrogen dependence to phosphorus dependence of primary production in Lake Kasumigaura, Japan, Archiv für Hydrobiologie, (1992) 129-148.

[12] M. Chujo, L. Pang, Y. Fujimura, Y. Amano, M. Machida, Composition of small *Thalassiosirales* under highly diluted conditions in a eutrophic lake., Journal of Environmental Information Science, 2019 (2019) 13-21.

[13] R.R. Guillard, C.J. Lorenzen, Yellow-green algae with chlorophyllide c1,2., J. Phycol., 8 (1972) 10-14.

[14] R. Anderson, R. Berges, P. Harrison, M. Watanabe, Appendix A-Recipes for freshwater and seawater media; freshwater synthetic media., Burlington, USA, 2005.

[15] D. Tilman, S.S. Kilham, Phosphade and silicate growth and uptake kinetics of the diatoms *Asterionella formosa* and *Cyclotella mnenghiniana* in batch and semicontinuous culture., J. Phycol., 12 (1976) 375-383.

[16] M. Mikawa, K. Sugimoto, Y. Amano, M. Machida, F. Imazeki, Competitive growth characteristics between *Microcystis aeruginosa* and *Cyclotella sp.* accompanying changes in river water inflow and their simulation model., Phycol. Res., 64 (2016) 123-132.

[17] M. Chujo, J. Li, T. Datta, Y. Amano, M. Machida, A Competitive Growth Model for the Simulation of Cyanobacterial Blooms Under Eutrophic Conditions, Environmental Engineering Science, (2020).

[18] Y. Amano, Y. Sakai, T. Sekiya, K. Takeya, K. Taki, M. Machida, Effect of phosphorus fluctuation caused by river water dilution in eutrophic lake on competition between blue-green alga *Microcystis aeruginosa* and diatom *Cyclotella* sp., J. Environ. Sci, 22 (2010) 1666-1673.

[19] H. Tatsumoto, Y. Amano, M. Machida, M. Aikawa, Y. Fujimura, D. George, S. Berk, K. Taki, Control of TN/TP ratio by sediment treatment for restraint of water blooms., JECE, 36 (2008) 357-364.

[20] Q. Hu, Y. Zhu, J. Song, Z. Li, J. Wen, Effects of pH and Eh on release of nitrogen and phosphorus from sediments of West Lake., J. Zhejiang Univ. Sci. A, 4 (2003)

358-362.

[21] Y. Wu, Y. Wen, J. Zhou, Y. Wu, Phosphorus release from lake sediments: Effects of pH, temperature and dissolved oxygen., KSCE J. Civ. Eng., 18 (2014) 323-329.

[22] F. Jun, T. Ting, L. Ting, H. Dong, M. Min, S. Jin, *Microcystis aeruginosa* flour as carbon and nitrogen source for aerobic denitrification and algicidal effect of *Raoultella* sp. R11., Ecol. Eng., 105 (2017) 162-169.

[23] L.E. Krausfeldt, A.T. Farmer, H.F. Castro, G.L. Boyer, S.R. Campagna, S.W. Wilhelm, Nitrogen flux into metabolites and microcystins changes in response to different nitrogen sources in *Microcystis aeruginosa* NIES-843., Environ. Microbiol., 22 (2020) 2419-2431.

[24] X. Liu, X. Lu, Y. Chen, The effects of temperature and nutrient ratios on *Microcystis* blooms in Lake Taihu, China: an 11-year investigation., Harmful Algae, 10 (2011) 337-343.

[25] S. Romo, J. Soria, F. Fernandez, Y. Ouahid, Á. BARÓN-SOLÁ, Water residence time and the dynamics of toxic cyanobacteria., Freshw. Biol., 58 (2013) 513-522.

[26] X. Wang, B. Qin, G. Gao, H.W. Paerl, Nutrient enrichment and selective predation by zooplankton promote *Microcystis* (Cyanobacteria) bloom formation., J. Plankton Res., 32 (2010) 457-470.

Chapter 5 General conclusion

In this study, the growth characteristics of *Microcystis* sp. and its main competitor *C. meneghiniana* under various temperatures, nutrient concentrations, and dilution rates were explored. Based on these patterns, a novel growth competition model to accurately predict cyanobacterial bloom occurrence was established. The main conclusions obtained in this study was shown as follows:

(1) *Microcystis* sp. and *C. meneghiniana* under various temperatures showed different growth responses based on the results of monoculture experiments. At low temperatures of 10^{o}C and 20^{o}C, *C. meneghiniana* had superior growth ability compared with *Microcystis* sp., while *Microcystis* sp. grew better at high temperatures (25^{o}C, 30^{o}C, and 35^{o}C). As demonstrated by the prediction of growth rate for two species as a function of temperature, *Microcystis* sp. had the highest temperature-dependent growth rate of 0.65 day^{-1} at 37^{o}C, meanwhile that of *C. meneghiniana* was 0.64 day^{-1} at 29^{o}C. The coefficient ε value reflecting the extent of the biovolume change affected by temperature was 19.4 for *C. meneghiniana* and that was 8.7 for *Microcystis* sp., indicating that *C. meneghiniana* was more sensitive to temperature compared to *Microcystis* sp. These characteristics related to temperature would affect the dominance of the two species when they grow together, thereby affecting the formation of *Microcystis* blooms. *C. meneghiniana* dominated in the low temperature group (20^{o}C) in the cocultivation experiment with *Microcystis* sp., while in the high temperature group (30^{o}C) *C. meneghiniana* was remarkably inhibited by *Microcystis* sp. The dominant characteristics were consistent with the results of monoculture experiments and the predictions of growth rate characteristics. These characteristics can be used to establish the temperature-related term that would enhance the accuracy of the previously developed interspecific competition model, so as to construct more effective methods to inhibit *Microcystis* blooms.

(2) The nitrogen limitation and proper dilution rate could suppress the proliferation of *Microcystis* sp. effectively at low temperature, which can prevent the

occurrence of *Microcystis* blooms. The improvement of the original nutrient uptake term has enhanced the accuracy of the prediction result in the competition experiments. As a result, the overestimation of nutrient uptake has also been reduced by modification of the nutrient uptake term. Under the nitrogen limitation at 20^{o}C, the *C. meneghiniana* could dominate over *Microcystis* sp. totally within the setting experimental conditions. Based on the prediction by the model, when nitrogen concentration was lower than 0.31 mg-N L^{-1} and daily renewal rate was higher than 3%, the growth of *Microcystis* would be suppressed most severely at 20^{o}C. To control the nutrient concentration and dilution rate like above mentioned, the risk of the *Microcystis* blooms will be suppressed efficiently.

(3) The replacement of medium (dilution) restricted the growth both of *Microcystis* sp. and *C. meneghiniana* in competition experiments. Especially, the restricted effect was more significant on the growth of *C. meneghiniana* compared with that of *Microcystis* sp. under the combined nutrient condition with limited phosphorus and sufficient nitrogen concentration. The differences of the growth for th two species were caused by the more excellent ability of nutrient uptake for *Microcystis* sp., and *C. meneghiniana* was easier to flow away. The broad accuracy of the developed growth competition model under various nutrient concentrations was also verified based on the prediction curves and competition experiment. The minimum effective dilution rate (*D*) to suppress *Microcystis* bloom in Lake Tega was estimated to be 13.3% by this model, which was in consistent with the field observation in Lake Tega. Since the accuracy of the new developed model in broad nutrient concentration range has been verified, it can be a powerful tool to apply for the management of *Microcystis* bloom in many actual lakes with complex nutrient conditions and several inflow rivers.

Chapter 6 Outlook

The effect of water temperature, nutrient limitation and dilution rate on the growth of *Microcystis* sp. was investigated in this study, and the effects were well clarified to develop a novel competition model to prevent the occurrence of *Microcystis* blooms. Nevertheless, because all experiments were conducted in stable incubators, there still be undeniable differences in environmental conditions compared with those in actual lakes. Therefore, besides the factors studied here, many other conditions, e.g. light intensity, other nutrient ion, and other coexisting algae, are needed to be further investigated to improve the accuracy of prediction by growth competition model.

The effect of water temperature on the growth of *Microcystis* sp. and its competitor *Cyclotella meneghiniana* was confirmed in laboratory with constant light intensity. Meanwhile, the temperature changes in actual conditions, according to seasonal or diurnal change, are accompanied by changes in light intensity. Thus, the combined impact of temperature and light intensity on algal growth should be further explored.

The relationship between nutrient concentrations and the proliferation of algae was estimated and modeled. The nutrient resource was supplied by inorganic nitrate and phosphate ion, overlooking the effects from other nutrient species. In addition to the two main nutrient resources, the mass ratio of carbon to nitrogen to phosphorus is also important for algal proliferation. Further experiments are necessary to verify and model the effect of those additional nutrient resources on algal proliferation and species succession. Furthermore, different metal ion concentrations and their combination can also be utilized to suppress the growth of *Microcystis* in future.

As the main competitor to *Microcystis* sp. in lake Tega, only the interspecific competition effect of *C. meneghiniana* was examined in this study. In wild aquatic ecosystems, predator-prey effect on algae can lead to changes in the

composition of the algal community in the ecosystem, which is one of the factors influencing the dominance of *Microcystis*. The effect of a superior predator on the dominant species succession so can be further investigated in the future.

The hydrodynamic effects of dilution on the proliferation of *Microcystis* sp. and *C. meneghiniana* were investigated by semi-continuous experiments. But, this kind of semi-continuous experiments is difficult to simulate the effect of disturbance from a continuous flow in the actual river. The proportion of toxic and non-toxic strains in the *Microcystis* sp. community also affects the proliferation trend and dominance characteristics of them without any discussion in this study. All these issues may need to be further investigated using instant monitoring techniques such as remote sensing and so on.

Appendix

Coefficient calculating program by Python

```
import numpy as np
import matplotlib.pyplot as plt
from scipy.optimize import curve_fit

#Using "curve fit" to fit the data to curve
def func (x, a, b, c):
    return a*(x-b)/(x-b+c)  # the formulation of variants and coefficient

#define the x and y
x = [ "0.0957, 0.04834, 0.04015, 0.0354" #the value of x ]
x = np.array(x)
num = ["0.606, 0.269, 0.0504, 0.0148" #the value of y]
y = np.array(num)

# Nonlinear least squares curve fitting
popt, pcov = curve_fit(func, x, y)

#obtain fitting constant from popt
print(popt)
a = popt[0]
b = popt[1]
c = popt[2]
yvals = func(x,a,b,c)
print('popt:', popt)
print('u_maxCN', a)
print('Q_CN', b)
print('K_C', c)
print('coefficient yvals:',yvals)

#Print figure out
plot1 = plt.plot(x, y, 's',lable = 'original values')
plot2 = plt.plot(x, yvals, 'r',lable = 'polyfit values')
plt.xlable('x')
plt.ylable('y')
plt.legend(loc=4) #Specified the position of legend
plt.title('curve_fit')
plt.show
```